1097

GENERAL ELECTRIC
SPACE DIVISION
PHILADELPHIA

PROGRAM INFORMATION REQUEST / RELEASE

	*CLASS. LTR.	OPERATION	PROGRAM	SEQUENCE NO.	REV. LTR.
PIR NO.	STEP	—	— PHIV —	270	

*USE "C" FOR CLASSIFIED AND "U" FOR UNCLASSIFIED

FROM	TO
E. Kelly	A. J. Poché

DATE SENT	DATE INFO. REQUIRED	PROJECT AND REQ. NO.	REFERENCE DIR. NO.
11/19/79			

SUBJECT

EXTENDED COLUMN THERMAL ENERGY STORAGE TEST RESULTS

INFORMATION REQUESTED/RELEASED

Attached are the results of the tests run at the G.E. Evendale Plant using a 100 inch long thermal energy storage bed with Syltherm™ 800 fluid and Hanna Mining Company iron ore pellets as the storage media.

RETURN TO:

SCOTT FAAS

The report is sectioned as follows:

1. Summary
2. Introduction
3. Description of Test Setup
4. Test Program

5.0 Static and Dynamic Holdup and Void Fraction

5.1 Charging Tests

5.2 Discharging Tests

5.3 Holding Tests

5.4 Inversion Test

5.5 Heat Transfer Coefficients

5.6 Fluid Distributor

5.7 Conclusions

Appendix A - Syltherm Properties

Copies To: W. Mertz, J. Bledsoe, A. Saydah, R. Laessig, R. Allred, V. Haley

PAGE NO. ____ OF ____

√ RETENTION REQUIREMENTS

COPIES FOR	MASTERS FOR
☐ 1 MO.	☐ 3 MOS.
☐ 3 MOS.	☐ 6 MOS.
☐ 6 MOS.	☐ 12 MOS.
☐ MOS.	☐ MOS.
☐	☐ DO NOT D

FORM 1020 B REV. (7/0)

1. Summary

An experiment has been performed at the General Electric Evendale Plant to gain knowledge of the performance of high temperature trickle mode thermal energy storage using a silicone oil as the working fluid. The incentive for considering trickle operation in a large system is the minimization of fluid inventory since high temperature heat transfer fluid costs are typically $20 per gallon.

The test program included measurement of static and dynamic fluid holdups, axial and radial temperature distributions during charging and discharging, holding tests and an inversion test.

Dow-Corning Syltherm^{TM} 800 was the working fluid; the storage material was Hanna Mines iron ore with a primary particle size of 3/8". The test temperature range was 350^{o}F (177^{o}C) to 450^{o}F (232^{o}C) whereas the actual system will operate at 500^{o}F (260^{o}C) to 750^{o}F (399^{o}C). Test flow rates were chosen to cover the range of the Reynolds number of the full scale system, 1.8 to 28.1 for fluid dynamic and thermal simulation.

The storage bed was 22.5 inches in diameter and 100 inches deep, with a void fraction of 40%.

Analysis of the data showed good agreement of static and dynamic holdup with correlations available in the literature. Static holdups in the range of 5 to 8% of bed volume are predicted for the full scale system. Dynamic holdups in the range of 2 to 10% are projected.

Charge/discharge data shows that large radial temperature gradients develop during initial charging, but go through a maximum and then diminish as charging/discharging proceeds. For the Shenandoah STEP program, series charging and

discharging will be used, consequently, these gradients will persist only at the bottom of the last tank. From the data analysis, in conjunction with a computer model, effective heat transfer coefficients in the range of 15 to 25 BTU/Ft^2hr^oF were deduced over the flow rate range from 550 to 2400 lbs/Ft^2hr. The tests showed the adequacy of the model to predict average thermocline shapes over the primary flow range of the full scale system, when the model heat transfer coefficient is reduced by a factor of 4. A previous test in a 28-inch long column, using water/glycerine solution as the fluid had indicated a reduction factor of eleven was needed. The sensitivity of charge/discharge efficiency to the heat transfer is not great; e.g., a reduction factor of 4 results in an 83% charge while a factor of 8 results in a 79% charge in the last large tank.

Holding test results indicate that serious distortion of the thermoclines will not occur in the full scale system with tanks of 10 to 20 feet in diameter.

The inversion test (moving the hot zone from the top to the bottom of the bed), showed that this process, although only of secondary importance in the full scale system, is feasible.

Difficulties in the test, which made analysis of the data less rigorous than desired, were primarily due to inlet fluid distributor problems, heat losses in the fluid exit line, and an insufficient batch fluid inventory to achieve full charges and discharges.

The overall conclusion is that the trickle mode of operation has a high probability of meeting the primary goals of the full scale system.

2. Introduction

The incentive for trickle mode operation is the reduction in fluid inventory required in comparison to dual media operation where the bed is completely filled with fluid. This is a signigicant consideration with high temperature heat transfer fluid costs at $20 per gallon.

The choice of fluids for high temperature operation is extremely limited and silicone oil was judged to offer the best potential for the STEP system. No data existed in the literature for high temperature silicone oil trickle mode operation. In order to confirm feasibility, an experiment was designed to obtain data in a small scale system. Of primary interest were the shapes of the thermoclines in the charging and discharging modes, along with void fraction measurement, static and dynamic fluid holdups, holding, and inversion (moving the hot zone of a partially charged bed from the top to the bottom of the bed). The comparison of measured thermocline shapes with a computer model would enable evaluation of effective heat transfer coefficients which would be used to size and predict the performance of the full scale system with a higher degree of confidence.

A previous test had been run on a short bed (28 inches deep) using a water/glycerine solution to simulate the viscosity of the silicone oil. This test was run over a temperature range of $80^{o}F$ ($27^{o}C$) to $180^{o}F$ ($82^{o}C$) with granite rock particles of large and irregular shapes (characteristic dimensions 3/8" to 1"). To match measured thermocline shapes with the model, the theoretical heat transfer coefficient as calculated in the model had to be reduced by a factor of 11. The short length of the bed did not allow

fully developed thermoclines to be established and in addition the large and irregular shaped particles were thought to have contributed to poor wetting with reduced heat transfer and channeling. Post test inspection of the fluid distributor showed clogging of some outlet holes which affected initial fluid distribution. In addition, a holding test of a partially discharged bed showed extreme distortion of the thermocline.

Because of the empirical inconclusiveness of these tests a second test described herein was designed. This test included the following changes and characteristics: 1) the column height was extended from 28 inches to 100 inches to allow measurement of full thermocline shape development as it proceeded through the bed, 2) spheroidal iron ore particles (3/8" diameter) as bed material (Granite was eliminated because compatibility tests showed high fluid degradation rates), 3) Syltherm^{TM} 800 silicone oil as the working fluid. It was recognized that fluid viscosity matching might not be sufficient, particularly as related to the question of fluid foaming which could reduce heat transfer rates. The surface tension of the fluid is believed to be an important parameter with regard to foaming. Consequently, the actual working fluid was used in these tests. The test temperature range was $350^{o}F$ ($177^{o}C$) to $450^{o}F$ ($232^{o}C$) compared to the actual system range of $500^{o}F$ ($260^{o}C$) to $750^{o}F$ ($399^{o}C$). Existing equipment limitations, schedules and costs precluded operation at $500^{o}F$ to $750^{o}F$. It was judged that this range would provide an acceptable degree of simulation of fluid dynamics and heat transfer characteristics so that fitting the model to test data at these temperatures would not result in significant error when the model was

used for full scale predictions. (See Appendix A for Sylthern^{TM} 800 properties as a function of temperature.)

Other changes included a redesign of the fluid distributor with the intent of obtaining a more uniform initial distribution, the addition of view ports at the top and bottom of the bed, re-design of the column support structure and insulation to control heat losses, and the use of a higher speed (13 channels per second) data acquisition system.

Table 1 summarizes the general operating conditions of the Phase 3 conceptual tests, the phase 4 extended column test and the STEP field installation.

TABLE 1

COMPARISON OF THE GENERAL OPERATING CONDITIONS OF THE TRICKLE OIL TES TESTS WITH THE SHENANDOAH FIELD APPLICATION

	Trickle Oil TES Tests		
	Phase III Conceptual Test	Phase IV Extended Column Test	STEP Shenandoah * Design
Heat Transfer Fluid	Water	S-800	S-800
Heat Storage Media	Granite	Iron Ore	Iron Ore
Temperature Range	80-180°F	350-450°F	500-750°F
Bed Height	28 in	100 in.	192 in. large 144 in. small
Cover Gas	N_2 (0 and 1 psig)	N_2 (5 psig and 1 psig)	N_2 (10 psig)

* Original 140 X 10^6 BTU design, 60 X 10^6 BTU System

Predictions not included in this report.

3. Description of Extended Column Test Setup

A 100-inch high iron ore column, 22-1/2" diameter was used with Syltherm^{TM} 800 oil in the temperature range for 350^{o}F to 450^{o}F at flows between 0.9 and 17.2 gpm.

Iron ore pellets approximately 3/8" in diameter were supported on a screen inside a 3 section stainless steel tank. The temperature profile of the bed was measured using sheathed thermocouples inserted into pellets located to provide both axial and radial data. The axial profile was measured along the column centerline at 2-inch intervals throughout the 100-inch depth. Radial profiles were measured on five selected planes.

Charging-discharging tests were accomplished by pre-establishing the desired temperature of a fixed inventory of oil and then pumping that oil through the ore tank. Separate source and sink tanks are used. By utilizing separate source and sink tanks, the need for a fast response facility temperature regulation system was eliminated.

Two centrifugal pumps were used in the test setup. One pump transfered oil from the source or sink tank to the fluid distributor at the top of the thermal storage tank. The second pump scavenged the oil from the bottom of the thermal storage tank and pumped it to the desired sink or source tank.

Both pumps are constant speed devices. The variable flow rates required for testing was achieved by "by-pass" regulation wherein part of the pump outlet flow was allowed to by-pass back to the pump inlet through an adjustable control valve.

Stainless steel (304) was used for the external storage tank, the source

and sink tanks and several other components but plain carbon was used extensively for piping, valves, etc. (The Shenandoah setup will use plain carbon steel almost exclusively).

The source and the sink tanks are actually a set of three 100 gal. tanks connected in parallel. Each of the three 100 gal. hot (source) tanks is equipped with clamp-around drum heaters with thermostatic controls to maintain a 450^{o}F environment around the tanks, minimize heat losses, and achieve a nearly constant source temperature. The three "cold" tanks were not equipped with clamp-around drum heaters since in general their function was to cool the oil prior to a "discharge" run. All tanks and piping were insulated.

Two parallel electric immersion heaters each rated at 6 KW are the means by which circulating oil was heated prior to a test run.

Fluid flow in and out of the thermal storage tank was measured with turbine type flow meters. The fluid flows and all temperatures are automatically recorded using an Acurex A-900 Data Logger. A magnetic tape cassette recording capability enabled data acquisition at approximately 13 channels/second and the use of a digital computer for fast, accurate and versatile date reduction and evaluation.

A nitrogen cover gas was used at all interior locations. The pressure level was established at approximately 5 psi by a nitrogen regulating valve connected through the ore tank. Vapor boil off below 450^{o}F was expected to be minimal and elaborate fluid pre-conditioning was not required.

Table 2 summarizes the significant thermal/mechanical characteristics of the extended column test.

Figure 1 (Dwg. No. 147D4026) shows the test setup flow schematic, detailing all valves, piping, gage locations, etc. By appropriate valve manipulation, various flow loops and paths required for the test (reference Table 3) were achieved.

Figure 2 is the top level assembly drawing for the test setup. The parts list defines all sub-tier drawings and equipment. Some features of the setup are:

An angle iron structure supports six 100 gallon tanks utilized for fluid storage. A separate structure supports the ore tank and provides a mid-height walk-on level.

The ore tank is supported at mid-flange location with 4 point structural contact in an effort to minimize heat conduction losses from the rock tank.

All tanks and pipes are insulated to control thermal loss. Filters have been installed at appropriate locations to prevent particulate matter from plugging critical flow paths.

Welded pipe joints were utilized as much as possible to avoid leakage problems with Syltherm^{TM} 800.

Figure 3 (Dwg. No. 147D4020) shows details of the fluid distribution manifold. It was intended to uniformly distribute the fluid over the upper cross sectional area of the tank. The manifold consists of five concentric circular tubes with 0.043 inch diameter holes drilled on the side facing the

TABLE 1

THERMAL CHARACTERISTICS OF TES EXTENDED COLUMN TEST SET-UP

Thermal Storage	
Storage Media	Hanna Mines Iron Ore Pellets
Characteristic Diameter	3/8" dia.
Bulk Density	137.1 lb/ft^3
Specific Heat @ 350,400,450^oF	0.2 Btu/lb-^oF
Pounds - Mass in Tank	3154 lbs.
Tank Weight (Total)	915 lbs.
Distributor System Wt.	122 lbs.
Upper Section Wt.	243 lbs.
Middle Section Wt.	187 lbs.
Bottom Section Wt.	363 lbs.
Tank Material	304 SS
Specific Heat	.11 Btu/lb-^oF
Fluid System	
Fluid	Syltherm 800
Viscosity at 400^oF	1 CP = 2.5 lb/ft-hr
Density @ 400^oF	48 lb/ft^3
Specific Heat @ 400^oF	0.46 Btu/lb-^oF
Oil Inventory	1730 lbs. (270) gallons
Hot Tank System	
Number of Tanks in Set	3 each
Individual Tank Capacity	100 gallons
Individual Tank Material	304 SS
Individual Tank Wt.	280 lbs.
Individual Tank Specific Heat	.11 Btu/lb-^oF

TABLE 1 (CONT'D.)

Individual Tank I.D. x Ht.	22.5" x 40"
Total Capacity	300 gallons
Total Weight	840 lbs
Cold Tank System	
Identical to Hot Tank System	
Pumps (Inlet & Scavenge Pump Identical)	Burks Turbine Pump
Rated Flow/Pressure (H_2O)	20 gpm/200 ft.
Max. Recommended Operating Temp.	550°F
NPSH (estimated)	2 ft.
Drive HP/Speed	3 HP/3450 RPM
In-line Heaters (Two in Parallel)	Chromalox
Each Heater Rated Capacity	6 KW
Thermal Density	13 watts/in^2
Design Range	150-550°F
Cooler Heat Exchanger	Graham
Shell Side Fluid/Pressure	H_2O/100 psi
Tube Side Fluid/Tube Dia.	Syltherm™800/0.5 inch
Heat Transfer Surface Area	9.63 ft^2

thermal storage bed. At 17 gpm the pressure head required at the shower inlet is 35 ft. of water (14.4 psi).

The major components and other system elements which make up the assembly are listed as follows:

Tanks. Six 100-gallon, Type 304 SS tanks detailed in Drawing No. 12808633.

Pumps. One circulating pump, and a scavenge pump. Both Burks Co. Model 330CS8MJ close coupled turbine pumps. 3 HP, 3450 RPM, 3 phase, 20 gpm at 200 ft. head, water jacketed mechanical face seal designed for 550^{o}F maximum fluid temperature.

Tank Heaters. Three Drum Tec Co. Model VHDR-55-460-3, 3.2 KW, 460 volts, 3 phase, 55 gal. drum heaters with 100^{o}-450^{o}F thermostat. Will cover only lower part of tank.

Circulation Heaters. Two Chromalox Co. Cat. No. MWHO-30615, 6.0 KW, 480 volts, 3 phase watt density 13 watts/in^{2}, with 150^{o}-550^{o}F thermostat.

Cooler Heat Exchanger. Graham Manufacturing Co., Heliflow Model 5X4C-14S, 1/2 inch Type 304 SS tubes, 9.63 ft^{2} surface area, cast iron shall 100 psi rating (water side).

Flow Meters. Two Flow Technology Inc., Turbine Type Model FT-8N10-LB, 1-10 gpm max, fluid temp. 450^{o}F. Two Model FT-12N20-LB, 2-20 gpm max, fluid temp. 450^{o}F. Model PRI-102A frequency to analog converter. Cox Model 950-D-A converter.

Valves. Gate-Vogt Model SW-12111 with socket weld connections, forged steel, max. temp. 850°F. Glove-Vogt Model SW-12141 with socket weld connections, forged steel. Max. Temp. 850°F.

Filter. Two 100μ filter elements, CUNO Model 2710-150 with AEP shop supplied S/S casings.

Piping. 3/4", 1", 1-1/2" Sch. 40, black steel with forged steel socket weld fittings.

Insulation.

Oil Tanks - Celotamp 1500 block for base, 4 inch thick; Type ETR Forty-Eight blankets on both sides and top 4 inch thick. Finish with 1 inch thick aluminum covered Armstrong "Rig-Flex."

Pipeline - Jim Micro-Lok Fiber Glass, 2 inch thick

Fittings - ETR Forty-Eight 2 inch thick covered with Textoglass cloth

Thermal Storage - ETR Forty-Eight 8 inch thick, with 1 inch thick Armstrong "Rig-Flex" on the outside.

Fluid. 270 gallons of Syltherm™ 800 (Dow Corning experimental fluid X2-1162).

Instrumentation

This section presents the instrumentation details for the extended column test setup.

An Acurex Autodata Logger Model A900 was utilized to record key HTS tank data. This recorder (with its auxiliaries) has the capability of scanning up to 140 input channels and printing the value of each channel on a paper tape at 2.5 channels/second. The A932-01 serial output interface provided an ASCII formatted serial output and enabled storage on a GE Magnetic Tape Terminal (MTT) cassette recorder. The logger records the following parameters:

Temperature

- Thermal storage tank inlet and outlet fluid temperature
- 88 temperatures in the iron ore bed

Flow

- Thermal storage tank inlet flow rate
- Thermal storage tank outlet flow rate

The Temperature readings associated with the tank were determined from Type T (copper constantan) sheathed thermocouples located in the iron ore bed along the axial centerline and radially at the five selected sections. Figure 4 (Dwg. No. 707E931) shows the mechanical design of the tank and identifies the thermocouple locations in the test bed as does Figure 4-A.

Figure 5 shows an instrumentation schematic diagram for the overall test setup and indicates the temperature and flow recording and monitoring equipment.

Due to the wide range of test flow requirements (.9 to 17.2 gpm) two overlapping flowmeters (in parallel) were used. Flow Technology Turbine Type Model FT-8N10-LB meter covers the 1-10 gpm range, while a Model FT-12N20-LB meter can measure flows up to 20 gpm. This is done at both the inlet and outlet of the storage tank. The flowmeters were calibrated with a fluid having a viscosity similar to Syltherm^{TM} 800 at 400^{o}F.

Strip Chart Recorders and Additional Temperature Instrumentation

Thermal storage tank inlet and outlet flow and temperature were recorded on separate single channel strip charts (Electronik Model 19 recorders). These charts were used to monitor the test progress and were useful for indicating break-out conditions.

Thirty (30) additonal Type K T/C's were used primarily for control of the test and to provide test bed heat loss and other related data.

Pressure Instrumentation

Pressure gages required for control of the facility were located throughout the facility and were not included in the automatic data logging system. The following list identifies the gages required.

LIST OF FACILITY PRESSURE GAGES

P1	Circulation Pump Inlet Pressure
P2	Circulation Pump Discharge
P3	N_2 Cover Gas Pressure
P4	Scavenge Pump Inlet Pressure
P5	Scavenge Pump Discharge
ΔP1	Flow Distributor to Rock Tank Diff. Press.
ΔP2	Filter ΔP

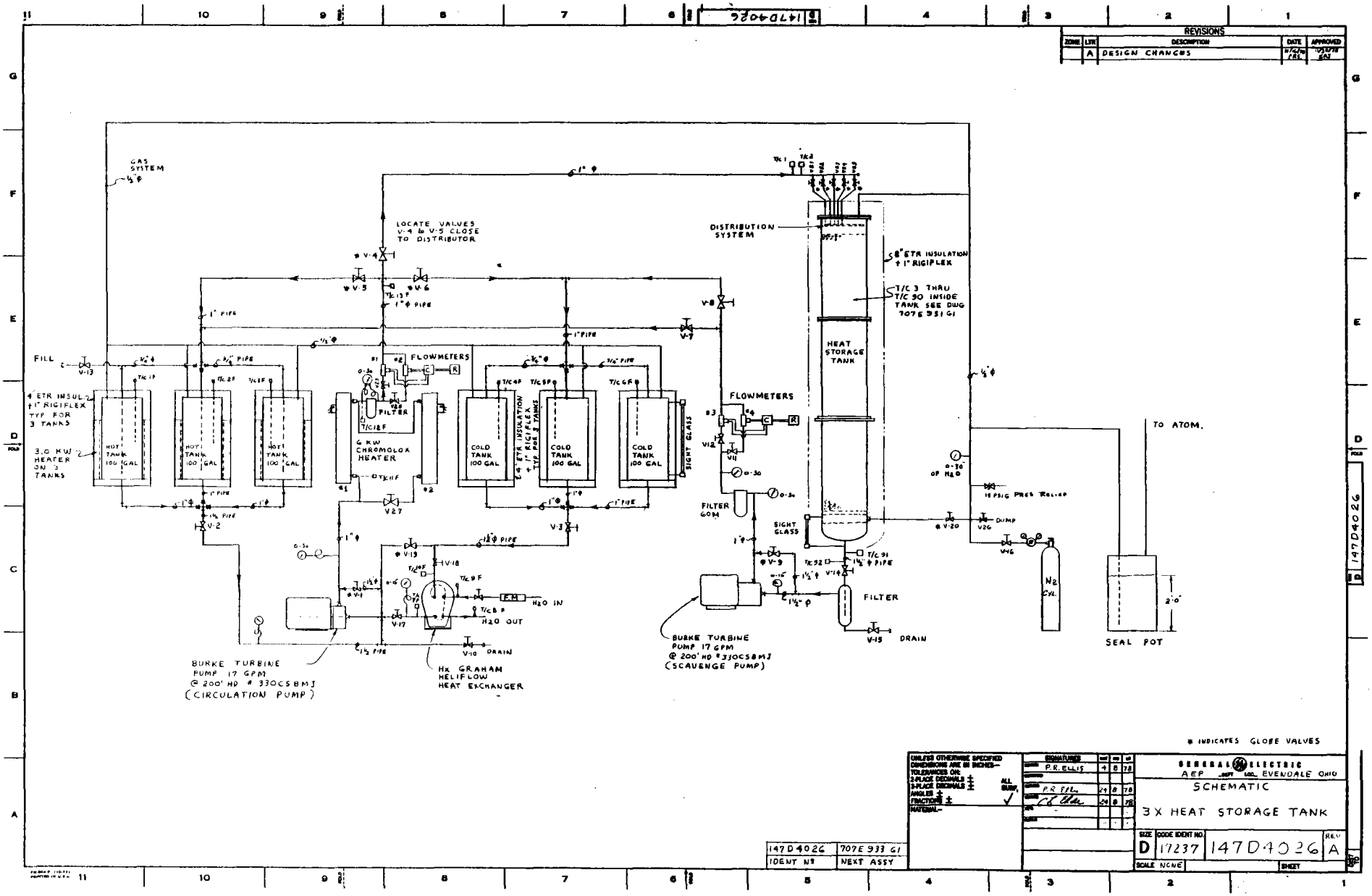
REVISIONS
ZONE | LTR | DESCRIPTION | DATE | APPROVED
A | DESIGN CHANGES
GAS SYSTEM
LOCATE VALVES V-4 & V-5 CLOSE TO DISTRIBUTOR
DISTRIBUTION SYSTEM
5.8" ETR INSULATION + 1" RIGIPLEX
T/C 3 THRU T/C 90 INSIDE TANK SEE DWG 707E 951 G1
HEAT STORAGE TANK
FILL
FLOWMETERS
4" ETR INSUL + 1" RIGIPLEX TYP FOR 3 TANKS
3.0 KW HEATER ON 3 TANKS
HOT TANK 100 GAL
6 KW CHROMOLOX HEATER
FILTER
COLD TANK 100 GAL
2.4" ETR INSULATION + 1" RIGIPLEX TYP FOR 3 TANKS
SIGHT GLASS
FILTER 60M
TO ATOM.
15 PSIG PRES REGULATOR
DUMP
N2 CYL.
SEAL POT
BURKE TURBINE PUMP 17 GPM @ 200' HD # 330CS8MJ (CIRCULATION PUMP)
Hx GRAHAM HELIFLOW HEAT EXCHANGER
BURKE TURBINE PUMP 17 GPM @ 200' HD #330CS8MJ (SCAVENGE PUMP)
H2O IN
H2O OUT
DRAIN
* INDICATES GLOBE VALVES
GENERAL ELECTRIC
AEP EVENDALE OHIO
SCHEMATIC
3X HEAT STORAGE TANK
SIZE D | CODE IDENT NO. 17237 | 147D4026 | REV A
SCALE NONE | SHEET
147D4026 | 707E933 G1
IDENT NO | NEXT ASSY

FIGURE 1

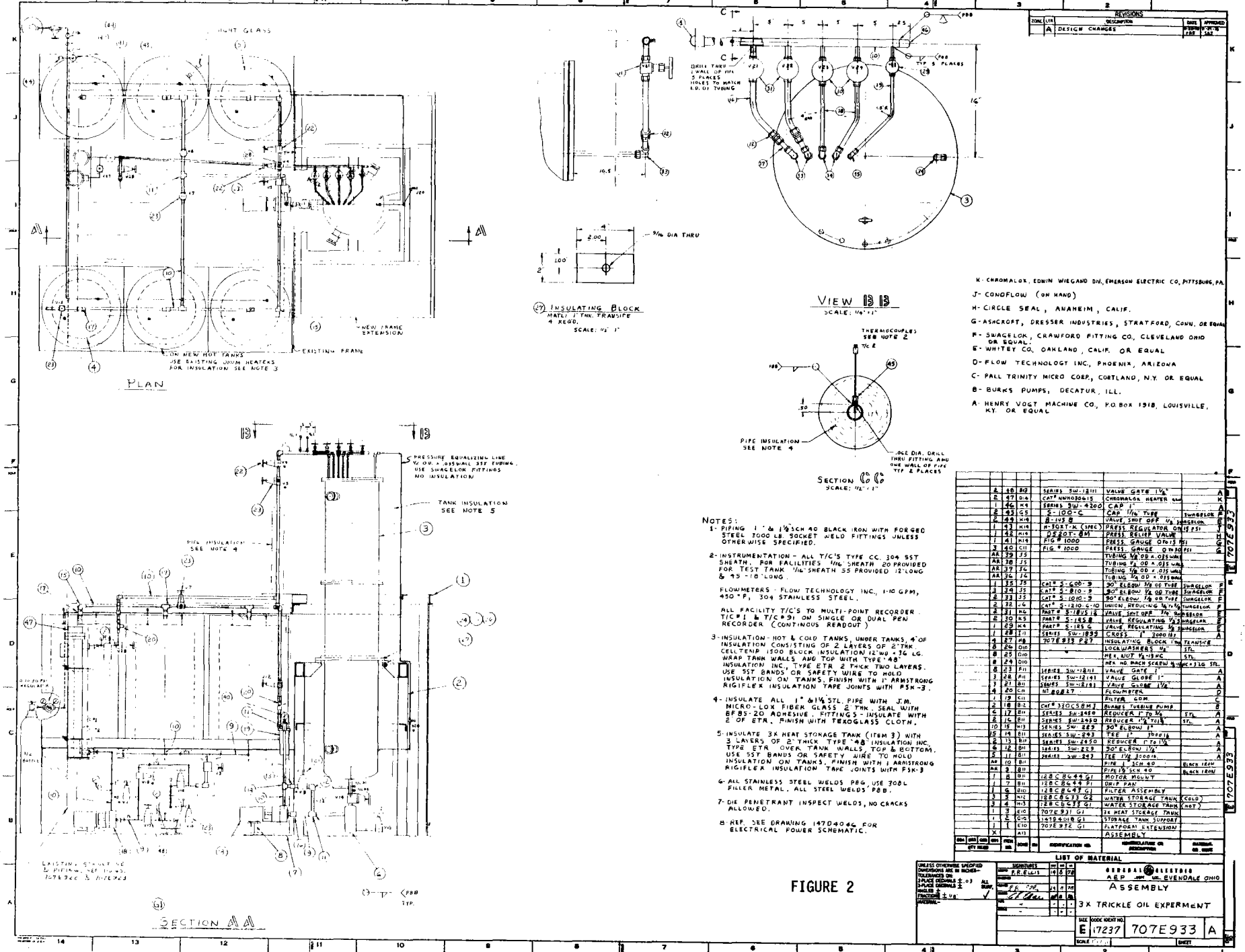

K- CHROMALOX, EDWIN WIEGAND DIV, EMERSON ELECTRIC CO, PITTSBURG, PA.

J- CONOFLOW (ON HAND)

H- CIRCLE SEAL, ANAHEIM, CALIF.

G- ASHCROFT, DRESSER INDUSTRIES, STRATFORD, CONN. OR EQUAL

F- SWAGELOK, CRAWFORD FITTING CO. CLEVELAND OHIO OR EQUAL.

E- WHITEY CO. OAKLAND, CALIF. OR EQUAL

D- FLOW TECHNOLOGY INC, PHOENIX, ARIZONA

C- PALL TRINITY MICRO CORP, CORTLAND, N.Y. OR EQUAL

B- BURKS PUMPS, DECATUR, ILL.

A- HENRY VOGT MACHINE CO, P.O. BOX 1918, LOUISVILLE, KY. OR EQUAL

NOTES:

1- PIPING 1" & 1½" SCH 40 BLACK IRON WITH FORGED STEEL 3000 LB SOCKET WELD FITTINGS UNLESS OTHERWISE SPECIFIED.

2- INSTRUMENTATION - ALL T/C'S TYPE CC. 304 SST SHEATH. FOR FACILITIES 1/16" SHEATH 20 PROVIDED FOR TEST TANK 1/16" SHEATH 55 PROVIDED 12' LONG & 95 - 18' LONG.

FLOWMETERS - FLOW TECHNOLOGY INC., 1-10 GPM, 450 °F, 304 STAINLESS STEEL.

ALL FACILITY T/C'S TO MULTI-POINT RECORDER T/C # 1 & T/C # 91 ON SINGLE OR DUAL PEN RECORDER (CONTINOUS READOUT)

3- INSULATION - HOT & COLD TANKS, UNDER TANKS, 4" OF INSULATION CONSISTING OF 2 LAYERS OF 2" THK CELLTEMP 1500 BLOCK INSULATION 12" WD. x 36 LG. WRAP TANK WALLS AND TOP WITH TYPE "AB" INSULATION INC., TYPE ETR 2 THK TWO LAYERS. USE SST BANDS OR SAFETY WIRE TO HOLD INSULATION ON TANKS, FINISH WITH 1" ARMSTRONG RIGIFLEX INSULATION TAPE JOINTS WITH FSK-3.

4- INSULATE ALL 1" & 1¼ STL. PIPE WITH J.M. MICRO-LOK FIBER GLASS 2 THK. SEAL WITH BFBS-20 ADHESIVE. FITTINGS - INSULATE WITH 2 OF ETR. FINISH WITH TEXGLASS CLOTH.

5- INSULATE 3X HEAT STORAGE TANK (ITEM 3) WITH 3 LAYERS OF 2" THICK TYPE "AB" INSULATION INC. TYPE ETR OVER TANK WALLS, TOP & BOTTOM. USE SST BANDS OR SAFETY WIRE TO HOLD INSULATION ON TANKS. FINISH WITH 1 ARMSTRONG RIGIFLEX INSULATION TAPE JOINTS WITH FSK-3

6- ALL STAINLESS STEEL WELDS PBG, USE 308L FILLER METAL. ALL STEEL WELDS PBB.

7- DIE PENETRANT INSPECT WELDS, NO CRACKS ALLOWED.

8- REF. SEE DRAWING 1470404G FOR ELECTRICAL POWER SCHEMATIC.

FIGURE 2

REVISIONS				
ZONE	LTR	DESCRIPTION	DATE	APPROVED
	A	DESIGN CHANGES	1-15-78	

	48	B12	SERIES SW-12111	VALVE GATE 1½"		A
2	47	B14	CAT# NHR3046-15	CHROMALOX HEATER 6KW		K
1	46	K9	SERIES SW-4200	CAP 1"		A
2	45	G5	S-100-C	CAP 1/16 TUBE	SWAGELOK	F
2	44	K18	B-1KS-B	VALVE, SHUT OFF 1/8	SWAGELOK	F
1	43	K18	R-3031-K (SPEC)	PRESS REGULATOR 0 TO 15 PSI		J
1	42	K18	D520T-8M	PRESS RELIEF VALVE		H
1	41	K19	FIG # 1000	PRESS. GAUGE 0 TO 15 PSI		G
3	40	C11	FIG # 1000	PRESS GAUGE 0 TO 30 PSI		G
AR	39	J5		TUBING 1/8 OD x .035 WALL		
AR	38	J5		TUBING ¼ OD x .035 WALL		
AR	37	J6		TUBING ½ OD x .035 WALL		
AR	36	J6		TUBING ¾ OD x .035 WALL		
1	35	J5	CAT# S-600-9	90° ELBOW 1/8 OD TUBE	SWAGELOK	F
2	34	J5	CAT# S-810-9	90° ELBOW ¼ OD TUBE	SWAGELOK	F
2	33	J5	CAT# S-1010-9	90° ELBOW ⅝ OD TUBE	SWAGELOK	F
2	32	J6	CAT# S-1210-6-10	UNION, REDUCING ¾"x⅝"	SWAGELOK	F
2	31	K6	PART # S-1BVS 16	VALVE SHUT OFF ¾"	SWAGELOK	F
2	30	K5	PART # S-1858	VALVE, REGULATING ½"	SWAGELOK	F
1	29	K4	PART # S-1856	VALVE, REGULATING ½"	SWAGELOK	F
1	28	F11	SERIES SW-1899	CROSS 1" 3000 lbs		A
4	27	H8	707E933 P27	INSULATING BLOCK 1" THK	TRANSITE	
8	26	D10		LOCKWASHERS ½"	STL.	
8	25	D10		HEX NUT ½"-13 NC	STL.	
8	24	D10		HEX HD BOLT SCREW ½"-13 NC x 2½ LG	STL.	
6	23	F11	SERIES SW-12111	VALVE GATE 1"		A
3	22	F11	SERIES SW-12101	VALVE GLOBE 1"		A
1	21	B11	SERIES SW-12181	VALVE GLOBE 1½"		A
4	20	C11	NT 80827	FLOWMETER		D
1	19	C11		FILTER ASM.		C
2	18	B12	CAT# 320CS8MJ	BURKS TURBINE PUMP		B
4	17	B11	SERIES SW-2450	REDUCER 1" TO ¾"	STL.	A
2	16	B11	SERIES SW-2450	REDUCER 1½" TO 1"	STL.	A
10	15	H13	SERIES SW-289	90° ELBOW 1"		A
12	14	B11	SERIES SW-243	TEE 1" 3000 lb		A
2	13	B11	SERIES SW-2450	REDUCER 1" TO ½"		A
6	12	B11	SERIES SW-229	90° ELBOW ½"		A
2	11	B11	SERIES SW-243	TEE 1½" 3000 lb		A
AR	10	B11		PIPE 1" SCH 40	BLACK IRON	
AR	9	B11		PIPE 1½" SCH 40	BLACK IRON	
1	8	B11	128C8644G1	MOTOR MOUNT		
1	7	B11	128C8644P1	DRIP PAN		
1	6	B10	128C8643G1	FILTER ASSEMBLY		
3	5	H12	128C8633G2	WATER STORAGE TANK (COLD)		
3	4	H13	128C8633G1	WATER STORAGE TANK (HOT)		
1	3	E10	707E931G1	3X HEAT STORAGE TANK		
1	2	C15	1418401851	STORAGE TANK SUPPORT		
1	1	E10	707E932G1	PLATFORM EXTENSION		
X		A13		ASSEMBLY		

QTY REQD	ITEM NO.	ZONE	IDENTIFICATION NO.	NOMENCLATURE OR DESCRIPTION	MATERIAL OR SIZE

LIST OF MATERIAL

UNLESS OTHERWISE SPECIFIED DIMENSIONS ARE IN INCHES	SIGNATURES	DATE
TOLERANCES ON:	DRAWN D.R. Ellis	1-15-78
3 PLACE DECIMALS ±.03	CHECKED	
2 PLACE DECIMALS ±	ENGR APPR.	
ANGLES ±	MFG APPR.	
FRACTIONS ± 1/16	Q.A.	
MATERIAL	COMM'L APPR.	

GENERAL ELECTRIC
AEP JOB NO. EVENDALE OHIO

ASSEMBLY

3X TRICKLE OIL EXPERMENT

SIZE	CODE IDENT NO.	DRAWING NO.	REV
E	17237	707E933	A

SCALE 1"=1" SHEET

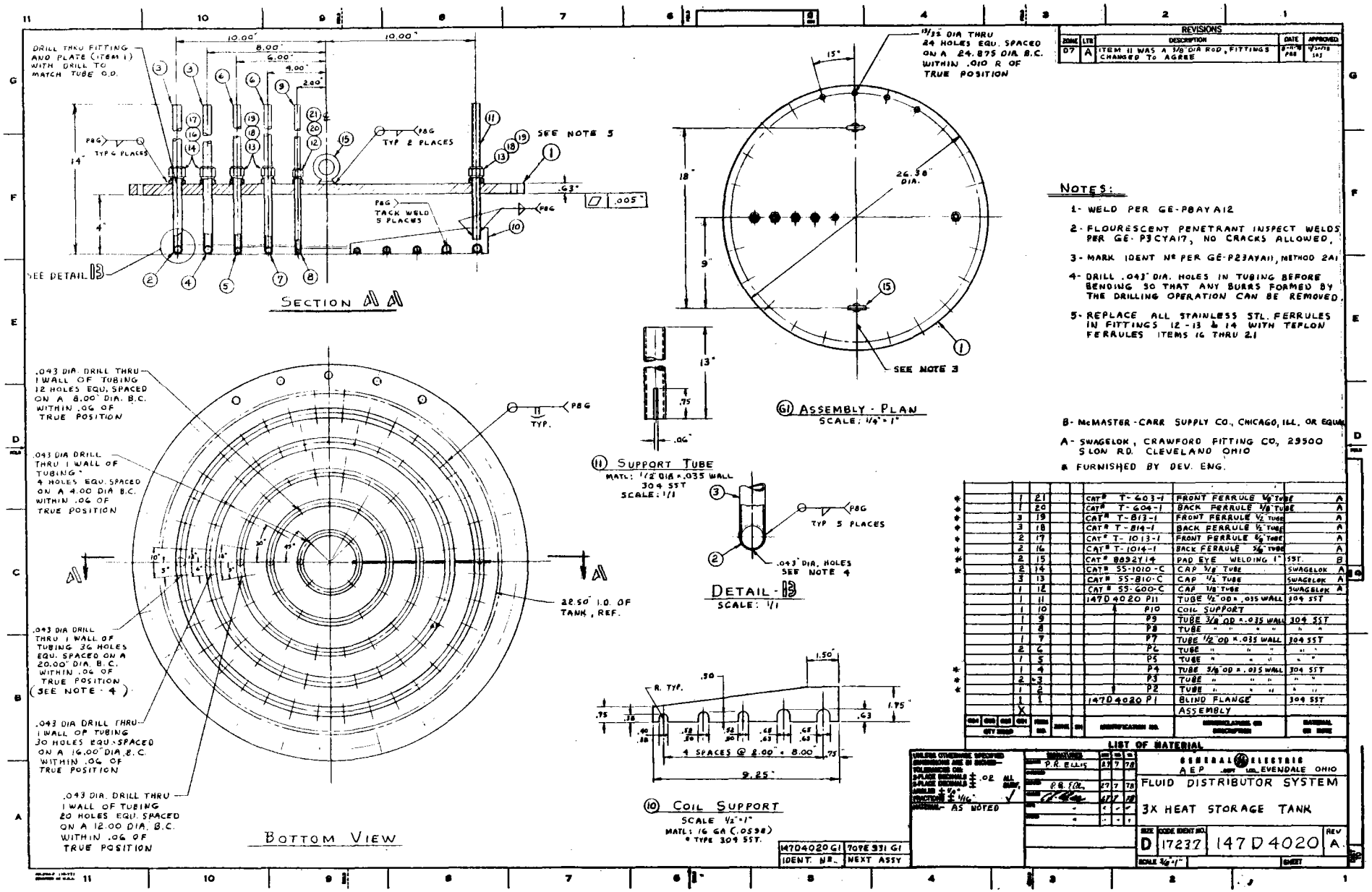

REVISIONS

ZONE	LTR	DESCRIPTION	DATE	APPROVED
07	A	ITEM 11 WAS A 3/8" DIA ROD, FITTINGS CHANGED TO AGREE	8-11-78	11-27-78

NOTES:

1- WELD PER GE-P8AYA12

2- FLOURESCENT PENETRANT INSPECT WELDS PER GE-P3CYA17, NO CRACKS ALLOWED.

3- MARK IDENT Nº PER GE-P23AYA11, METHOD 2A1

4- DRILL .043" DIA. HOLES IN TUBING BEFORE BENDING SO THAT ANY BURRS FORMED BY THE DRILLING OPERATION CAN BE REMOVED.

5- REPLACE ALL STAINLESS STL. FERRULES IN FITTINGS 12-13 & 14 WITH TEFLON FERRULES ITEMS 16 THRU 21

B- McMASTER-CARR SUPPLY CO., CHICAGO, ILL. OR EQUAL

A- SWAGELOK, CRAWFORD FITTING CO, 29500 SLON RD. CLEVELAND OHIO

* FURNISHED BY DEV. ENG.

LIST OF MATERIAL

	QTY REQD	ITEM	CAT NO	DESCRIPTION	MATERIAL OR SOURCE	
*	1	21	CAT# T-603-1	FRONT FERRULE 1/8" TUBE		A
*	1	20	CAT# T-604-1	BACK FERRULE 1/8" TUBE		A
*	3	19	CAT# T-813-1	FRONT FERRULE 1/2" TUBE		A
*	3	18	CAT# T-814-1	BACK FERRULE 1/2" TUBE		A
*	2	17	CAT# T-1013-1	FRONT FERRULE 5/8" TUBE		A
*	2	16	CAT# T-1014-1	BACK FERRULE 5/8" TUBE		A
*	2	15	CAT# B8924Y14	PAD EYE WELDING 1"	SST.	B
*	2	14	CAT# SS-1010-C	CAP 5/8" TUBE	SWAGELOK	A
	3	13	CAT# SS-810-C	CAP 1/2" TUBE	SWAGELOK	A
	1	12	CAT# SS-600-C	CAP 1/8" TUBE	SWAGELOK	A
	1	11	147D4020 P11	TUBE 1/2" OD x .035 WALL	304 SST	
	1	10	P10	Coil Support		
	1	9	P9	TUBE 3/8 OD x .035 WALL	304 SST	
	1	8	P8	TUBE " " " "	" "	
	1	7	P7	TUBE 1/2" OD x .035 WALL	304 SST	
	2	6	P6	TUBE " " " "	" "	
	1	5	P5	TUBE " " " "	" "	
*	1	4	P4	TUBE 5/8" OD x .035 WALL	304 SST	
*	2	3	P3	TUBE " " " "	" "	
*	1	2	P2	TUBE " " " "	" "	
	1	1	147D4020 P1	BLIND FLANGE	304 SST	
	X			ASSEMBLY		

UNLESS OTHERWISE SPECIFIED DIMENSIONS ARE IN INCHES
TOLERANCES ON:
2-PLACE DECIMALS ± .02 ALL SURF. ✓
3-PLACE DECIMALS ±
ANGLES ± 1/2°
FRACTIONS ± 1/16"
MATERIAL AS NOTED

	NAME	DATE
DRAWN	P.R. ELLIS	8 7 78
CHECKED		
ENGR APPR.	P.R. Ellis	8 7 78
MFG APPR.		
Q.A.		
COMM'L APPR.		

GENERAL ELECTRIC
AEP DEPT. EVENDALE OHIO

FLUID DISTRIBUTOR SYSTEM

3X HEAT STORAGE TANK

SIZE	CODE IDENT NO.		REV
D	17232	147D4020	A

SCALE 3/8"=1" SHEET

147D4020 G1 | 709E931 G1
IDENT. NO. | NEXT ASSY

FIGURE 3

APPENDIX A

SYLTHERM™ PROPERTIES

750°F	μ	= .6292 lb/Fthr	450°F	μ	= 1.98
	ρ	= 37.02 lbs/Ft^3 (.593 qm/cc)		ρ	= 47 (.753 qm/cc)
	k	= .06375 BTU/Fthr°F		k	= .070
	C_p	= .525 BTU/lb°F		C_p	= .465
	P_r	= 5.18		P_r	= 13.75
	σ	= 3.5 dyne/cm		σ	= 9.4 dyne/cm
500°F	μ	= 1.585	350°F	μ	= 3.27
	ρ	= 45.26 (.725 qm/cc)			= 50 (.801 qm/cc)
	k	= .0691		k	= .0718
	C_p	= .475		C_p	= .445
	P_r	= 10.9		P_r	= 20.27
	σ	= 8 dyne/cm		σ	= 12 dyne/cm
625°F	μ	= .97	400°F	μ	= 2.52
	ρ	= 41.2 (.66 qm/cc)		ρ	= 48.4 (.775 qm/cc)
	k	= .0668		k	= .0709
	C_p	= .50		C_p	= .455
	P_r	= 7.33		P_r	= 16.17
	σ	= 5.5 dyne/cm		σ	= 10.6 dyne/cm
Room Temp.	μ	= 21.8 lb/Fthr			
	ρ	= 58.3 lbs/Ft^3 (.934 qm/cc)			
	k	= .078			
	C_p	= .395			
	P_r	= 110.4			
	σ	= 20 dyne/cm			

REVISIONS

1 | 7/11/79 P&LR INC EWH 79-07-110 LSE

OPERATION

Steam Generator operating ranges, limits, setpoints, and setpoint tolerances are as follows:

a.	Steam Flow	0 - 10500 lb/hr
b.	Steam Temperature (Superheated Mode)	720°F (+25°, - 70°)
c.	Steam Pressure Setpoint/ Tolerance (Saturated Mode)	700 psig/ ± 2 psig
d.	Steam Pressure Setpoint/ Tolerance (Saturated Mode)	110 psig/ ± 2 psig
e.	Steam Purity	99.5%
f.	Maximum total solids carryover	1ppm
g.	S-800 Inlet Pressure	50 psig $\begin{cases} +15 \\ -5 \end{cases}$
h.	S-800 Inlet Temp.	685° - 750°F
i.	S-800 Outlet Temp.	475°-525°F.
J.	S-800 ΔT	200°F Minimum
k.	S-800 Pressure Drop	12 psi Max.
l.	Feedwater Inlet Temp.	338°F ± 4°F
m.	Feedwater Inlet Pres.	850 psig (max)
n.	Blowdown Flow	1-5% of Feedwater Flow (± 1/4%)
o.	Blowdown Water Discharge Temp.	80°F. (max)
p.	Flash Tank Operating Pressure	105 psig ± 5
q.	Shell Side Fouling Resistance	.001 Water/.0005 Steam (max)
r.	Tube Side Fouling Resistance	.001 (max)
s.	Tube Side Design Pres./Temp	150 psig/750°F
t.	Shell Side Design Pres./ Temp. Preheater & Steam Generator	750 psig/550°F
u.	Superheater.	750 psig/750°F
	Nitrogen Supply Pressure	1-5 psig

2.2.2 PHYSICAL

All components comprising the steam generating unit shall be mounted on a common steel skid base. Maximum envelope dimensions are 20'L x 10'H x 4'W. S-800 valves shall be mounted with stems horizontal to prevent leakage from soaking into insulation.

STE/PC-5

PRINTS TO

REVISIONS

1 | 7/11/78 PC&R INC EWH 79-07-110 LSE

OPERATION

Steam Generator operating ranges, limits, setpoints, and setpoint tolerances are as follows:

a.	Steam Flow	0 - 10500 lb/hr
b.	Steam Temperature (Superheated Mode)	720°F (+25°, - 70°)
c.	Steam Pressure Setpoint/ Tolerance (Saturated Mode)	700 psig/ ± 2 psig
d.	Steam Pressure Setpoint/ Tolerance (Saturated Mode)	110 psig/ ± 2 psig
e.	Steam Purity	99.5%
f.	Maximum total solids carryover	1ppm
g.	S-800 Inlet Pressure	50 psig $\begin{cases} +15 \\ -5 \end{cases}$
h.	S-800 Inlet Temp.	685° - 750°F
i.	S-800 Outlet Temp.	475°-525°F.
j.	S-800 ΔT	200°F Minimum
k.	S-800 Pressure Drop	12 psi Max.
l.	Feedwater Inlet Temp.	338°F ± 4°F
m.	Feedwater Inlet Pres.	850 psig (max)
n.	Blowdown Flow	1-5% of Feedwater Flow (± 1/4%)
o.	Blowdown Water Discharge Temp.	80°F. (max)
p.	Flash Tank Operating Pressure	105 psig ± 5
q.	Shell Side Fouling Resistance	.001 Water/.0005 Steam (max)
r.	Tube Side Fouling Resistance	.001 (max)
s.	Tube Side Design Pres./Temp	150 psig/750°F
t.	Shell Side Design Pres./ Temp. Preheater & Steam Generator	750 psig/550°F
u.	Superheater.	750 psig/750°F
	Nitrogen Supply Pressure	1-5 psig

2.2.2 PHYSICAL

All components comprising the steam generating unit shall be mounted on a common steel skid base. Maximum envelope dimensions are 20'L x 10'H x 4'W. S-800 valves shall be mounted with stems horizontal to prevent leakage from soaking into insulation.

STE/PC-
PRINTS TO

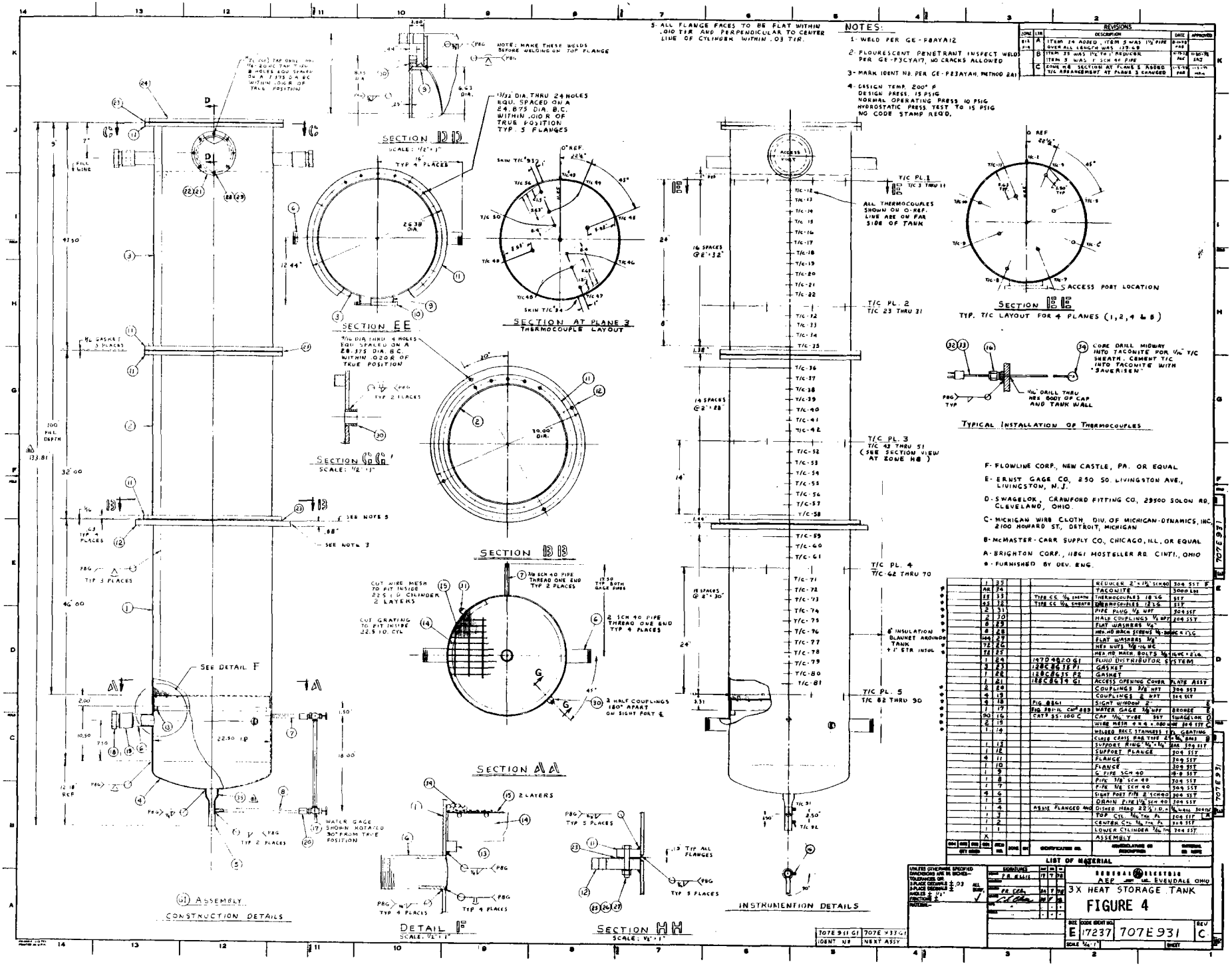
NOTES:
1- WELD PER GE - P8AYA12
2- FLOURESCENT PENETRANT INSPECT WELDS PER GE-P3CYA17, NO CRACKS ALLOWED
3- MARK IDENT NO. PER GE-P23AYAH, METHOD 2A1
4- DESIGN TEMP. 200° F
DESIGN PRESS. 15 PSIG
NORMAL OPERATING PRESS 10 PSIG
HYDROSTATIC PRESS TEST TO 15 PSIG
NO CODE STAMP REQ'D.
5- ALL FLANGE FACES TO BE FLAT WITHIN .010 T.I.R. AND PERPENDICULAR TO CENTER LINE OF CYLINDER WITHIN .03 T.I.R.
REVISIONS
SECTION EE
SECTION AT PLANE 2 THERMOCOUPLE LAYOUT
SECTION GG
SECTION HH
SECTION AA
SECTION FF
TYP. T/C LAYOUT FOR 4 PLANES (1, 2, 4 & 8)
ACCESS PORT LOCATION
TYPICAL INSTALLATION OF THERMOCOUPLES
CORE DRILL MIDWAY INTO TACONITE FOR 1/16" T/C SHEATH. CEMENT T/C INTO TACONITE WITH "SAUERISEN"
1/16" DRILL THRU HEX BODY OF CAP AND TANK WALL
T/C PL. 1 T/C 1 THRU 11
T/C PL. 2 T/C 23 THRU 31
T/C PL. 3 T/C 43 THRU 51 (SEE SECTION VIEW AT ZONE H8)
T/C PL. 4 T/C 62 THRU 70
T/C PL. 5 T/C 82 THRU 90
ALL THERMOCOUPLES SHOWN ON O-REF. LINE ARE ON FAR SIDE OF TANK
6" INSULATION BLANKET AROUND TANK + 1" STR INSUL
SEE DETAIL F
SEE NOTE 5
SEE NOTE 3
F- FLOWLINE CORP., NEW CASTLE, PA. OR EQUAL
E- ERNST GAGE CO, 250 SO. LIVINGSTON AVE., LIVINGSTON, N.J.
D- SWAGELOK, CRAWFORD FITTING CO, 29500 SOLON RD, CLEVELAND, OHIO.
C- MICHIGAN WIRE CLOTH DIV. OF MICHIGAN-DYNAMICS, INC. 2100 HOWARD ST., DETROIT, MICHIGAN
B- McMASTER-CARR SUPPLY CO., CHICAGO, ILL., OR EQUAL
A- BRIGHTON CORP., 11861 MOSTELLER RD. CINTI., OHIO
* - FURNISHED BY DEV. ENG.
LIST OF MATERIAL
(1) ASSEMBLY CONSTRUCTION DETAILS
DETAIL F
INSTRUMENTION DETAILS
BENDIX ELECTRONICS AEP AVENDALE OHIO
3X HEAT STORAGE TANK
FIGURE 4
707E931 C
E 17237

FIG. 4A T.C. LOCATIONS IN 5 PLANES

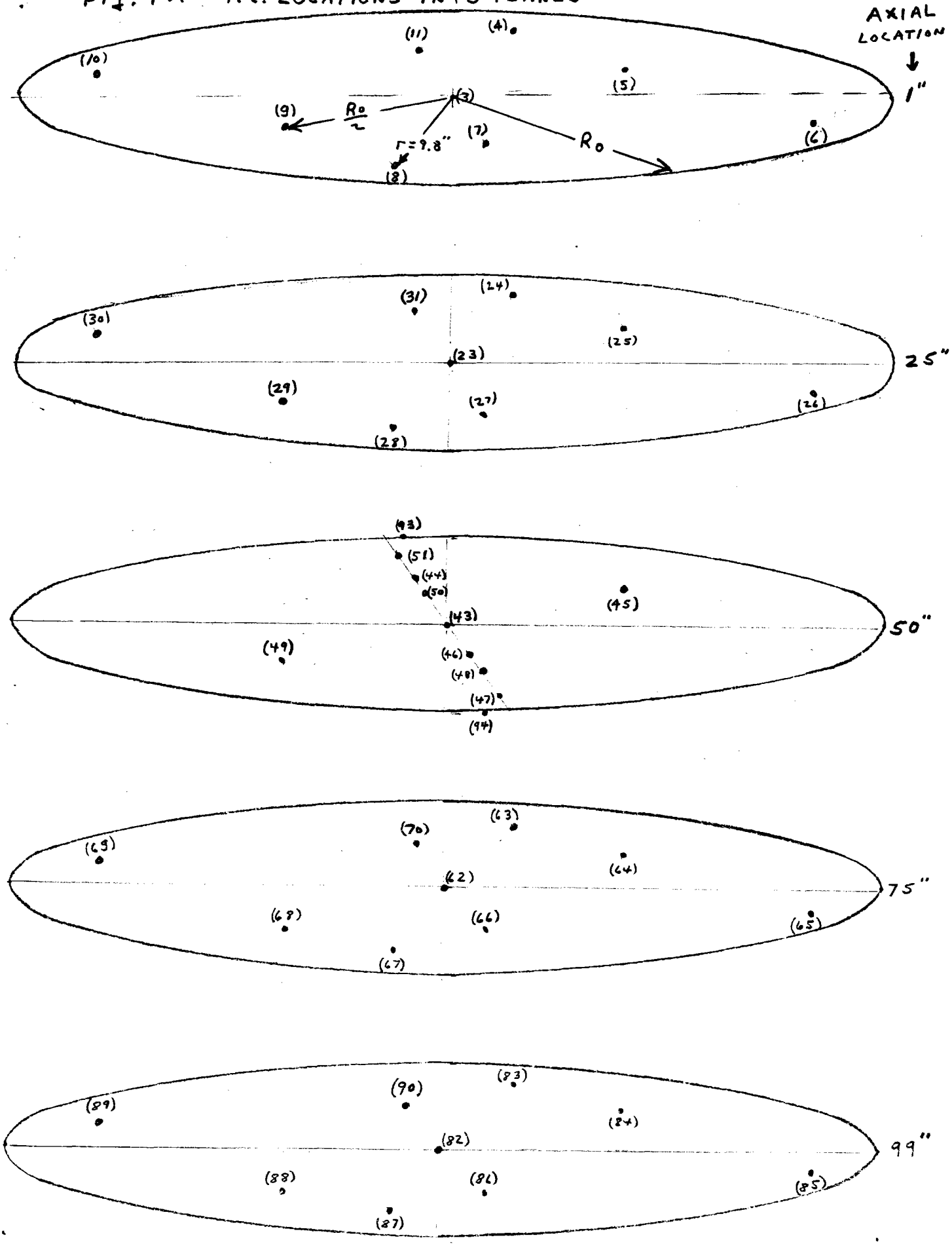

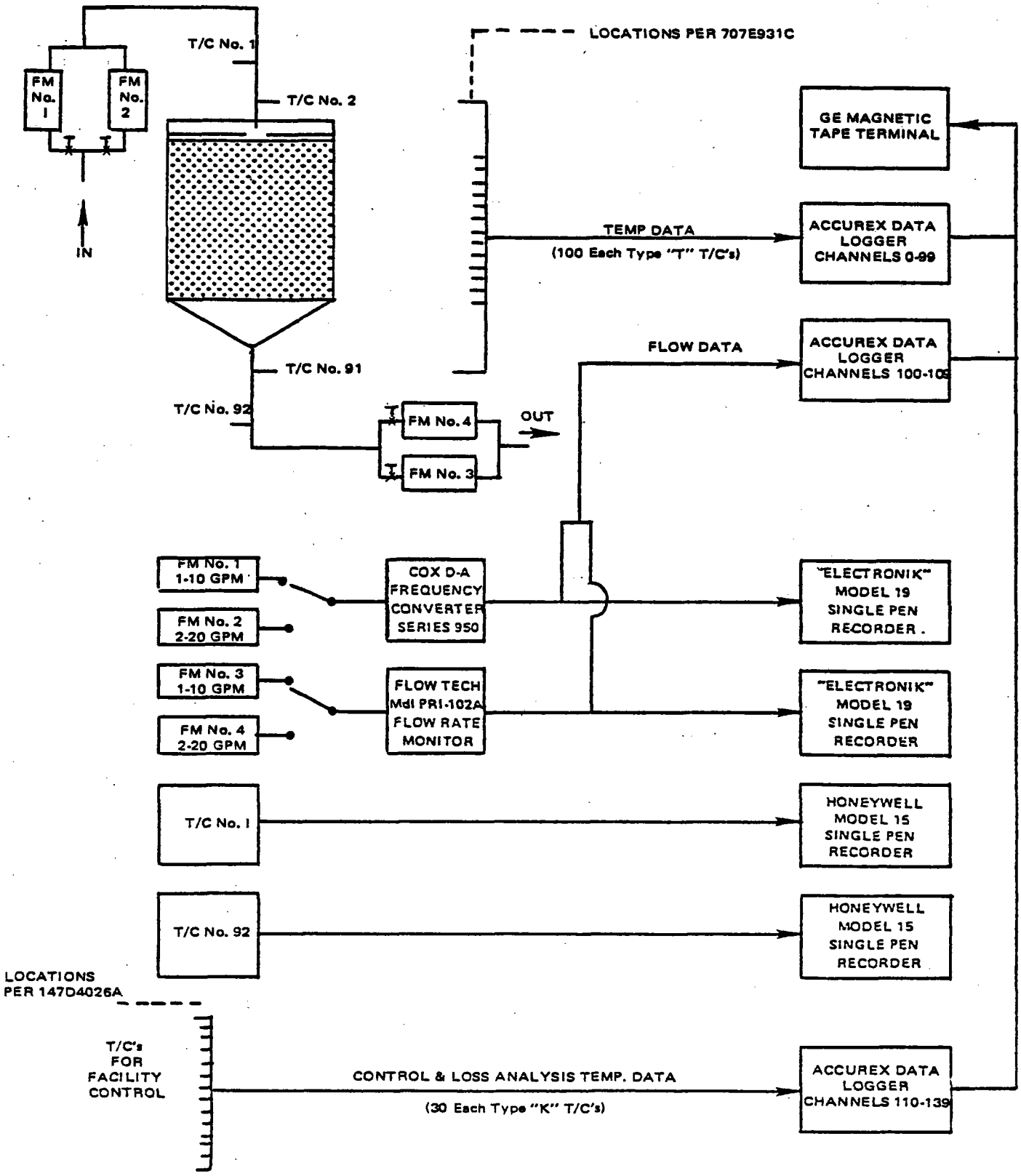

Figure 5 . Instrumentation Schematic for Extended Column TES Experiment

4. Test Program

The primary objectives of the test were (1) to obtain axial and radial temperature distributions through the bed as a function of time for a range of flow rates to simulate the full scale system, (2) to determine static and dynamic liquid holdups, (3) to obtain temperature distribution during the holding and inversion modes.

To accomplish the best simulation, it was judged that the Reynolds number was the most significant parameter that should be matched. The test flow rates were then selected to cover the Reynolds number range of the full scale system. This matching is shown in Table 1 for the charging and discharging tests. It is also seen from the Table that the Reynold matching combined with the selected operating temperature range provides a good simulation of the heat flux parameter ($\frac{MC_p\Delta T}{A}$). From this comparison, the specific points for the planned test program to cover the required range were selected and shown in Table 2. The actual tests deviated only slightly from the plan, as follows: test run #2, the actual flow rate was 4 GPM (determined by recalibration of the flow meter after this test) instead of 3.5 GPM, and the charging temperature was 430^{o}F; run #4, the actual flow rate was 17.2 GPM instead of 16.5 GPM (increased to extend the upper range since later inputs indicated flow rates slightly over 400 GPM were possible in the full scale system), the inversion test was run at 8 GPM. In addition full charge and discharges were not achieved because of insufficient fluid capacity in the batch holding tanks. The procedure for the operation is shown in Table 3.

TABLE 1

REYNOLDS NUMBER SUMMARY FOR EXTENDED COLUMN TEST POINTS AT MAX & MIN. STEP FLOW CONDITIONS

Shenandoah STE-LSE				REYNOLDS NUMBER	Extended Column Test			
Flow Rate (gpm)	Inlet Temp. (^oF)	Mass Flux $\frac{lb/hr}{ft^2}$ M/A	Heat Flux $\frac{Btu/hr}{ft^2}$	$\frac{DG}{\mu}$	Flow Rate (gpm)	Inlet Temp. (^oF)	Mass Flux $\frac{lb/hr}{ft^2}$ M/A	Heat Flux $\frac{Btu/hr}{ft^2}$
Charging			$\frac{M}{A} C_p \Delta T$					$\frac{M}{A} C_p \Delta T$
Small Tank (Dia = 13.0')					Storage Tank (Dia = 22.5")			
50	750	112	14,000	3.6	2.1	450	283	13,200
198	750	443	55,400	14.3	8.4	450	1144	52,600
387 (403)	750	877	109,000	28.1	16.5 (17.2)	450	2248	103,400
Large Tank (Dia = 20.6')								
50	750	44.5	5,560	1.4	.84	450	114	5,260
198	750	176	22,000	5.7	3.3	450	456	21,000
387 (403)	750	347	43,400	11.2	6.6	450	896	41,200
Discharging								
Small Tank								
50	500	137	17,100	4.4	2.4	350	352	16,200
198	500	542	67,800	17.4	9.6	350	1400	64,400
Large Tank								
50	500	54	6,800	1.8	.96	350	140	6,400
198	500	216	27,000	7.0	3.8	350	557	25,600

$\bar{\mu}$, viscosity, @625^{o}F = .97 lb/Ft hr
@400^{o}F = 2.5

TABLE 2
EXTENDED COLUMN TEST PROGRAM SUMMARY

Activity					Comments
Static Holdup Evaluation					Room Temperature Test accomplished after initial filling of bed
Dynamic Hold-up Tests					Hot circulation tests at .9, 8, and 16.5 gpm
Charging-Discharing and Holding Loss	CHARGING		DISCHARGING		
	Run No.	Rate (gpm)	Rate (gpm)	Holding Time	
Full charge/discharge	1	0.9	0.9	Minimum	
Full charge/discharge	2	3.5(4.0)	3.5	"	
Full charge/discharge	3	8.0	9.6	"	
Full charge/discharge	3(a)	8.0	9.6 at 1 psig		
Full charge/discharge	4	16.5(17.2)	9.6	6 hours	
50% Discharge/hold	5	3.5	3.5	6 hours	
50% Charge/hold	6	3.5	3.5	6 hours	
Inversion	7	3.5 (8 gpm)			

TABLE 3

OPERATIONAL PROCEDURE FOR CHARGING-DISCHARGING EVALUATION

PROCEDURE SEQUENCE	COMMENTS	FLOW SCHEMATIC
PRELIMINARY WARM-UP		
1. BATCH OIL HEAT UP TO 350°F	OIL CIRCULATES IN SOURCE TANK - HEATER LOOP	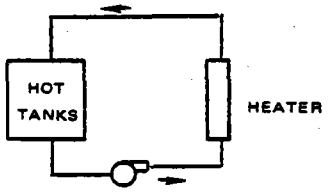
2. ORE TANK HEAT UP TO 350°F	OIL CIRCULATES IN SOURCE TANK - HEATER- ORE TANK LOOP. BOTH PUMPS REQUIRED	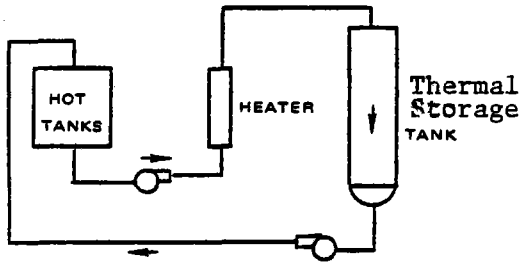
3. BATCH OIL HEAT UP TO 450°F	OIL CIRCULATES IN SOURCE TANK - HEATER LOOP	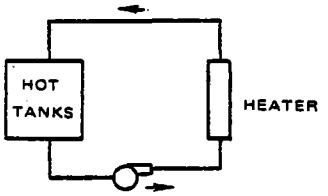
CHARGING RUN		
4. 450°F OIL PUMPED THRU ore BED TO SINK TANKS	ENTIRE HOT OIL INVENTORY PUMPED THRU ORE BED AT DESIRED RATE. SCAVENGE PUMP TRANSFER OIL TO COLD TANKS	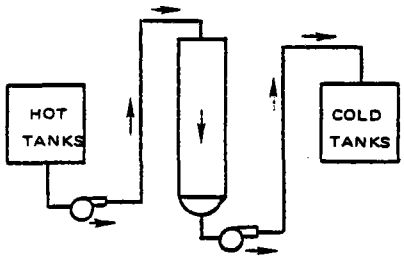
HOLDING LOSS EVALUATION		
5. RECORD ORE BED TEMPERATURE PROFILE	AUTOMATIC DATA LOGGER WILL RECORD KEY ORE BED AND TEST FACILITY TEMPERATURES	STATIC TEST
PRE-DISCHARGE STABILIZATION		
6. BATCH OIL TEMPERATURE STABILIZATION AT 350°F	OIL CIRCULATES FROM SINK TANK THRU HEATER OR COOLER AS NECESSARY TO ESTABLISH 350°F	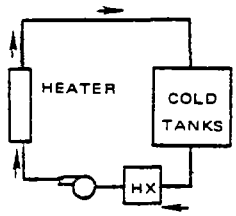
DISCHARGE RUN		
7. 350°F OIL PUMPED THRU ORE BED TO SOURCE TANKS	ENTIRE OIL INVENTORY PUMPED THRU ore BED AT DESIRED RATE. SCAVENGE PUMP TRANSFERS OIL TO HOT TANKS	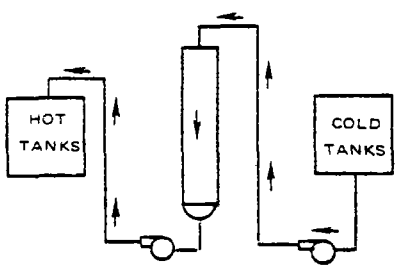

STATIC HOLDUP

VOID FRACTION

DYNAMIC HOLDUP

5.0.1 STATIC HOLDUP AND VOID FRACTION

Static Holdup

Knowledge of the bed static holdup is necessary to calculate system fluid inventory requirements and to calculate fluid make-up rates due to fluid degradation. The static holdup consists of (1) fluid clinging to the surface of individual particles, (2) fluid held at the inter-particle contact areas, and (3) fluid held in the particle pore structure.

The static holdup was determined at room temperature by filling the dry bed with a measured quantity of Syltherm oil and then draining the bed and measuring the quantity drained. The calculated holdup was 4.8% of the bed weight. This was translated into a fluid volume per unit of bed volume and is plotted in figure 1 along with a correlation from Ref. (1). The value is in good agreement with the extrapolated curve for porous particles. From independent measurements made on single bed particles the internal particle porosity is known to be 15%. The EÖTVÖS number, which contains the fluid density, surface tension and particle diameter, was calculated at 500°F and 750°F and the extrapolated curve used to determine the static holdup for the full scale system. These correspond to 7.6% at 500°F and 4.6% at 750°F for particles in the range from 3/8 to ½".

Void Fraction

At the same time the static holdup was measured the bed void fraction was also determined from the known quantity of fluid input and drained from the bed. The void fraction was determined to be 40%. Details of the static holdup and void fraction determination are in Ref. (2).

Ref. (1) Int. Chem. Eng., Vol 17, No. 1, Jan. 1977
Ref. (2) S. Abujawdeh - U-LSE PhIV-193(VIF) PIR 79-1-3 (Evendale)

FIG. 1 STATIC HOLDUP

359 — 125

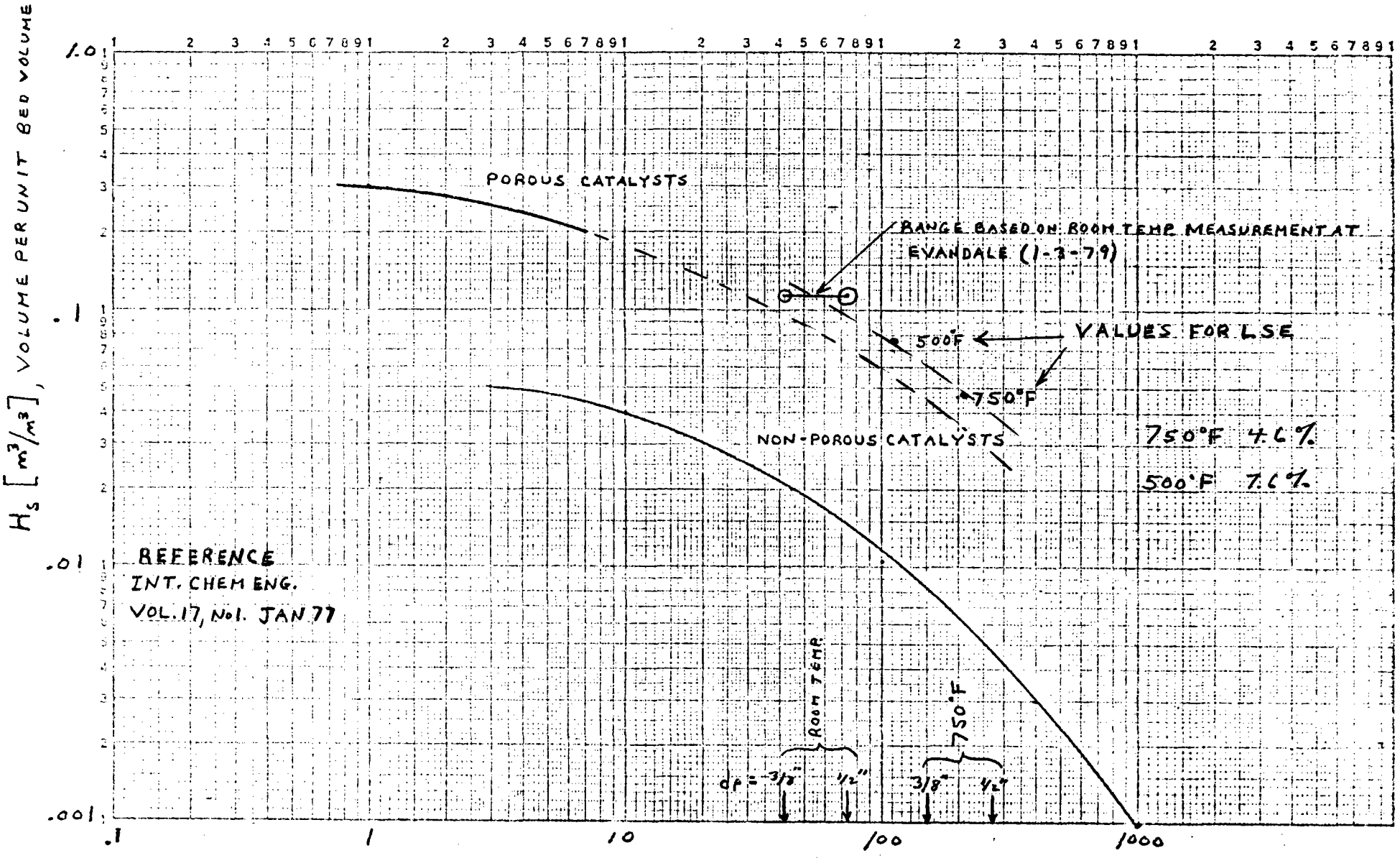

EÖTVÖS NUMBER – $E\ddot{o} = \frac{\rho_L g d^2}{\gamma_L}$

Dynamic Holdup

Dynamic holdup is that portion of the total fluid holdup in the bed under flow conditions which drains from the bed after flow is stopped. Dynamic holdup is a function of flow rate and is needed to enable calculations of required fluid inventories, fluid residence time in the bed, and fluid make-up rates. Dynamic holdup was measured by circulating fluid through the bed at a constant flow rate; simultaneously closing the fluid inlet and outlet valves; then measuring the fluid level rise in the reservoir at the tank bottom. Dynamic holdup is defined as the fraction of bed voids filled and is correlated with the Reynold's number, Galileo number, surface area per unit volume, particle size and bed void fraction. Figure 2 shows the measured data in comparison with the values predicted from the correlation of reference (3). Agreement between theory and model is good at the higher flow rates and diverges at the lower rates. This is due to poorer fluid distribution at the lower flow rates which is discussed later. The dynamic holdup predictions for the large scale system are shown in figure 3.

From the dynamic holdup, the fluid residence time in the bed can be predicted as shown in figure 4. Direct observation of residence time was made at 3.5 and 15 GPM and is shown in figure 4. Residence time predictions for the full scale system are shown in figure 5.

Ref. (3) Ginnetto, Baldi, and Specchia - A.I.Ch.E.J. Nov. 1978

FIG. 2 DYNAMIC HOLDUP - 100 INCH COLUM TEST

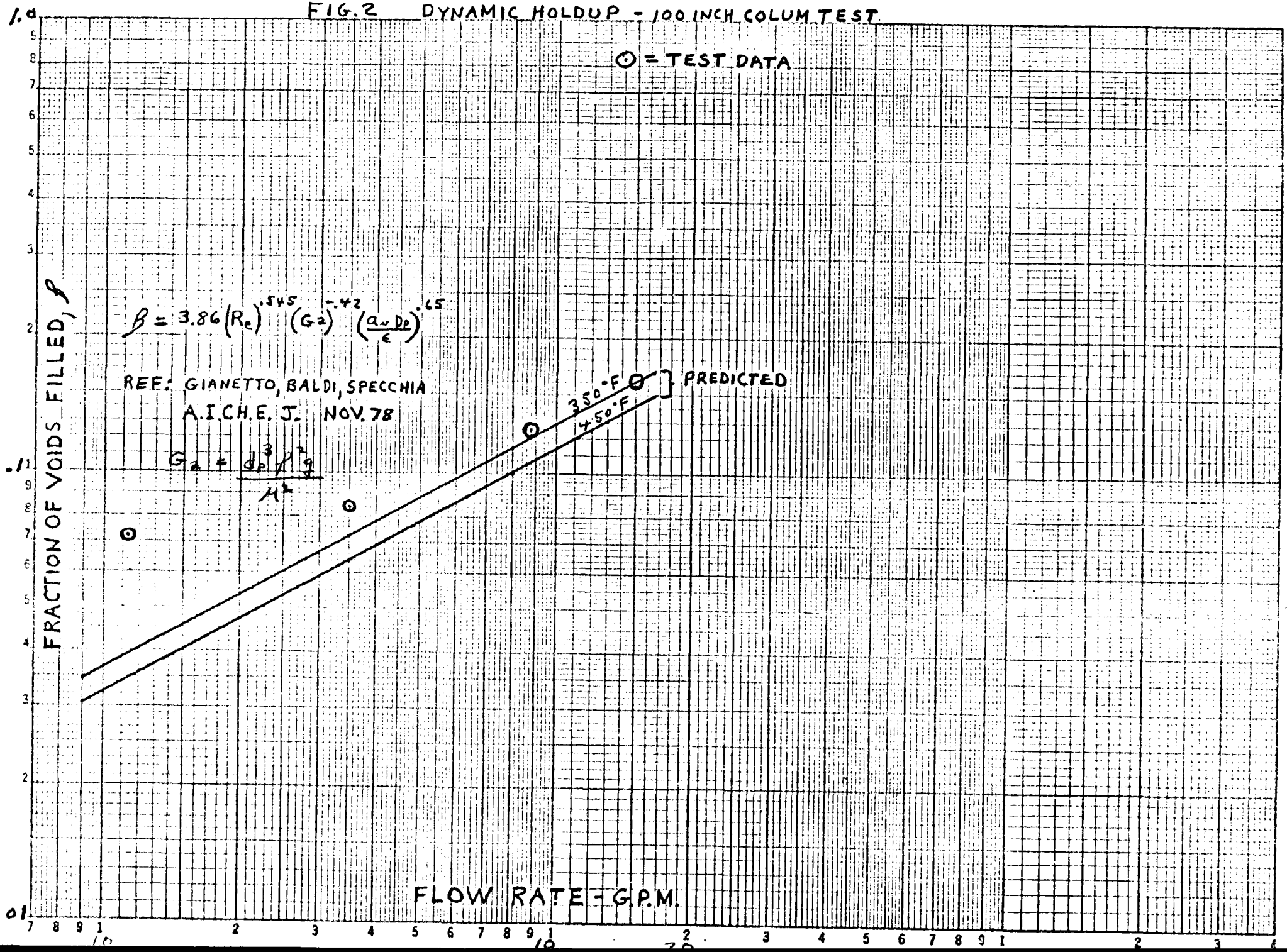

FIG. 3 DYNAMIC HOLDUP - STEP

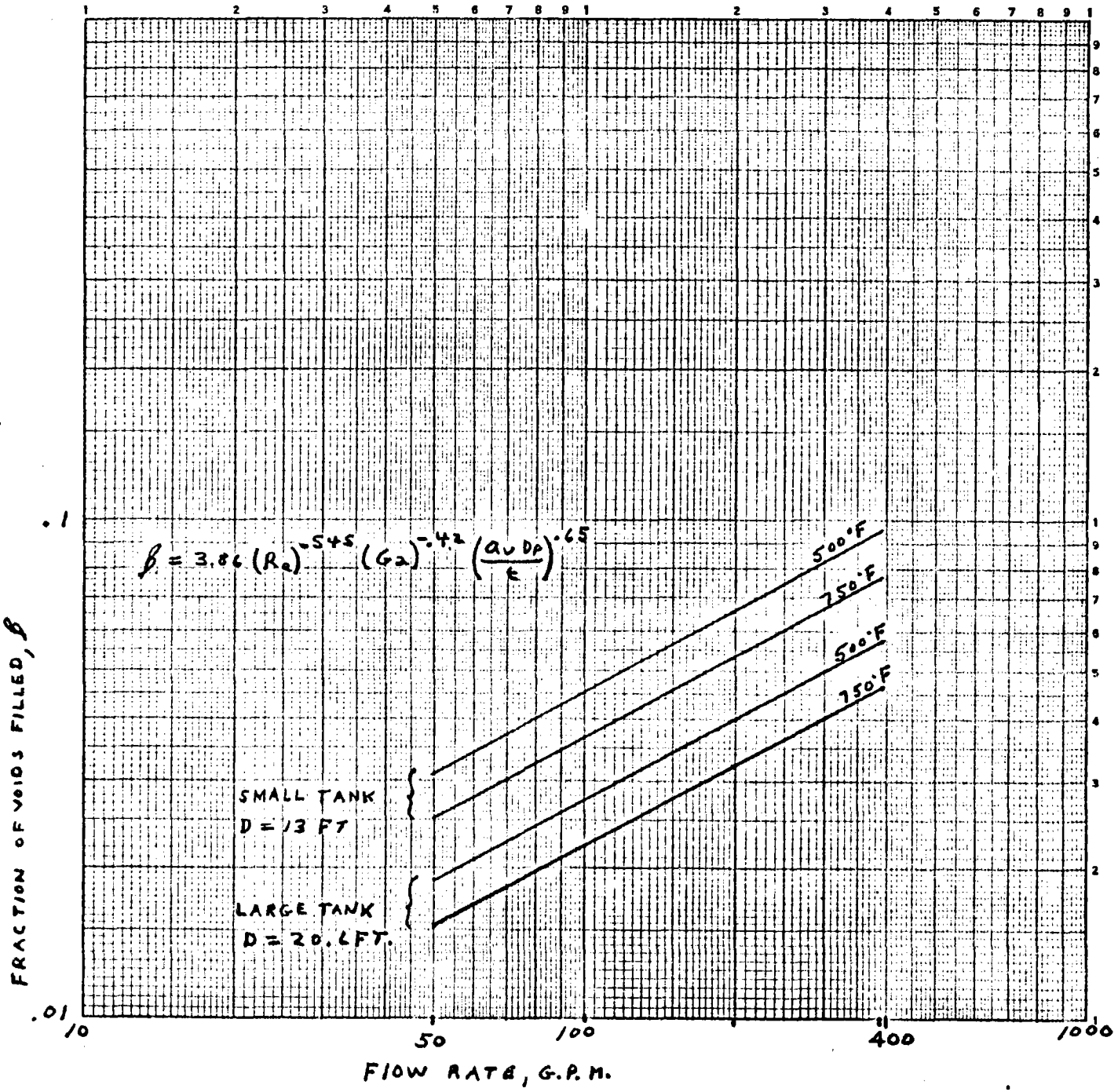

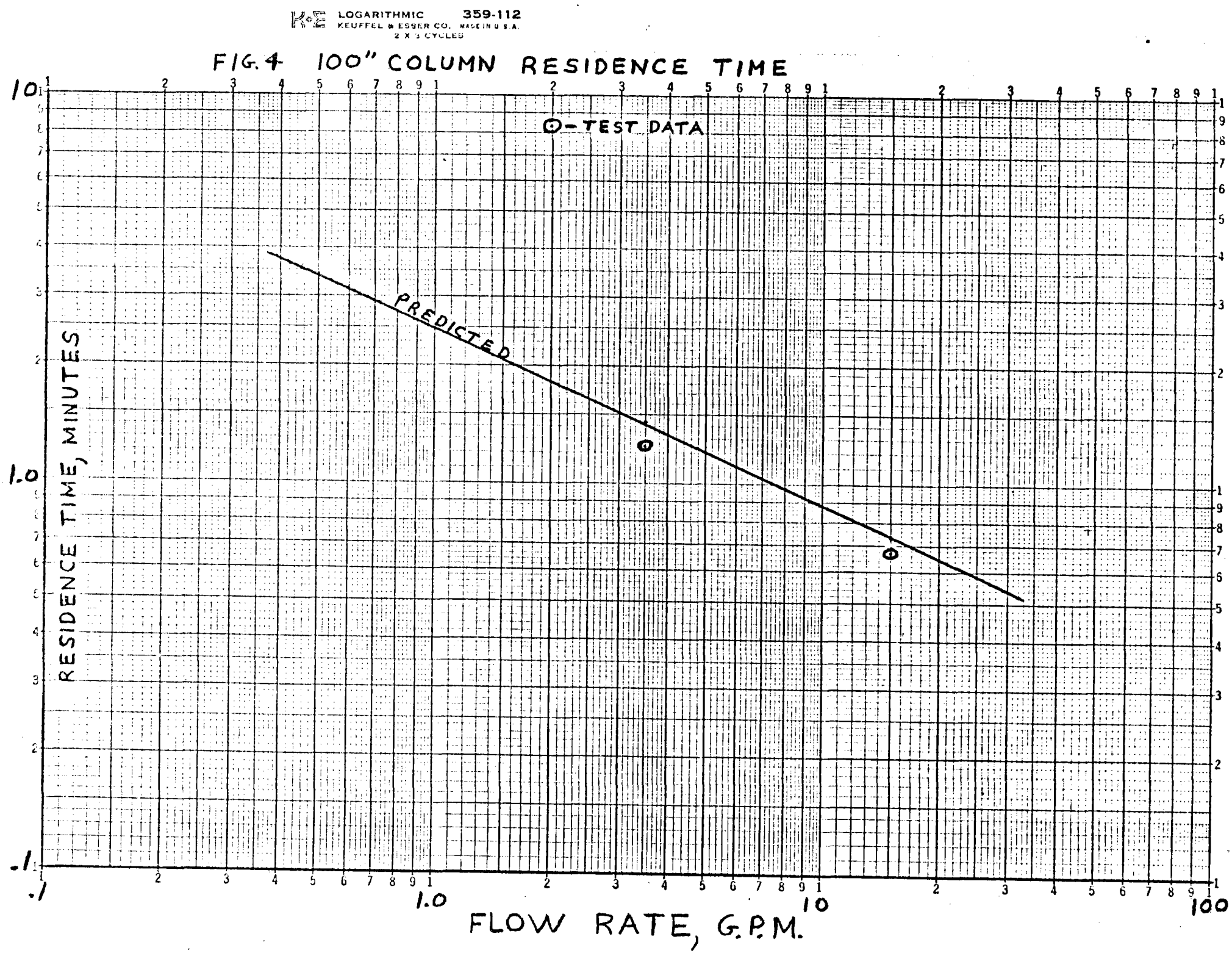
K&E LOGARITHMIC 359-112
KEUFFEL & ESSER CO. MADE IN U.S.A.
2 X 3 CYCLES
FIG. 4 100" COLUMN RESIDENCE TIME
⊙-TEST DATA
PREDICTED
RESIDENCE TIME, MINUTES
FLOW RATE, G.P.M.
10
1.0
.1
1.0
10
100

FIG. 5

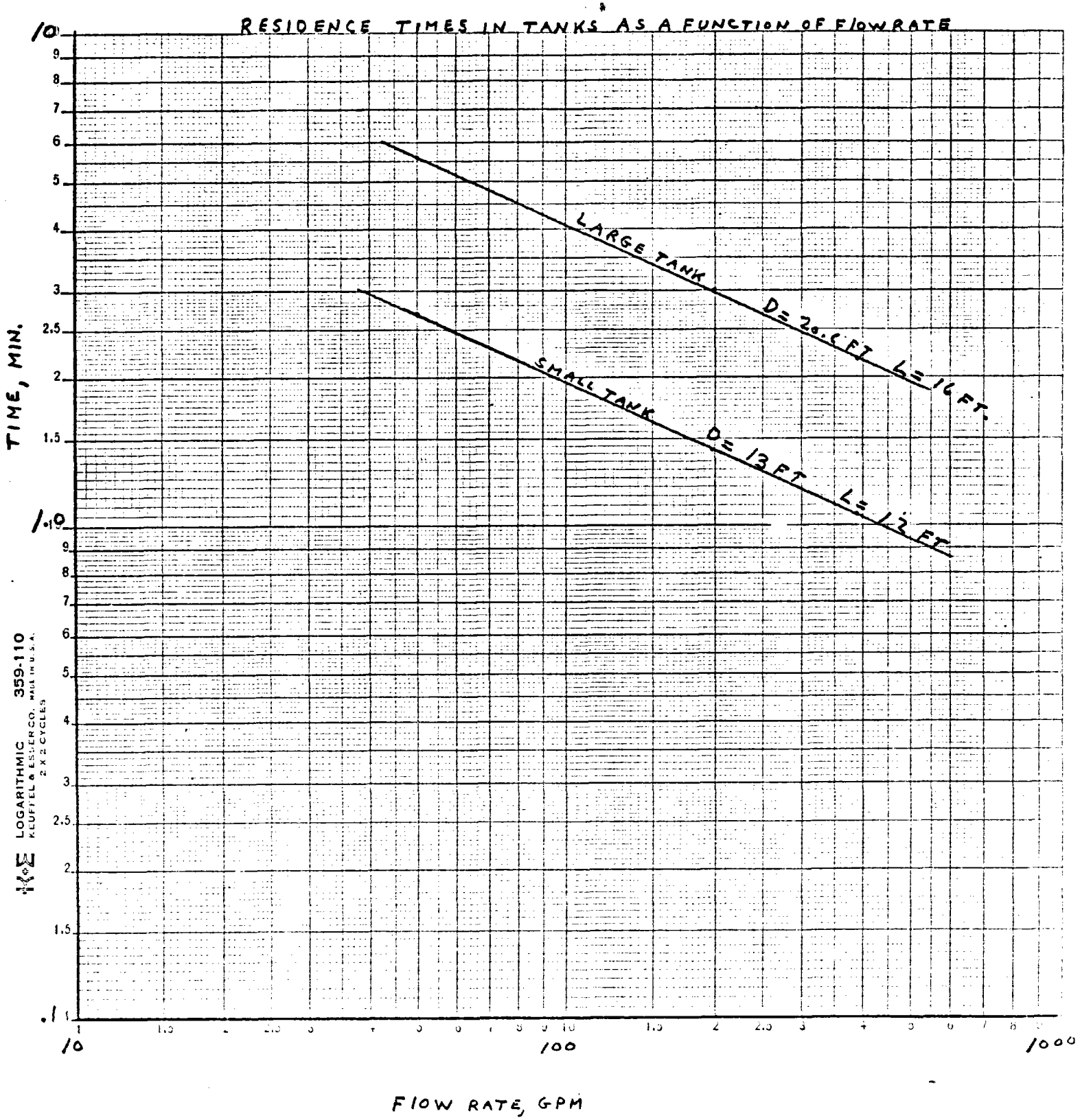
RESIDENCE TIMES IN TANKS AS A FUNCTION OF FLOWRATE
TIME, MIN.
FLOW RATE, GPM
LARGE TANK D= 20.6 FT L= 16 FT.
SMALL TANK D= 13 FT L= 12 FT.
LOGARITHMIC 359-110
KEUFFEL & ESSER CO. MADE IN U.S.A.
2 X 2 CYCLES

CHARGING TESTS

5.1 Charging Tests

Charging tests were run at flow rates of 17.2, 8, 4 and 0.9 GPM. This section shows the measured temperature profiles at the bed centerline as well as the radial temperature distributions which were measured at 5 locations in the bed. Also shown are the measured fluid exit temperatures as a function of time.

5.1.1 17.2 GPM Charge

Fig. 5.1 shows the temperature profiles measured along the bed centerline initially and for three times during the test, 5, 11 and 16 minutes. (The numbers along the top of the plot are the thermocouple identification numbers.)

Fig. 5.2 shows the initial radial temperature distribution. The initial radial gradient are $10^{o}F$ to $15^{o}F$ from the centerline to wall.

Fig. 5.3 shows the bed centerline temperature profile and the radial temperatures measured at the midpoint between the centerline and the wall ($r=\frac{Ro}{2}$). Also shown are a family of predicted curves from the model for heat transfer coefficients in the range from h to $\frac{h}{8}$. h is the theoretical heat transfer coefficient calculated in the model. A good fit to the data is shown in figure 5.4 for $\frac{h}{4}$= 25 BTU/Ft^2hr^oF. Fig. 5.5 again shows the bed centerline but also the temperature measured 1.4 inches ($r=9.8"$) from the wall. It is seen that $h=25$ is a reasonable duplication of the temperature axial gradient and off centerline temperature levels.

Fig. 5.6 shows the bed centerline profile and temperature at $\frac{RO}{2}$ for t=11 minutes, as well as the family of theoretical curves for a

range of heat transfer coefficients. Again $\frac{h}{4}$ or 25 BTU/Ft^{2}hr^{o}F is a good fit to the slope at the thermoclines, as shown in figure 5.7. Figure 5.8 shows the radial temperatures measured 1.4 inches from the wall along with the centerline temperatures. The slope of the $\frac{h}{4}$ curve is a reasonable fit. The limited number of thermocouples in the radial positions make it difficult to define the off centerline slopes with great certainty. But the charge efficiency is not a strong function of h in this flow rate range. For example, in charging a large tank, if h is in the range $\frac{h}{4}$ to $\frac{h}{8}$ the charge efficiency varies from 83% to 79%.

Figures 5.9 and 5.10 show the centerline and radial temperatures measured at $\frac{Ro}{2}$ and near the wall, respectively for t=16 minutes. Again $\frac{h}{4}$ is a reasonable fit to the slope of the thermoclines.

It has been seen in the plots presented, that there exist large radial temperature gradients in the bed during charging. Radial gradients to some degree are inherent in a trickle charge operation with a finite number of fluid distributor sources. In these tests the situation was aggravated by the fact that the fluid distribution rings tended to allow a greater flow per unit area in the outer rings. (See Section 5.6 for details.) This condition became more severe as the flow rate decreased till at 1 GPM the flow was almost entirely out of the outer rings. Consequently, as the fluid moves axially down the bed and spreads radially it's cooler fluid reaches the centerline, resulting in the lag in centerline temperatures which becomes more severe at the lower flow

rates. However, these radial gradients are washed out with time. Figure 5.11 shows the radial distribution at the plane near the top of the bed as a function of time. At t=o the spread in temperature was $14^{o}F$, after 29 seconds the spread increased to $60^{o}F$ then diminished till after 5 minutes the spread was only $5^{o}F$. Figures 5.12 and 5.13 show the spreads along the bed after charging at position $\frac{Ro}{2}$ and near the wall. (Complete charging of the bed was not achieved because of insufficient capacity in the 3 fluid holding tanks. In the charge runs a second smaller batch of fluid was heated to obtain a more fully charged bed for the discharge runs, however, complete charging was not achieved because of the time involved in reheating the entire batch back up to $450^{o}F$.) It is seen that the radial gradients diminish as charging proceeds. Figure 5.14 shows this phenomena at the 5 planes as a function of time. It is seen that the radial temperature spread goes through a maximum at each plane, and large gradients do not persist. This is particularly important because it means that in the trickle mode of operation, the series charging of the tanks will result in gradients in only the end of the last tank.

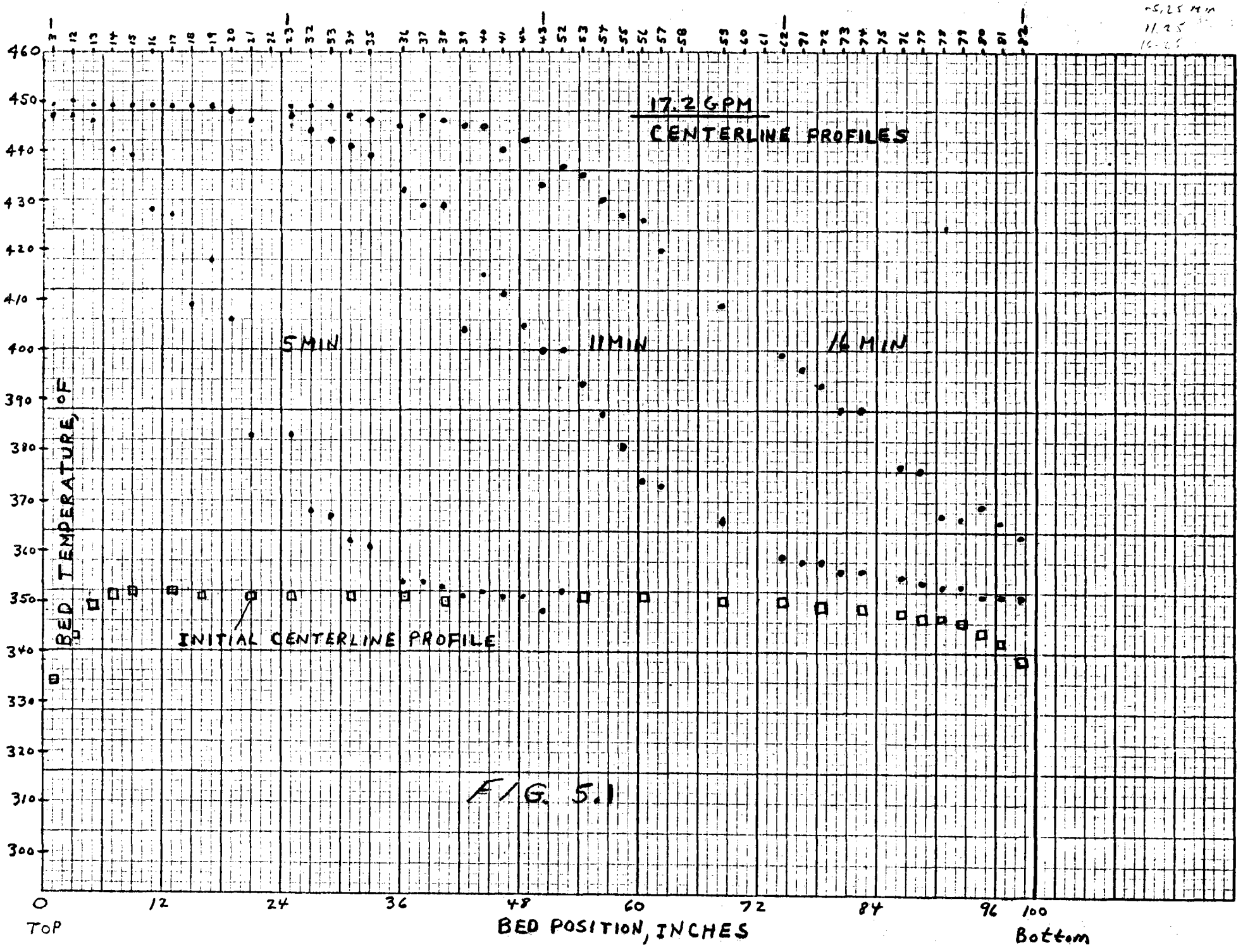

FIG. 5.1

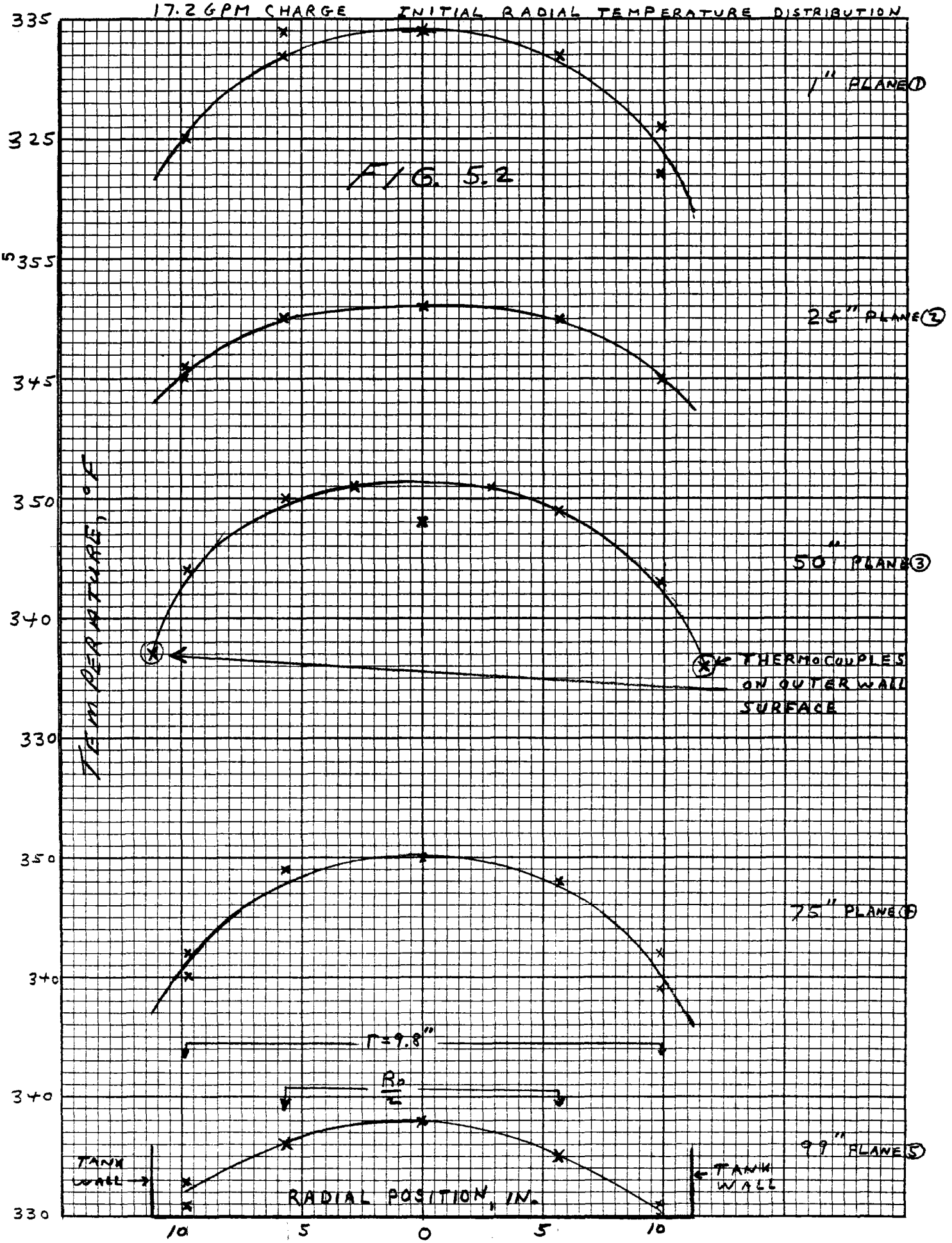
17.2 GPM CHARGE INITIAL RADIAL TEMPERATURE DISTRIBUTION
FIG. 5.2
1" PLANE ①
25" PLANE ②
50" PLANE ③
75" PLANE ④
99" PLANE ⑤
THERMOCOUPLES ON OUTER WALL SURFACE
TEMPERATURE, °F
335
325
355
345
350
340
330
350
340
340
330
r=9.8"
$\frac{R_b}{2}$
TANK WALL
TANK WALL
RADIAL POSITION, IN.
10
5
0
5
10

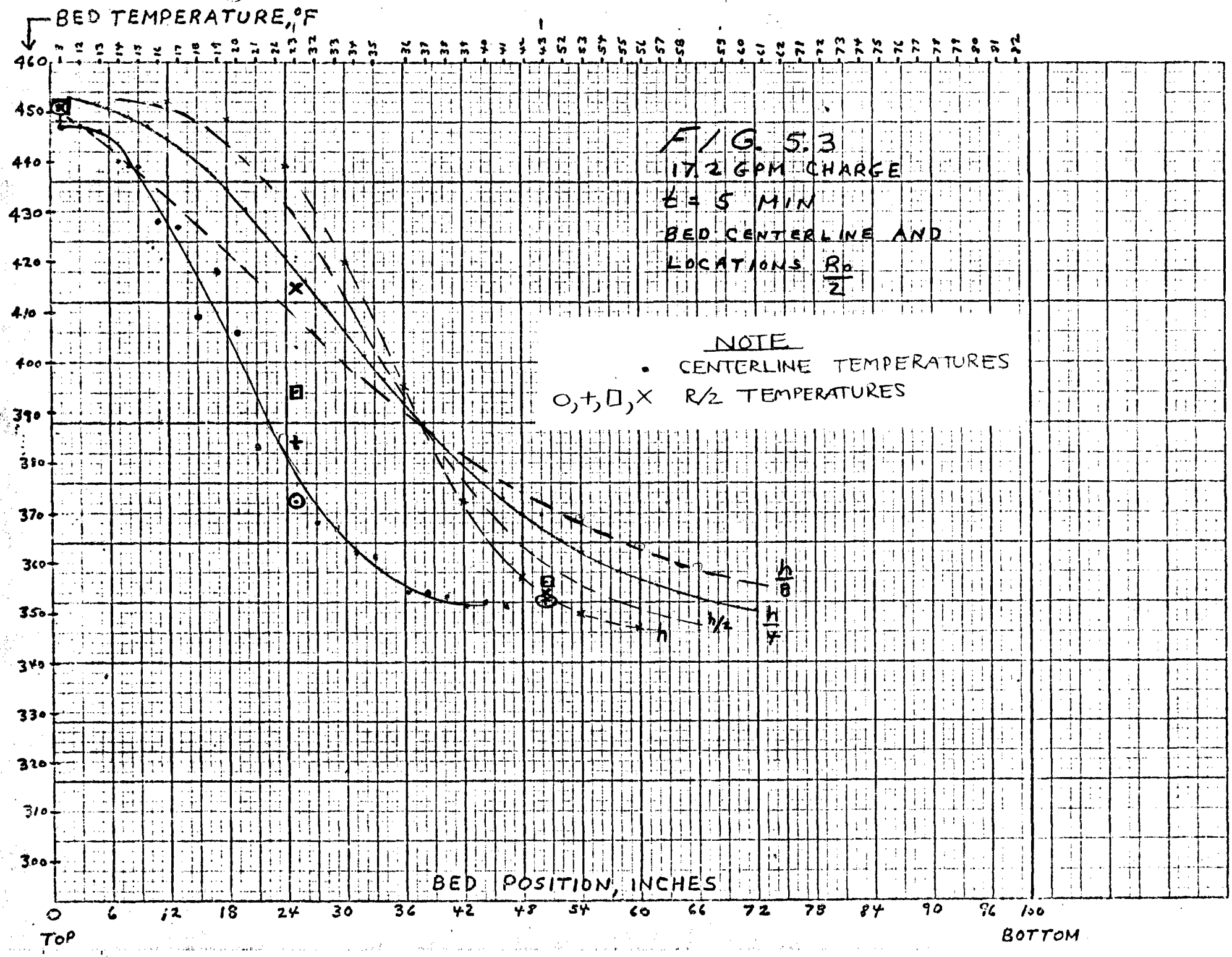
BED TEMPERATURE, °F
460
450
440
430
420
410
400
390
380
370
360
350
340
330
320
310
300
FIG. 5.3
17.2 GPM CHARGE
t = 5 MIN
BED CENTERLINE AND
LOCATIONS $\frac{R_o}{2}$
NOTE
• CENTERLINE TEMPERATURES
o, +, □, X R/2 TEMPERATURES
h/8
h/4
h/2
h
BED POSITION, INCHES
0
6
12
18
24
30
36
42
48
54
60
66
72
78
84
90
96
100
TOP
BOTTOM

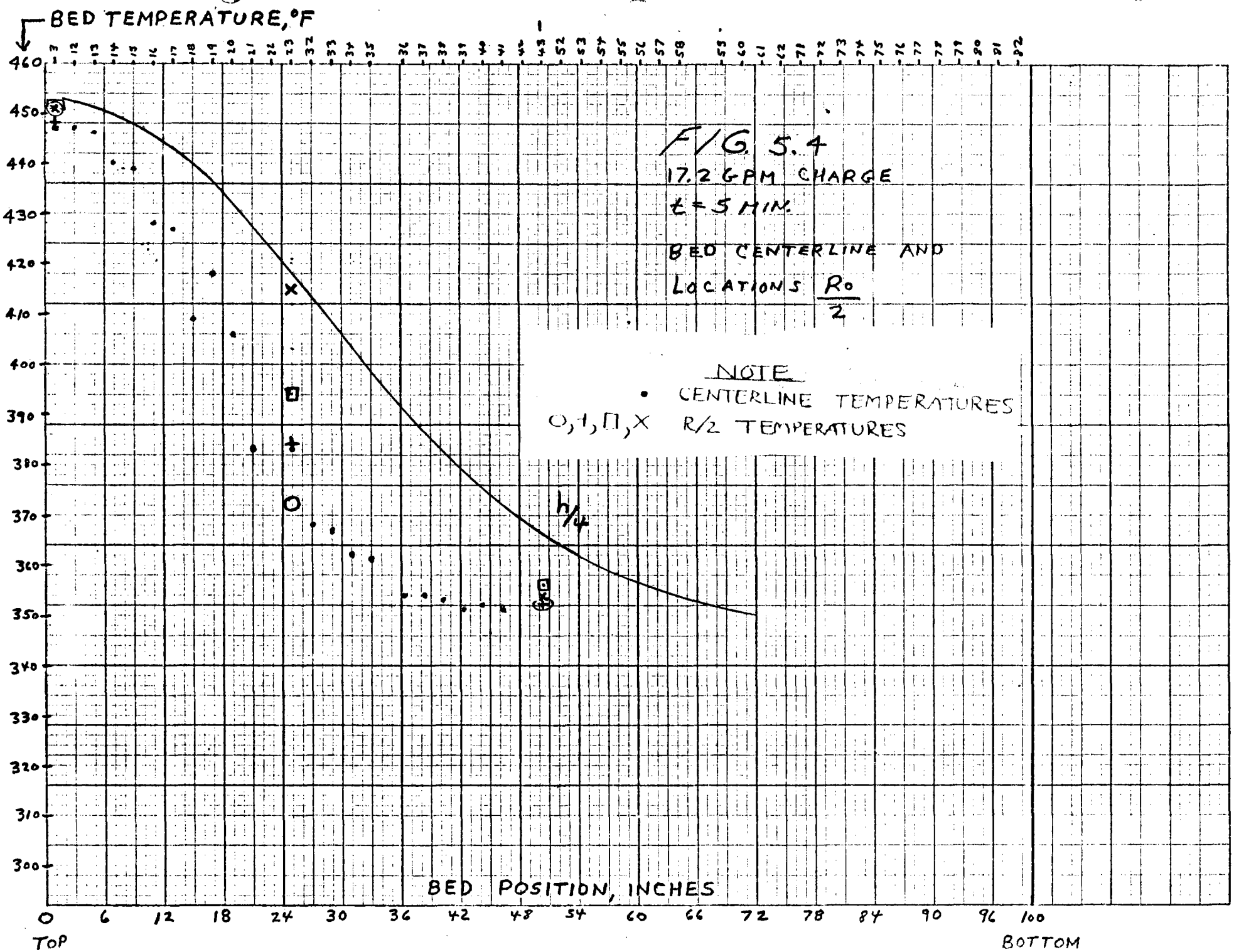
BED TEMPERATURE, °F
460
450
440
430
420
410
400
390
380
370
360
350
340
330
320
310
300
FIG. 5.4
17.2 GPM CHARGE
t = 5 MIN.
BED CENTERLINE AND
LOCATIONS Ro/2
NOTE
• CENTERLINE TEMPERATURES
O, 1, Π, X R/2 TEMPERATURES
h/4
BED POSITION, INCHES
0 6 12 18 24 30 36 42 48 54 60 66 72 78 84 90 96 100
TOP
BOTTOM

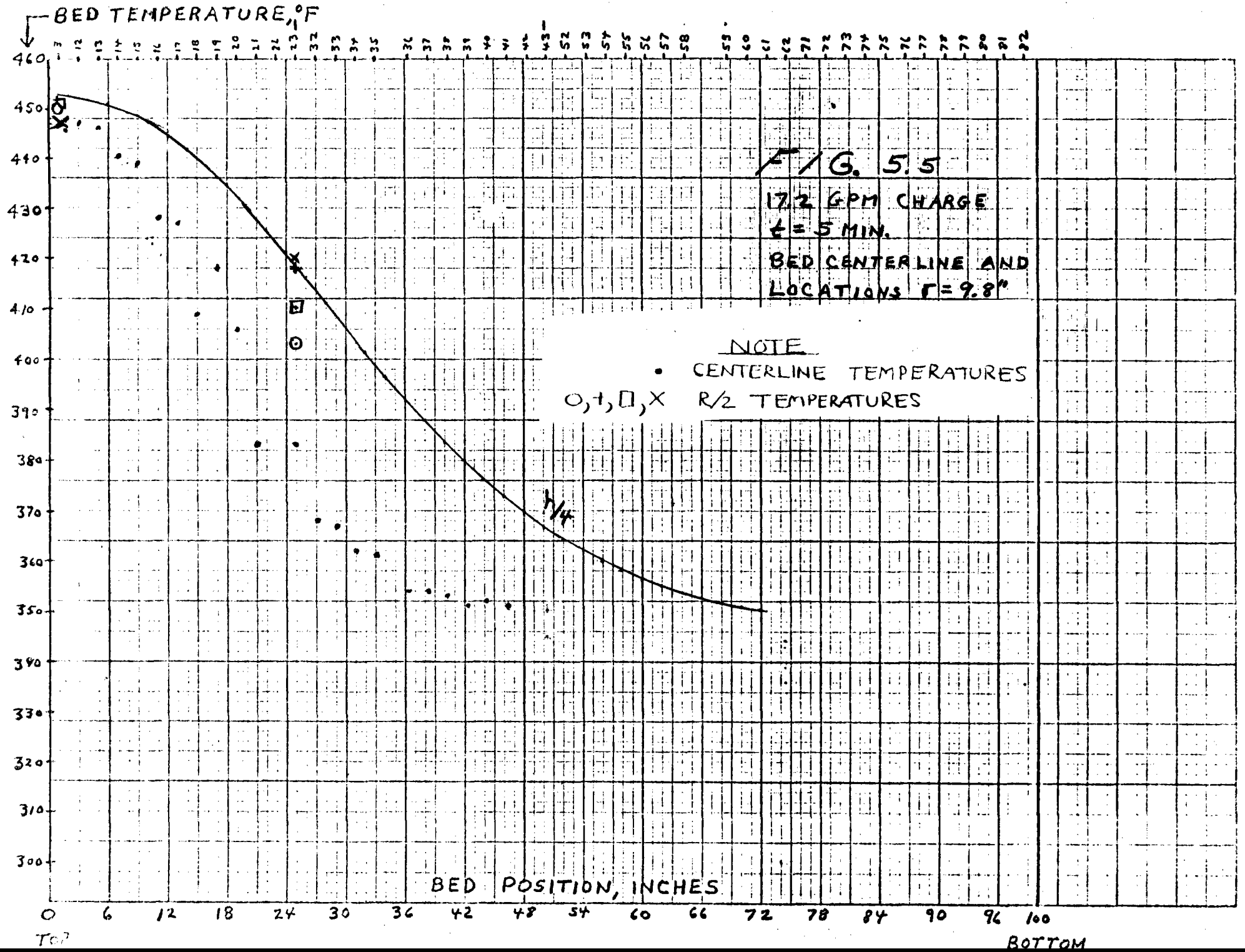
BED TEMPERATURE, °F
460
450
440
430
420
410
400
390
380
370
360
350
340
330
320
310
300
FIG. 5.5
17.2 GPM CHARGE
t = 5 MIN.
BED CENTERLINE AND
LOCATIONS r = 9.8"
NOTE
• CENTERLINE TEMPERATURES
O, +, □, X R/2 TEMPERATURES
R/4
BED POSITION, INCHES
0
6
12
18
24
30
36
42
48
54
60
66
72
78
84
90
96
100
TOP
BOTTOM

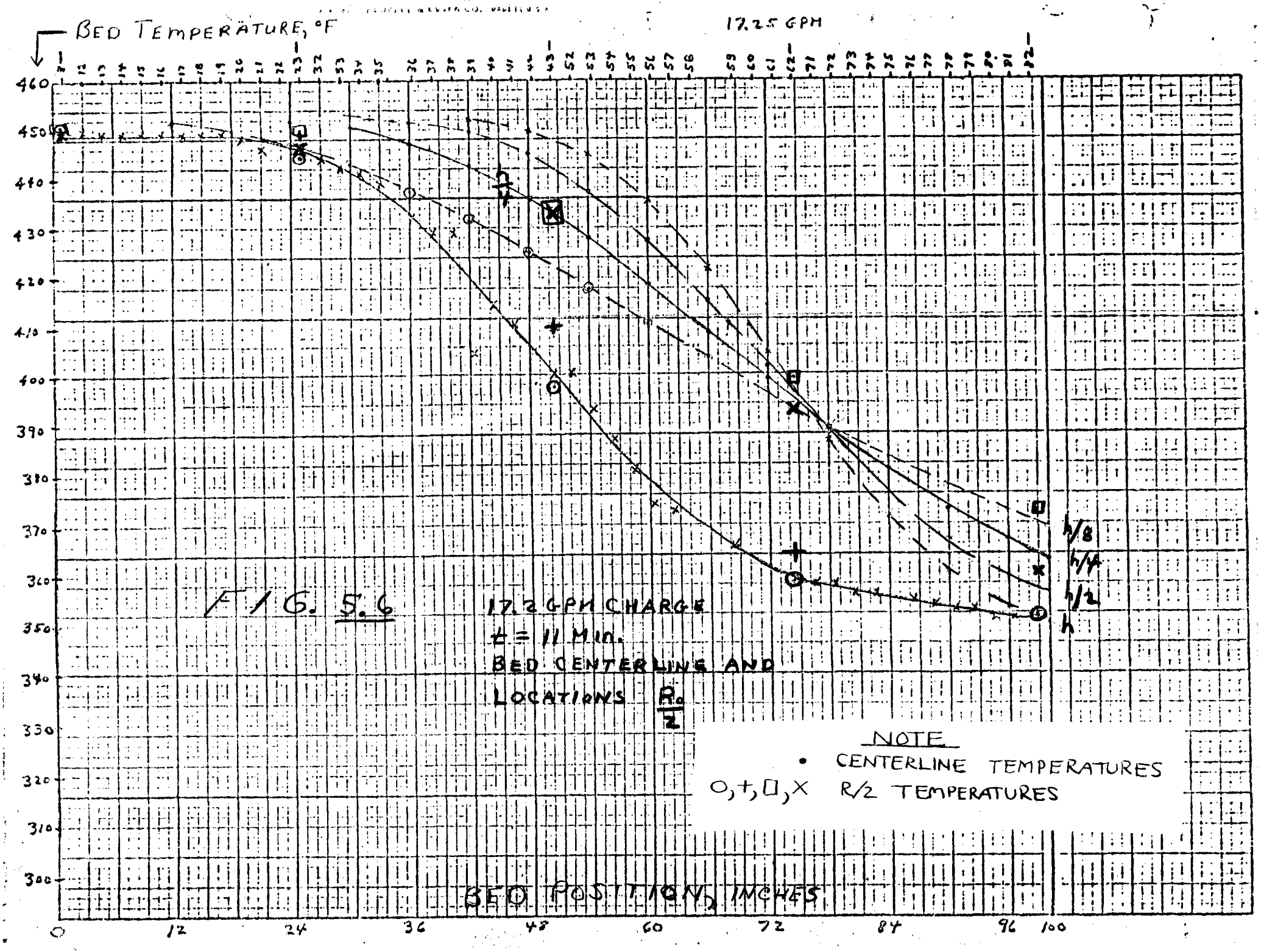
BED TEMPERATURE, °F
17.25 GPM
460
450
440
430
420
410
400
390
380
370
360
350
340
330
320
310
300
h/8
h/4
h/2
h
FIG. 5.6
17.2 GPM CHARGE
t = 11 Min.
BED CENTERLINE AND
LOCATIONS R₀/2
NOTE
• CENTERLINE TEMPERATURES
○,+,□,X R/2 TEMPERATURES
BED POSITION, INCHES
0
12
24
36
48
60
72
84
96
100

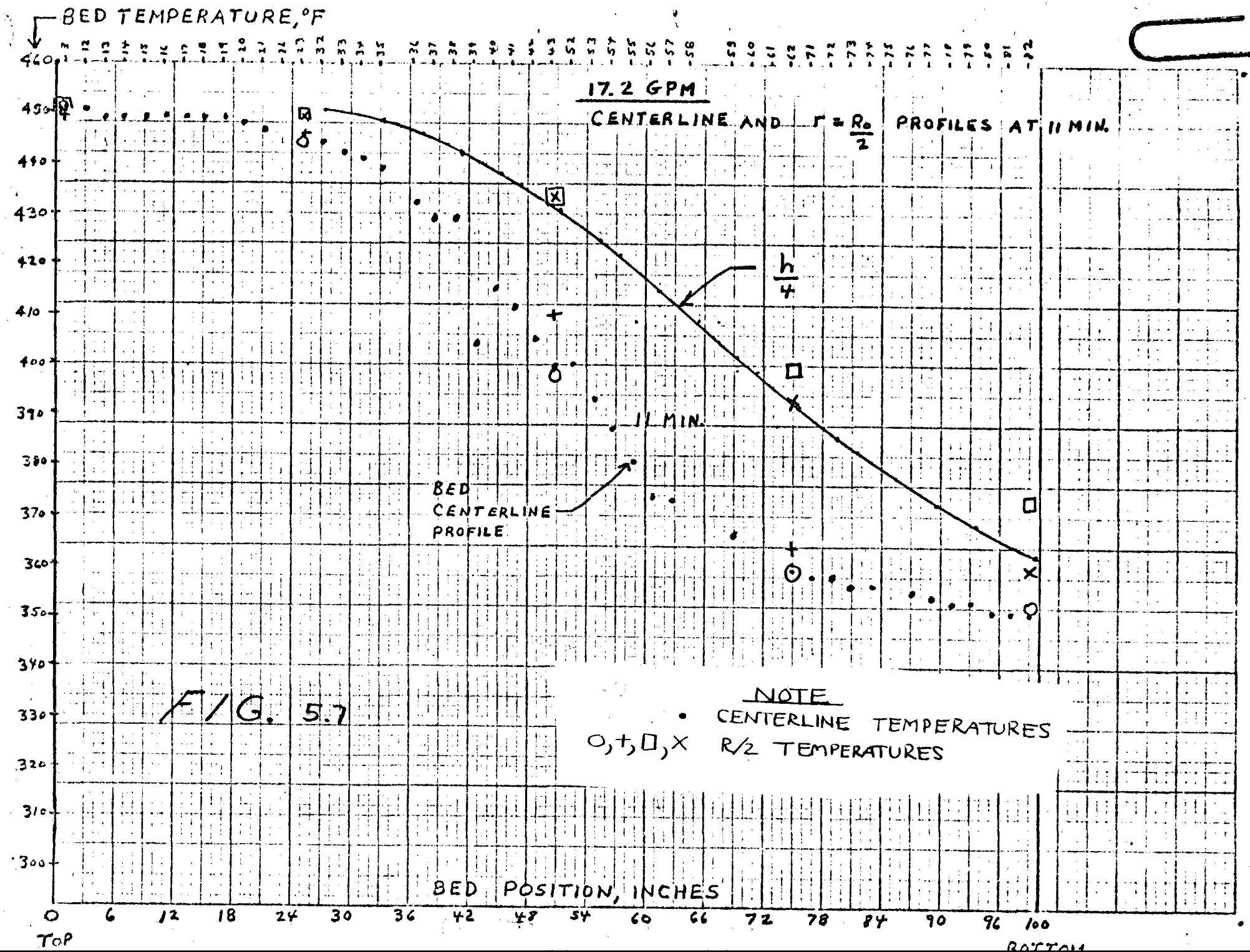
BED TEMPERATURE, °F
17.2 GPM
CENTERLINE AND $r = \frac{R_o}{2}$ PROFILES AT 11 MIN.
$\frac{h}{4}$
11 MIN.
BED CENTERLINE PROFILE
NOTE
• CENTERLINE TEMPERATURES
○, +, □, × R/2 TEMPERATURES
BED POSITION, INCHES
TOP
BOTTOM

FIG. 5.7

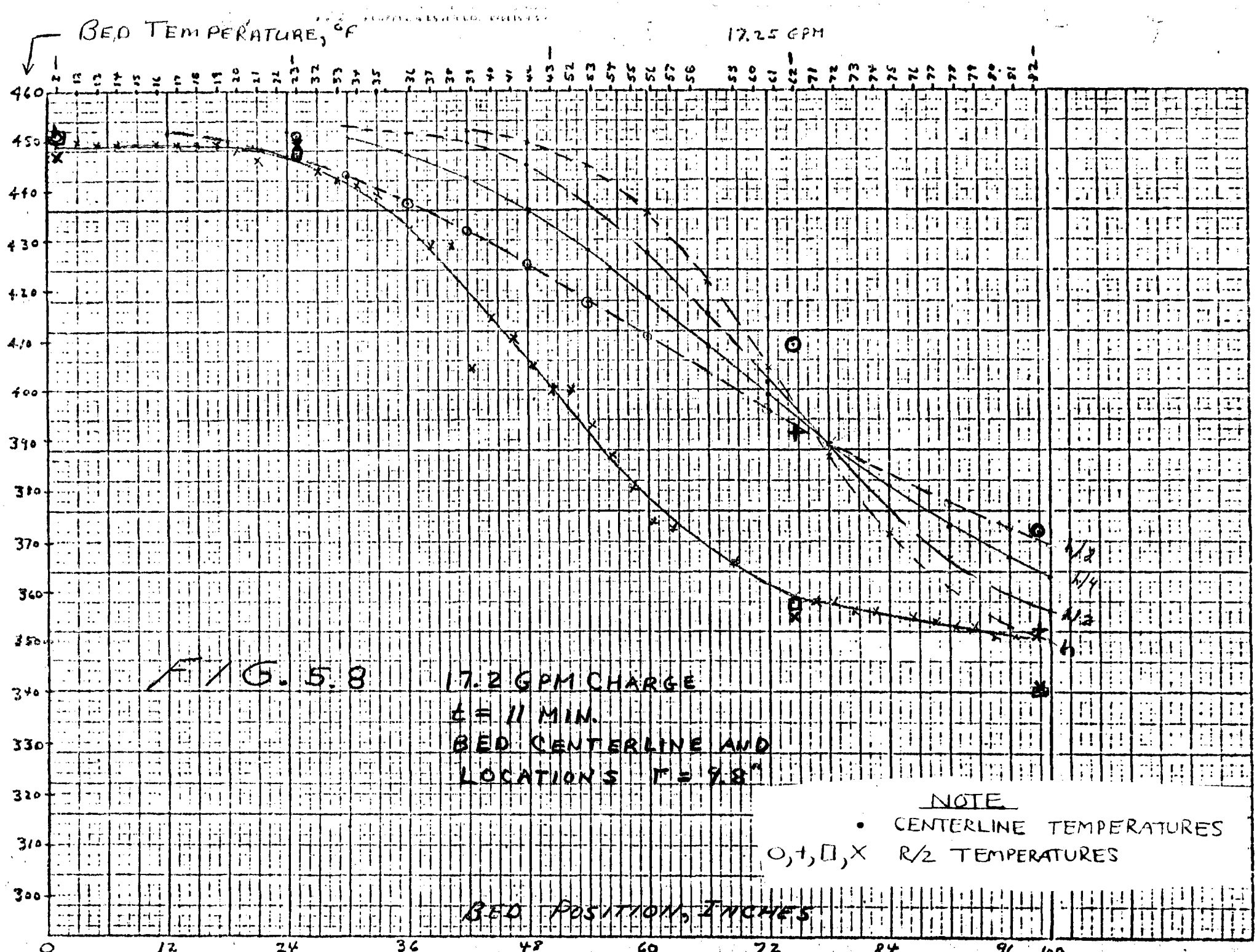

FIG. 5.8 17.2 GPM CHARGE
$t = 11$ MIN.
BED CENTERLINE AND
LOCATIONS $r = 9.8$"

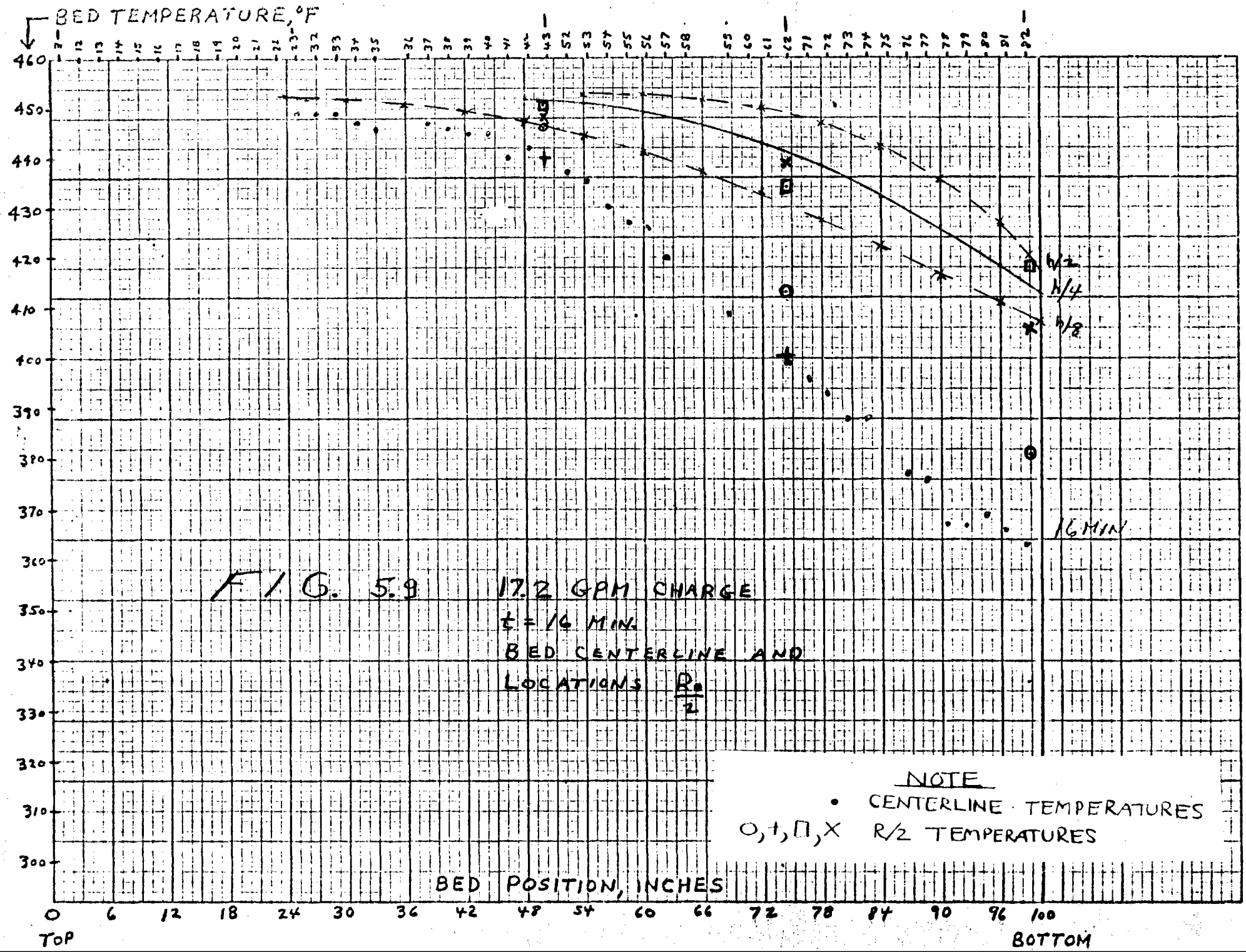
BED TEMPERATURE, °F
460
450
440
430
420
410
400
390
380
370
360
350
340
330
320
310
300
R/2
R/4
R/8
16 MIN
FIG. 5.9
17.2 GPM CHARGE
t = 16 MIN.
BED CENTERLINE AND
LOCATIONS R/2
NOTE
• CENTERLINE TEMPERATURES
O, t, □, X R/2 TEMPERATURES
BED POSITION, INCHES
0 6 12 18 24 30 36 42 48 54 60 66 72 78 84 90 96 100
TOP
BOTTOM

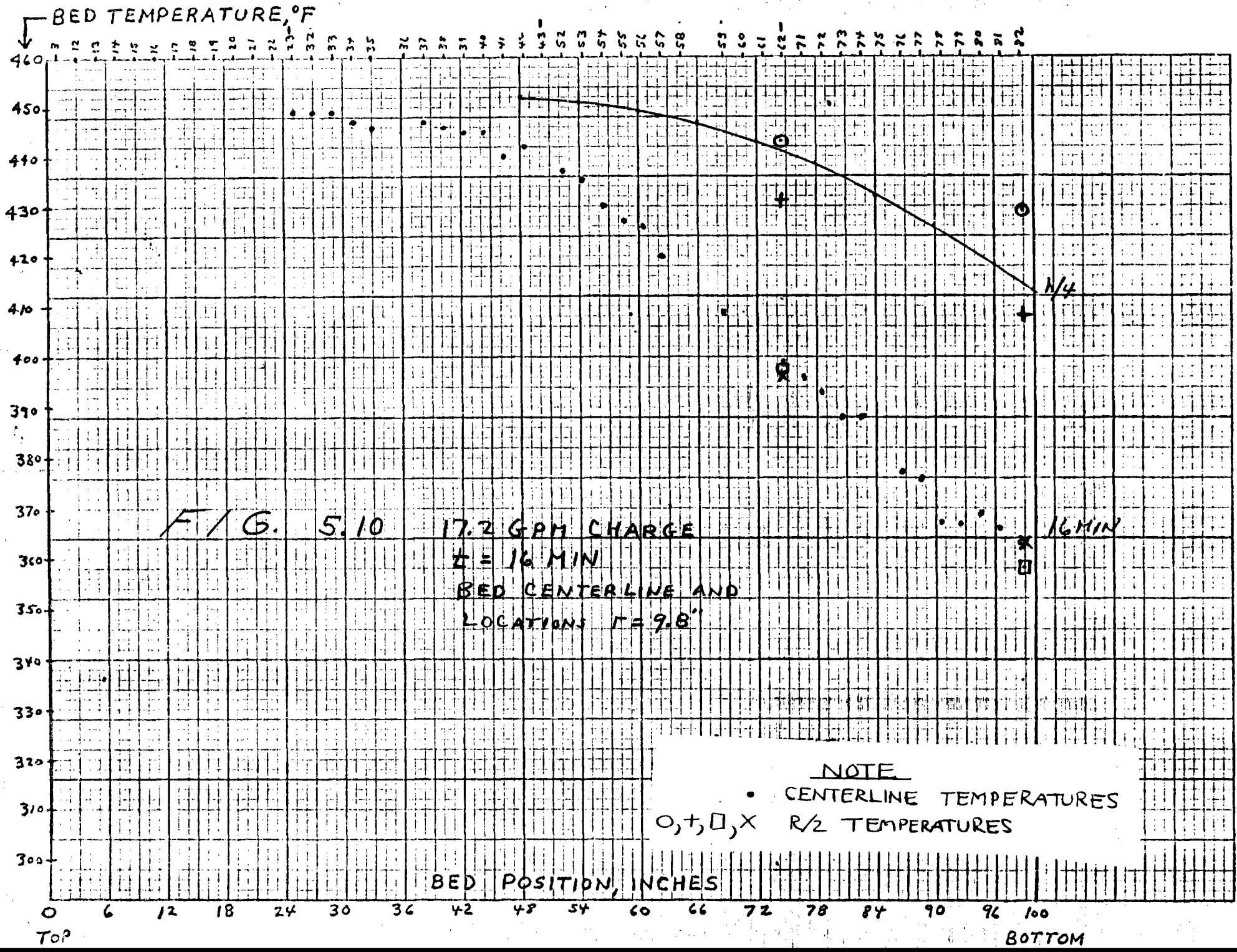
BED TEMPERATURE, °F
460
450
440
430
420
410
400
390
380
370
360
350
340
330
320
310
300
N/4
16 MIN
FIG. 5.10 17.2 GPM CHARGE
Z = 16 MIN
BED CENTERLINE AND
LOCATIONS r = 9.8"
NOTE
• CENTERLINE TEMPERATURES
O, +, □, X R/2 TEMPERATURES
BED POSITION, INCHES
0 6 12 18 24 30 36 42 48 54 60 66 72 78 84 90 96 100
TOP
BOTTOM

FIG. 5.11

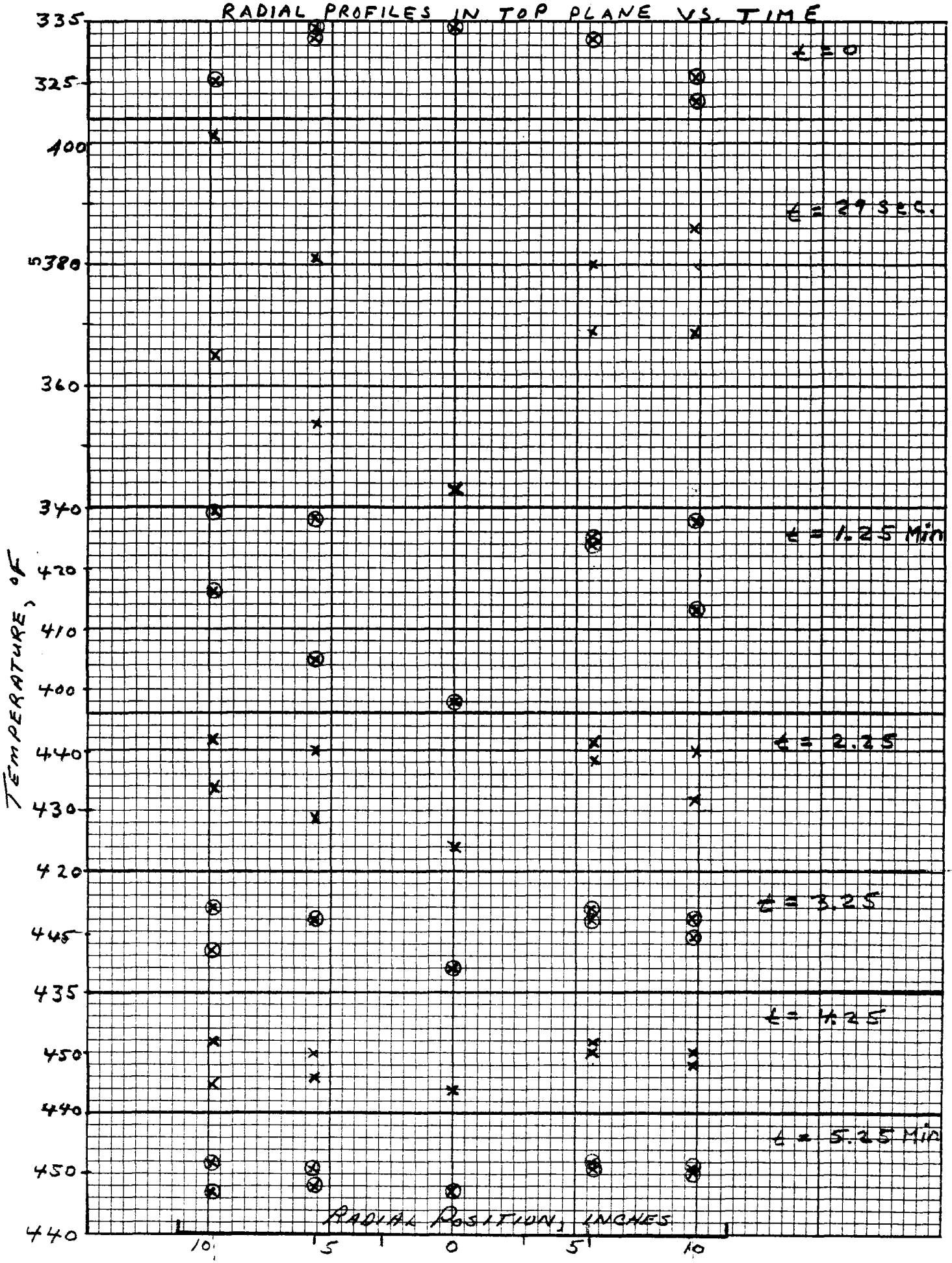
RADIAL PROFILES IN TOP PLANE VS. TIME
t = 0
t = 29 sec.
t = 1.25 Min
t = 2.25
t = 3.25
t = 4.25
t = 5.25 Min
TEMPERATURE, °F
335
325
400
380
360
340
420
410
400
440
430
420
445
435
450
440
450
440
RADIAL POSITION, INCHES
10
5
0
5
10

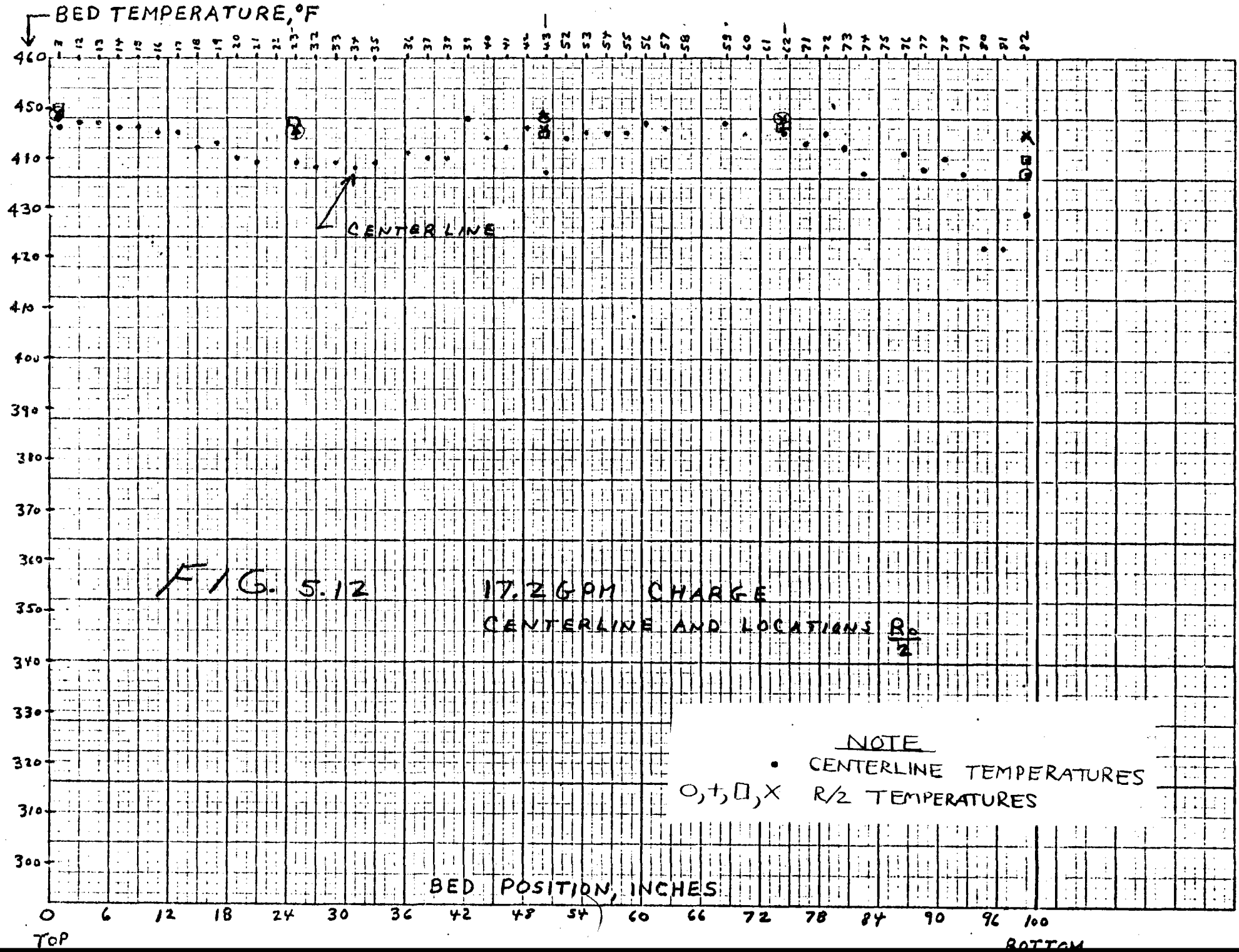
BED TEMPERATURE, °F
460
450
440
430
420
410
400
390
380
370
360
350
340
330
320
310
300
CENTER LINE
FIG. 5.12
17.2 GPM CHARGE
CENTERLINE AND LOCATIONS $\frac{R_o}{2}$
NOTE
• CENTERLINE TEMPERATURES
O, +, □, X R/2 TEMPERATURES
BED POSITION, INCHES
0 6 12 18 24 30 36 42 48 54 60 66 72 78 84 90 96 100
TOP
BOTTOM

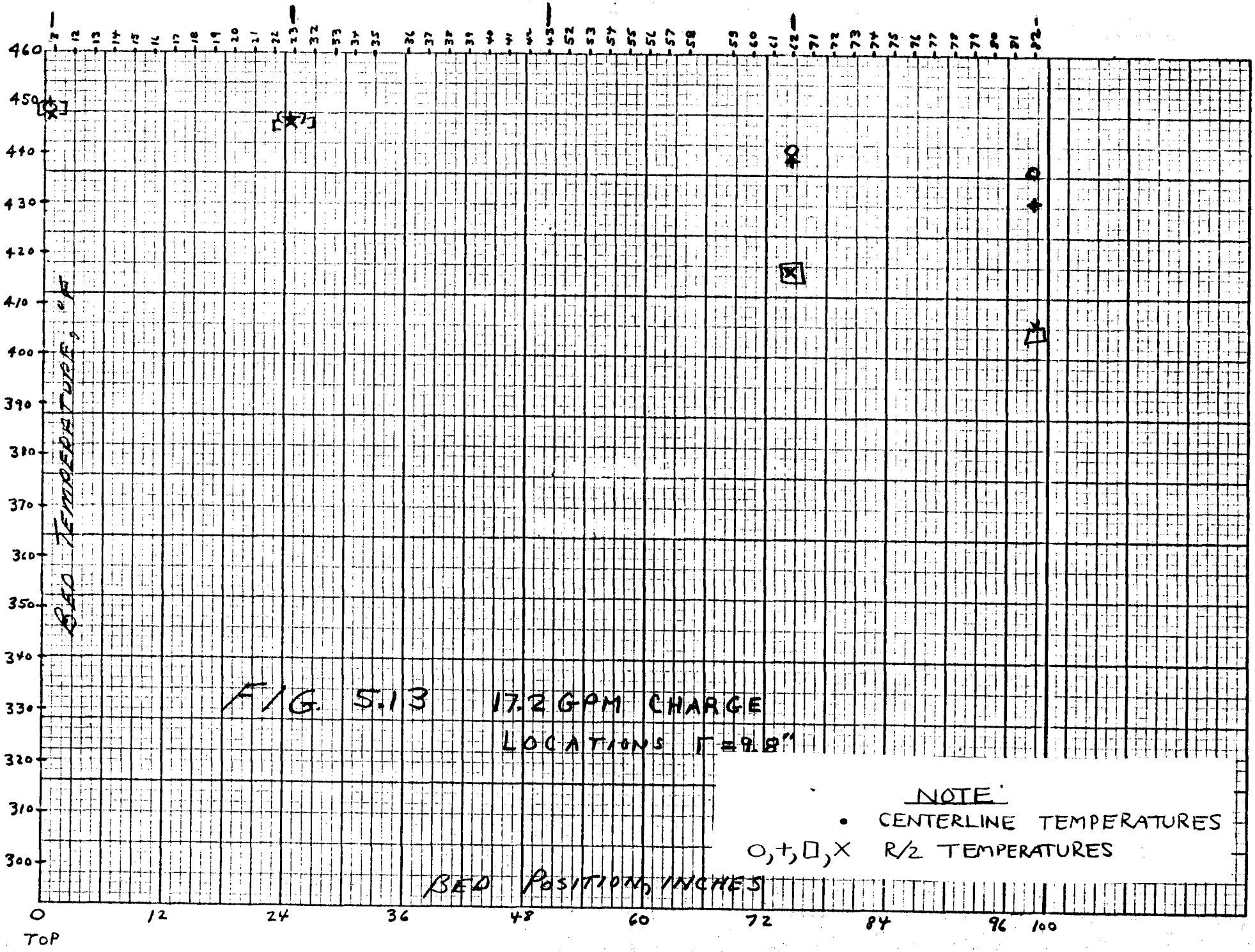

FIG. 5.13 17.2 GPM CHARGE
LOCATIONS r = 9.8"

FIG. 5.14

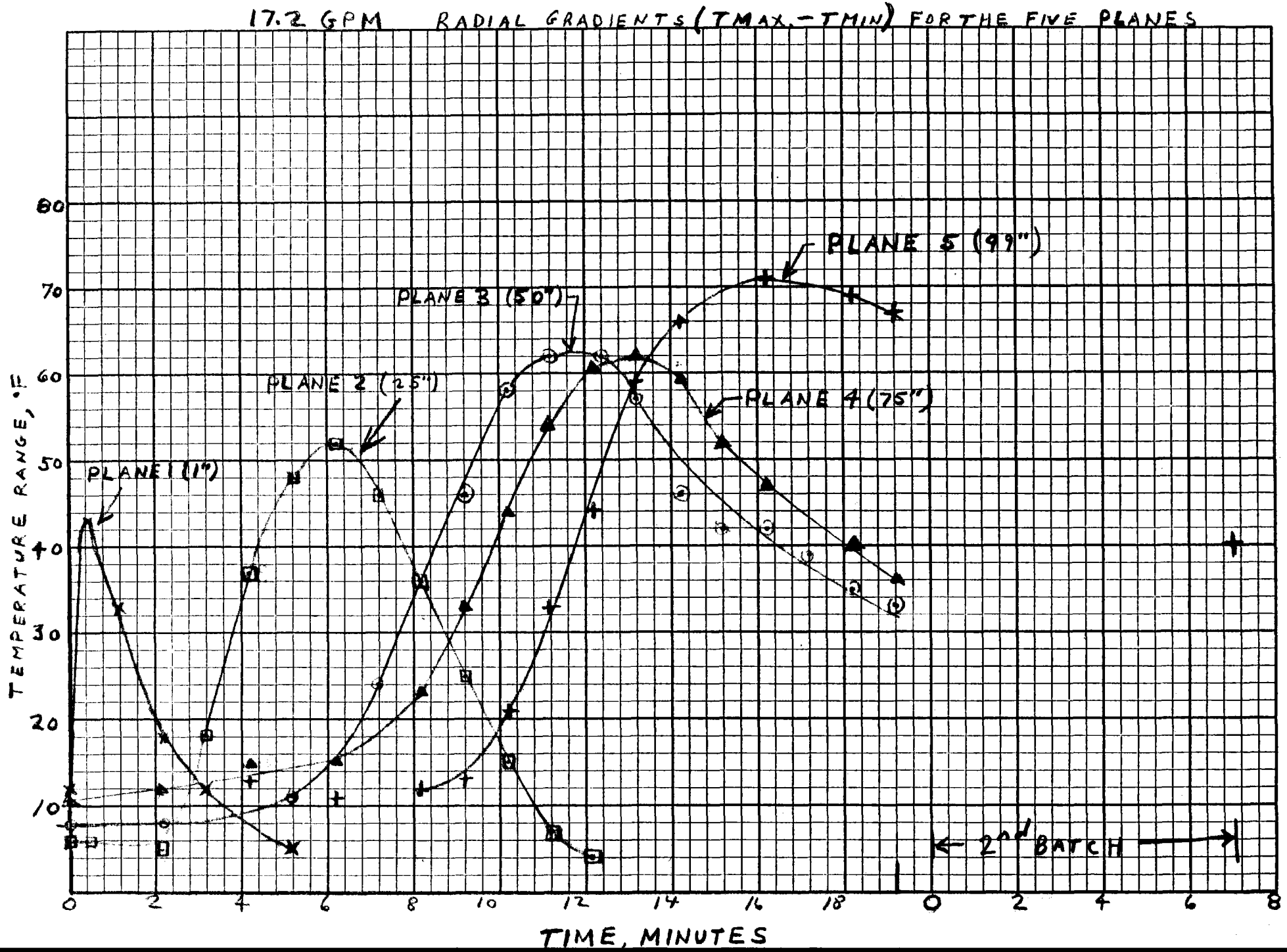
17.2 GPM RADIAL GRADIENTS (TMAX. - TMIN) FOR THE FIVE PLANES
PLANE 5 (99")
PLANE 3 (50")
PLANE 2 (25")
PLANE 4 (75")
PLANE 1 (1")
← 2nd BATCH
TEMPERATURE RANGE, °F
TIME, MINUTES
80
70
60
50
40
30
20
10
0
2
4
6
8
10
12
14
16
18
0
2
4
6
8

5.1.1.1 Fluid Exit Temperature

Figure 5.15 shows the measured fluid exit temperature and the model prediction for $\underline{h}_4$. The model was run using the measured fluid inlet temperature and the integrated average bed temperature at the 5 planes as shown in figure 5.16.

The measured fluid exit temperature starts at 156^{o}F. This is due to cooling of outlet pipe by the coolant loop used to protect the outlet pump from overheating. The coolant pump was located only a few feet downstream from the tank bottom. In 3 minutes the fluid exit rises to a near steady state value, however, there is still a heat loss to the pipe which results in the measured fluid exit temperature being lower than the average temperature of the bottom of the bed. This effect becomes more pronounced at the lower flow rates. The measured fluid exit temperature rise slope after breakthrough is in good agreement with the predicted curve but displaced in time by 2 minutes.

Fig. 5. 15

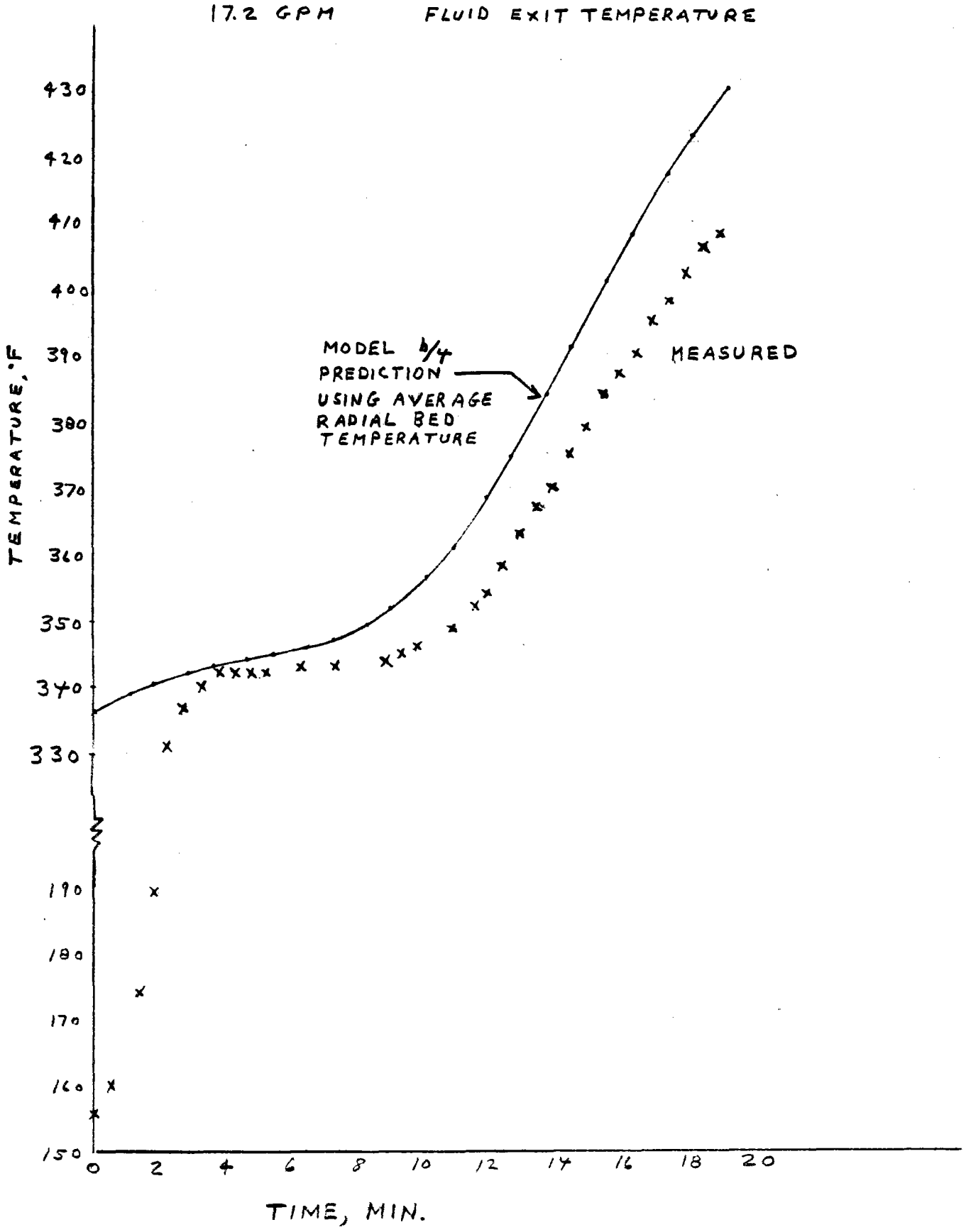
17.2 GPM
FLUID EXIT TEMPERATURE
TEMPERATURE, °F
430
420
410
400
390
380
370
360
350
340
330
190
180
170
160
150
0
2
4
6
8
10
12
14
16
18
20
TIME, MIN.
MODEL h/4 PREDICTION USING AVERAGE RADIAL BED TEMPERATURE
MEASURED

FIG. 5.16

17.2 G.P.M.

INITIAL AXIAL PROFILE

FROM RADIAL AVERAGE IN 5 PLANES

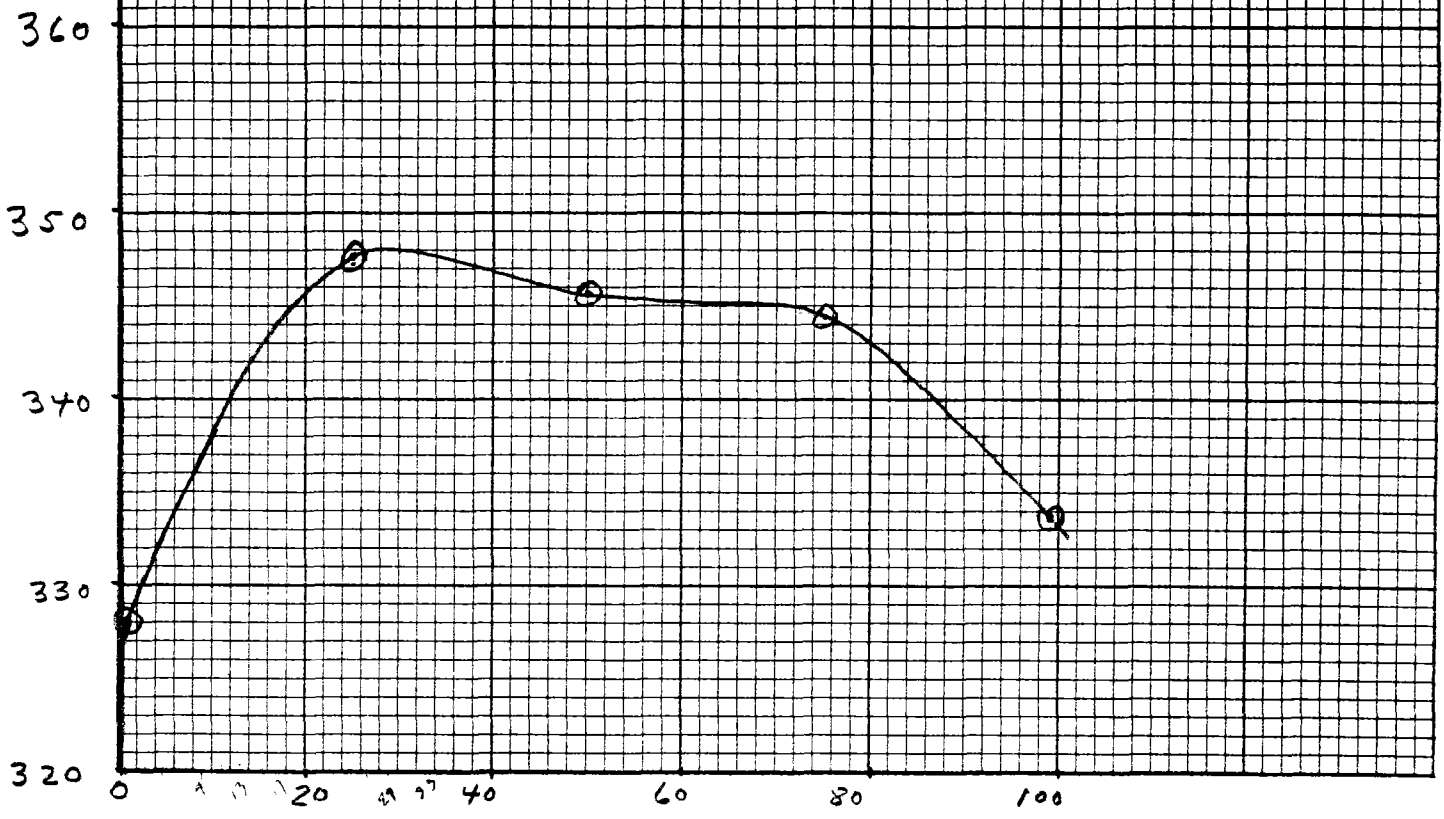

5.1.2 8 GPM Charge

Two tests were run at 8 GPM to determine if there was an effect on the shape of the thermocline due to system pressure. Theoretically, a more dense gas phase might have an effect on the fluid-solid heat transfer rate. Tests were run at 1 psig and 5 psig. Higher pressures could not be achieved due to safety considerations.

5.1.2.1 5 psig Charge

Figure 5.17 shows the initial bed centerline profile and the profiles measured at 13, 26, and 36 minutes. Figure 5.18 shows the bed centerline temperatures and the radial profiles measured a $\frac{Ro}{2}$ along with the model prediction for $\frac{h}{4}$. Figure 5.19 is a similar plot where the radial temperatures measured near the wall are shown. The model fit $\frac{h}{4}$ is again a good fit to the slope of the measured temperature profiles. As at 17 GPM, it is seen that the radial gradients do not persist as charging proceeds.

Figure 5.20 shows the initial radial temperature profiles, from which the integrated average profile shown in figure 5.21 was calculated. This profile along with the inlet fluid temperature history were used as the initial conditions in the model.

5.1.2.1.1 Fluid Exit Temperature

Figure 5.22 shows the measured and model fluid exit temperature for $\frac{h}{4}=t$. The measured temperature, as at 17.2 GMP, lags the model, however, the slopes are in good agreement.

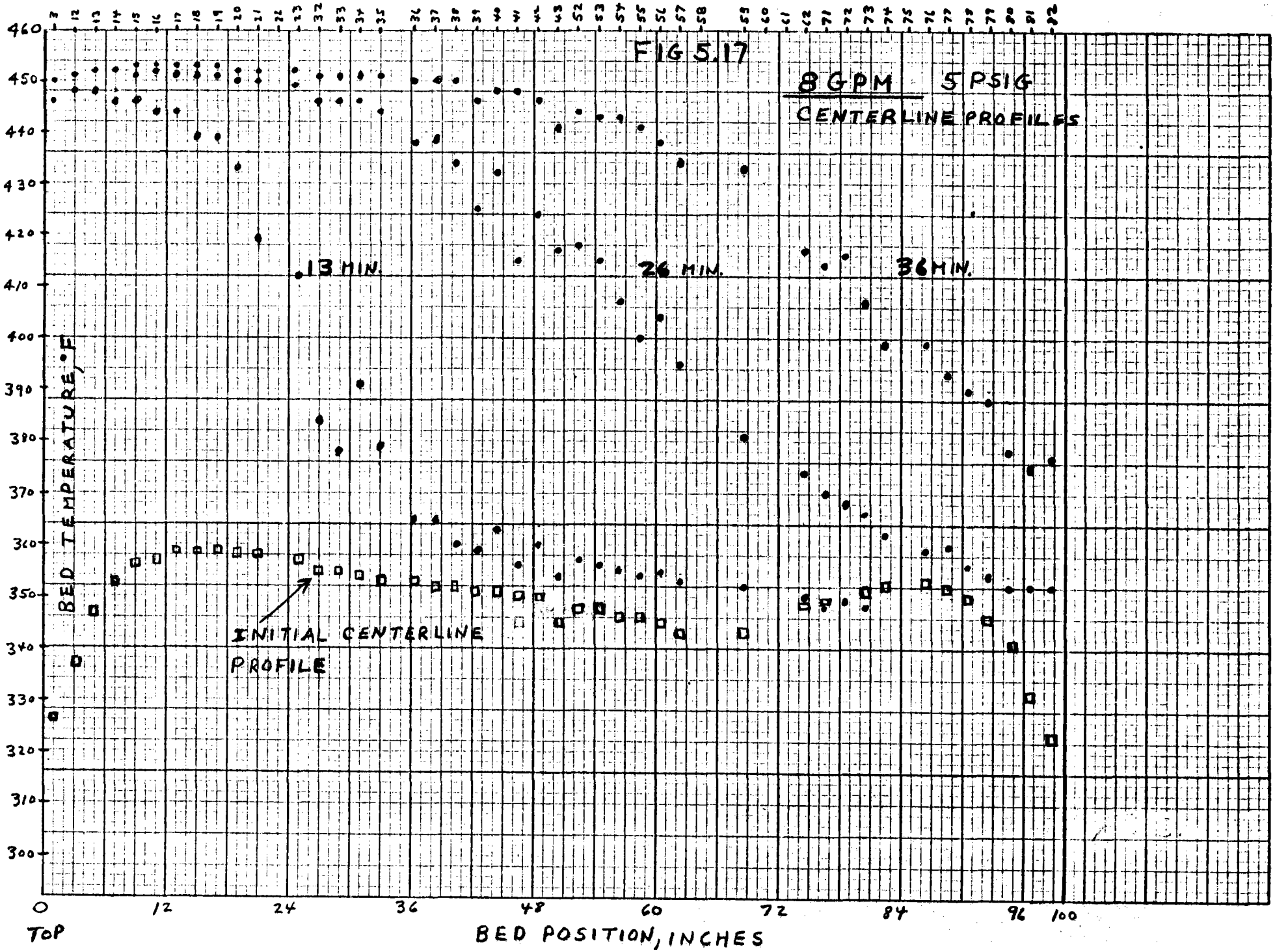

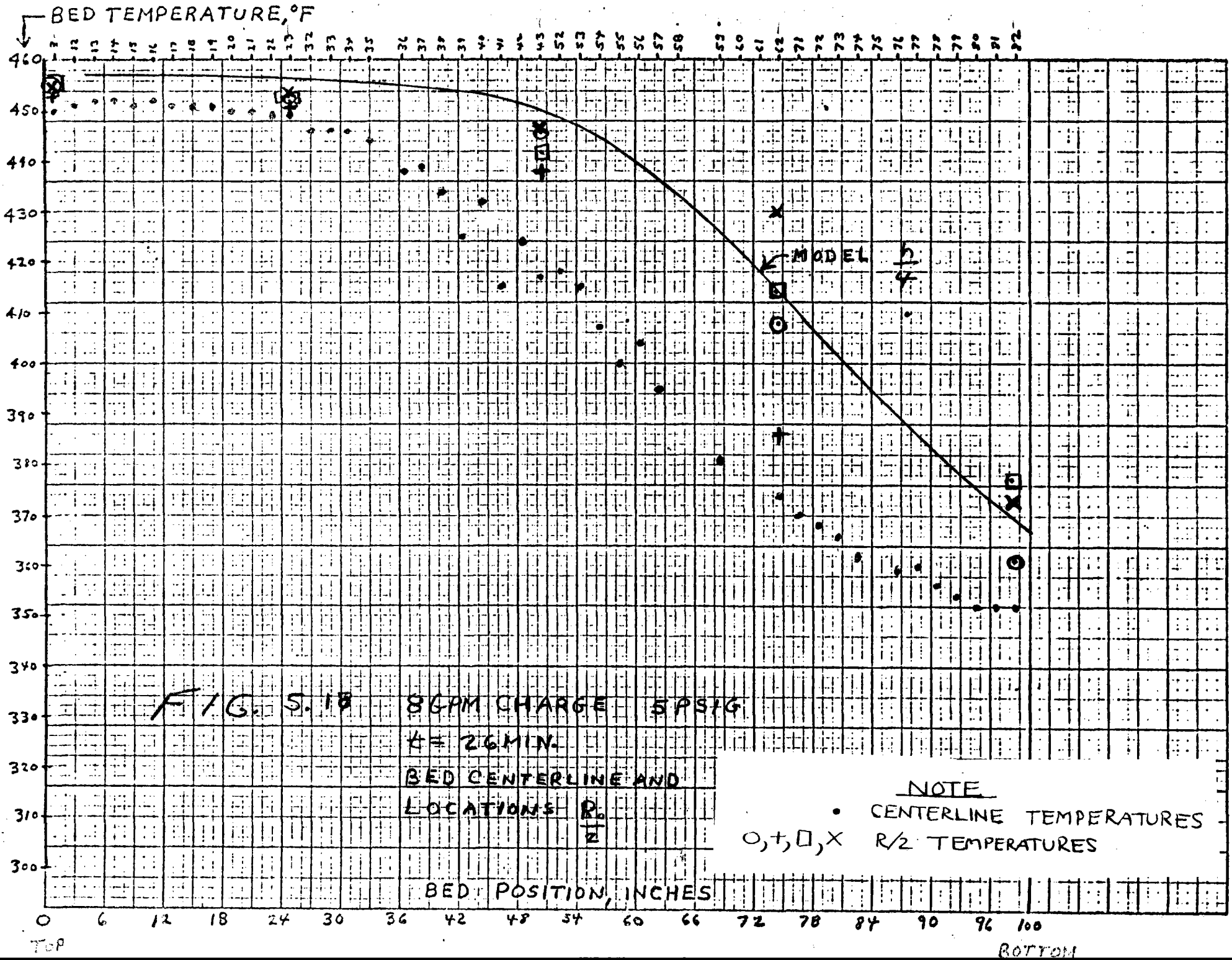
BED TEMPERATURE, °F
460
450
440
430
420
410
400
390
380
370
360
350
340
330
320
310
300
MODEL h/4
FIG. 5.18 86PM CHARGE 5PSIG
t = 26MIN.
BED CENTERLINE AND
LOCATIONS R/2
NOTE
• CENTERLINE TEMPERATURES
O, +, □, X R/2 TEMPERATURES
BED POSITION, INCHES
0 6 12 18 24 30 36 42 48 54 60 66 72 78 84 90 96 100
TOP
BOTTOM

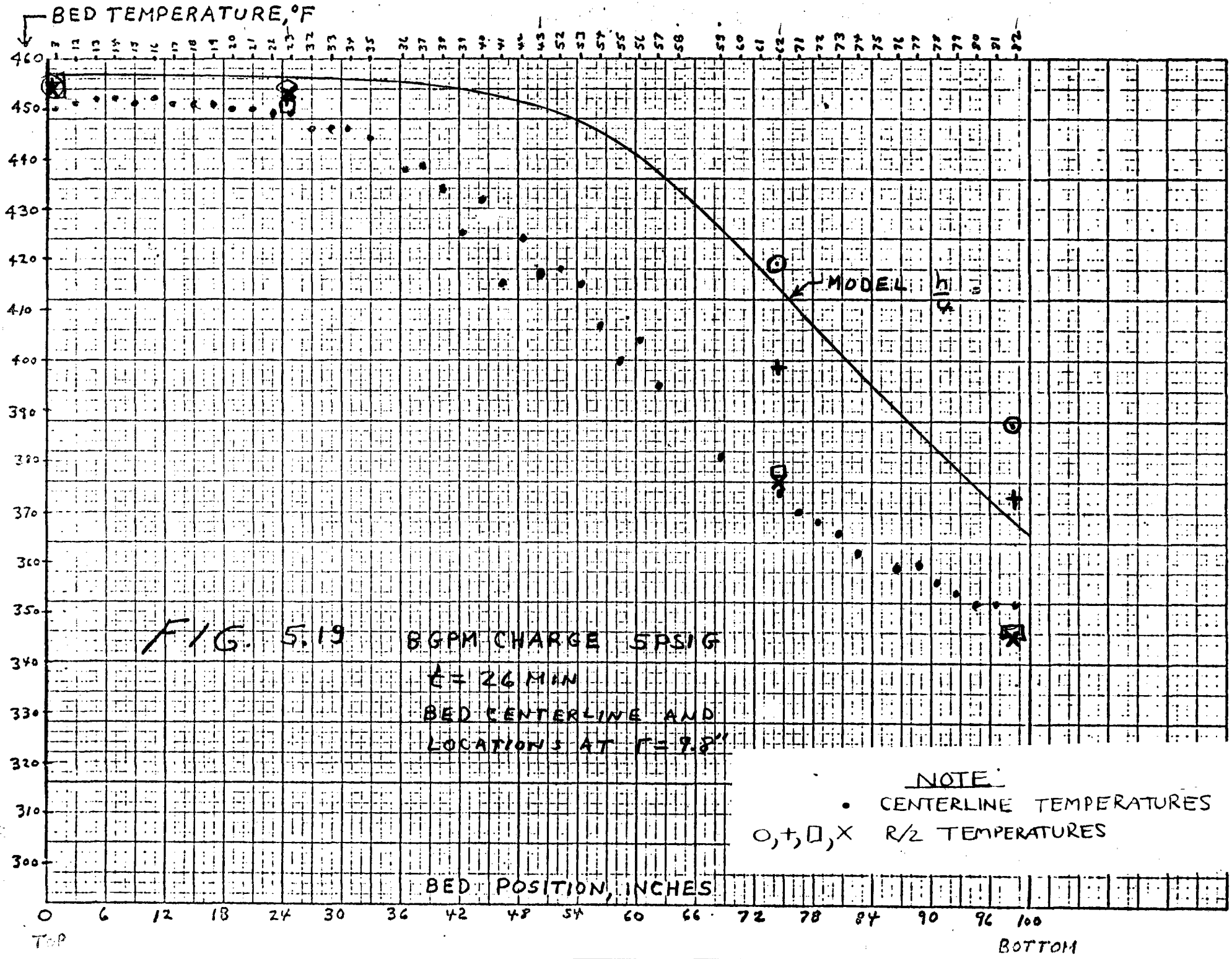

FIG. 5.19 60PM CHARGE 5PSIG
t = 26 MIN
BED CENTERLINE AND
LOCATIONS AT r = 9.8"

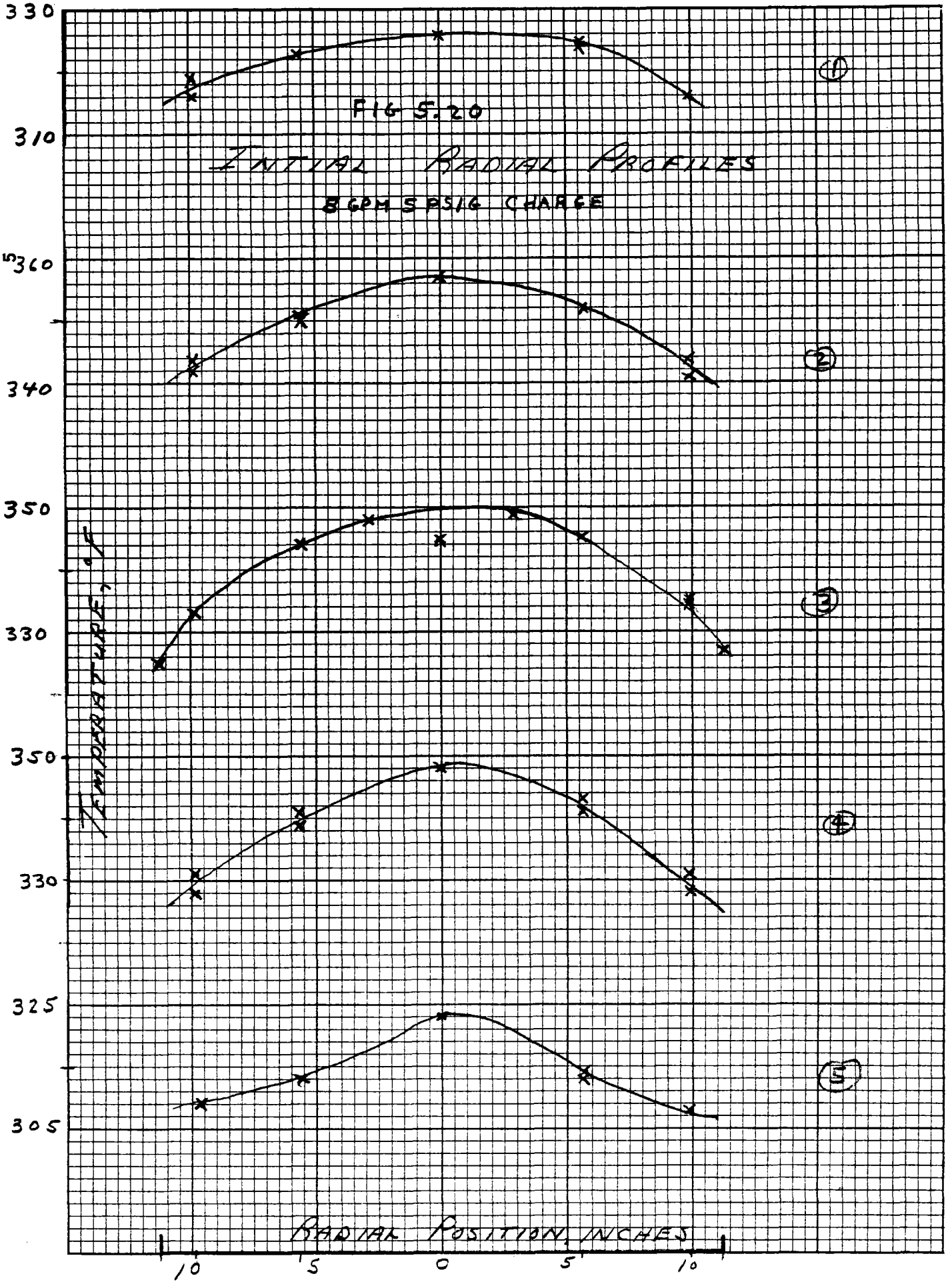

FIG 5.20

INITIAL RADIAL PROFILES

8 GPM 5 PSIG CHARGE

FIG. 5.21

INITIAL AXIAL PROFILE

8 GPM 5 PSIG CHARGE

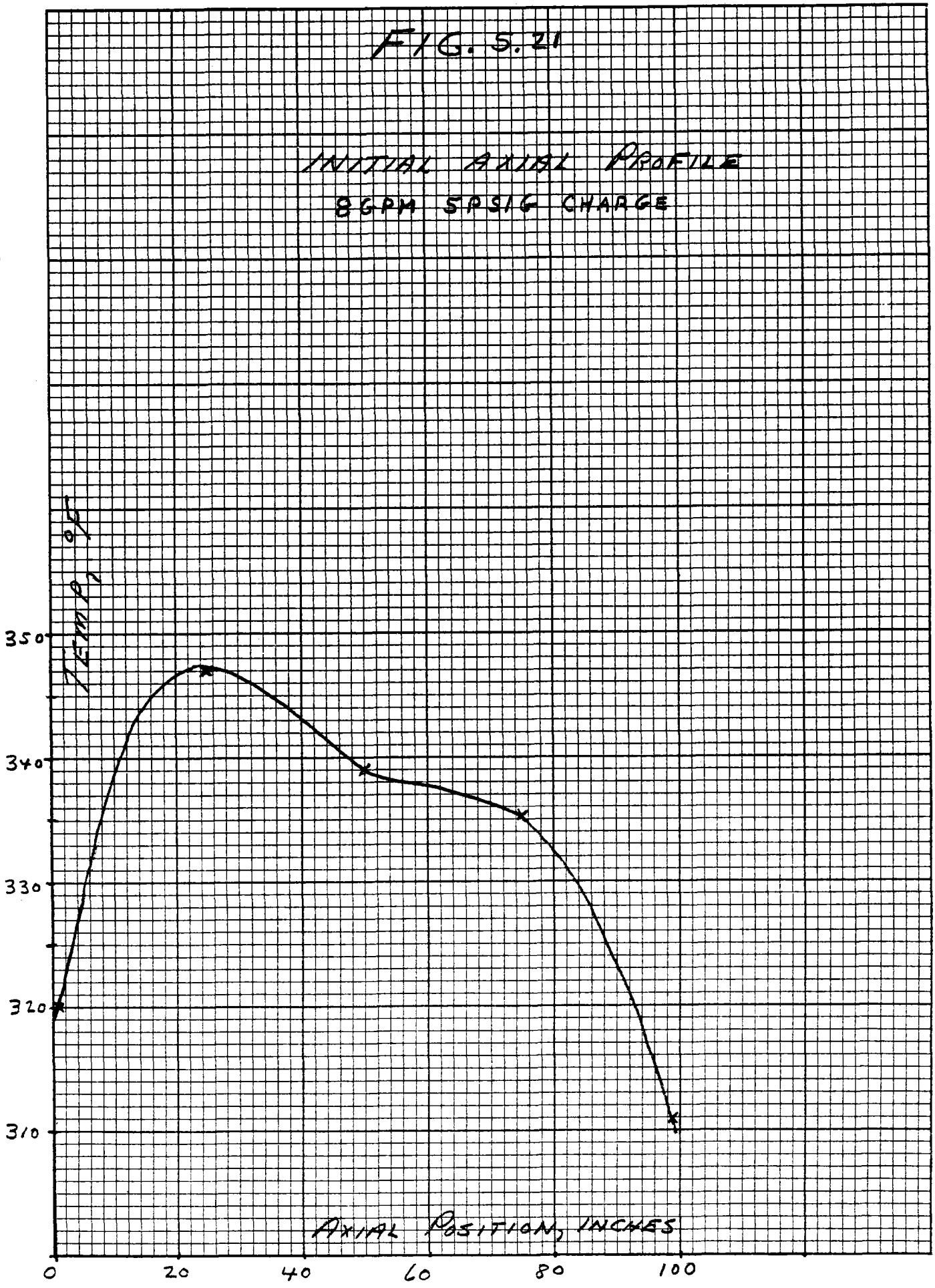

FIG. 5.22 FLUID EXIT TEMPERATURE 8 GPM CHARGE 50 PSIG

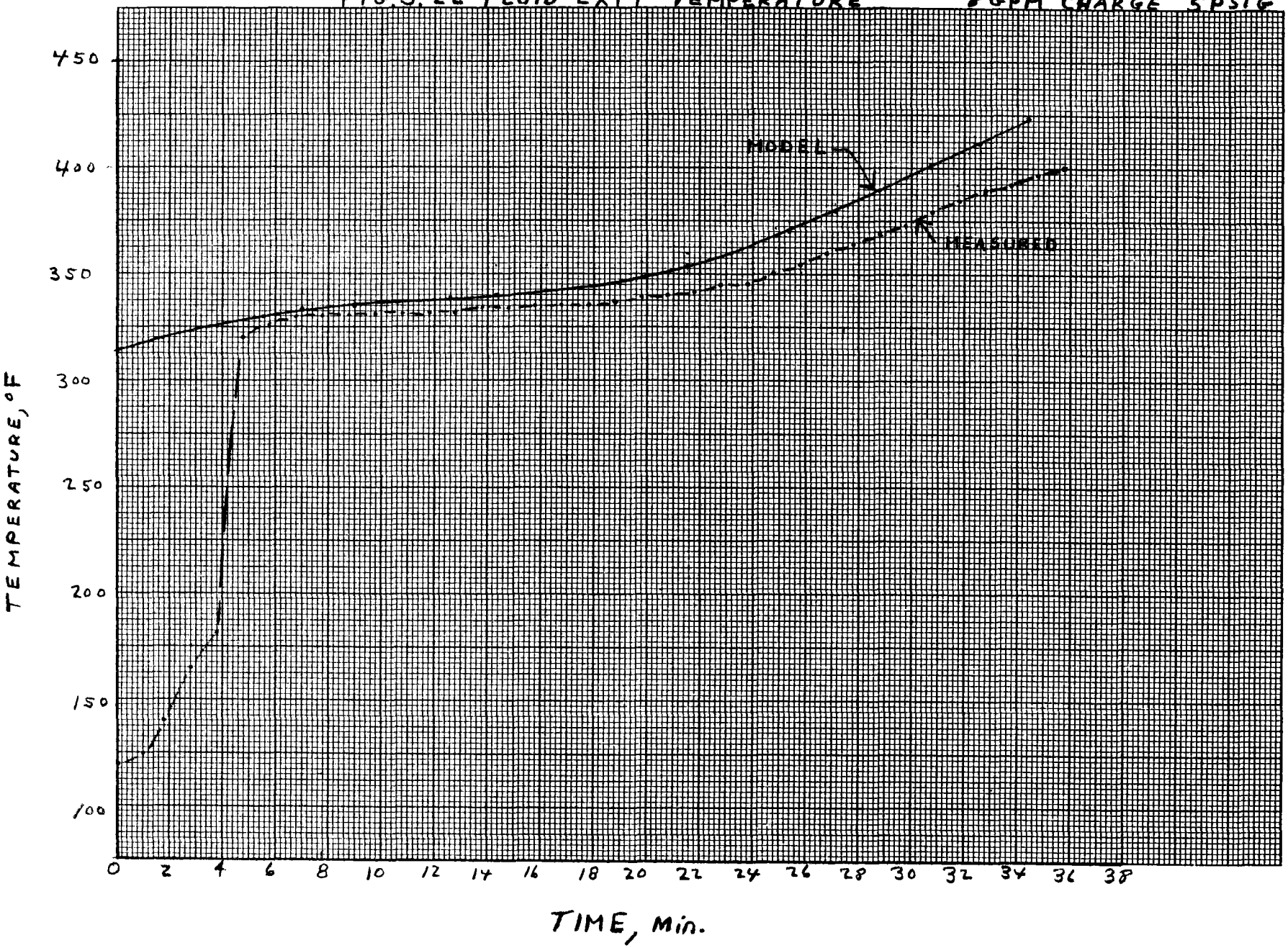

5.1.2.2 8 GPM, 1 psig Charge

Figure 5.23 shows the initial bed centerline temperature and the bed temperatures measured at 13, 26 and 36 minutes. Figures 5.24 and 5.25 show the 26 minute profiles at $\frac{Ro}{2}$ and near the wall for $\frac{h}{4} = 20$ The model, $\frac{h}{4}$, again fits the measured thermocline slopes. The initial bed radial profiles are shown in figure 5.26. The integrated average profile was not calculated because the only effect is to shift the model curve slightly to the left but not change the slope. Consequently, the input to the model was the bed centerline profile and the measured fluid inlet temperature history.

5.1.2.2.1 Fluid Exit Temperature

Figure 5.27 shows the measured and model fluid exit temperatures. These show the same characteristics as the previous profiles.

5.1.2.2.2 Thermocline Comparison at 1 and 5 psig

Figure 5.28 shows the thermoclines measured at the centerline for both test pressures. There is no significant difference between the slopes of the thermoclines at the two pressures as they progress through the bed.

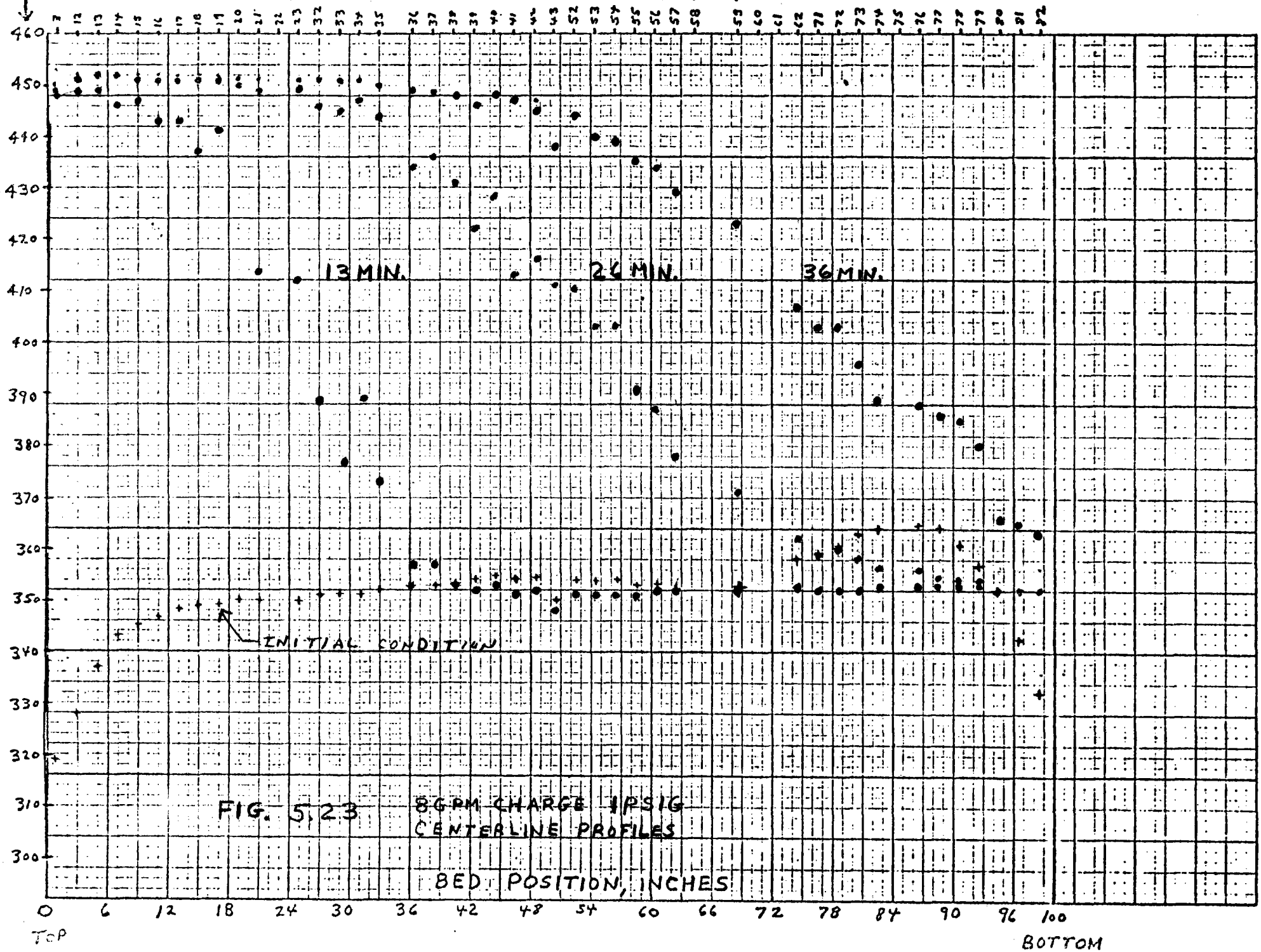

FIG. 5.23 8 GPM CHARGE 1PSIG CENTERLINE PROFILES

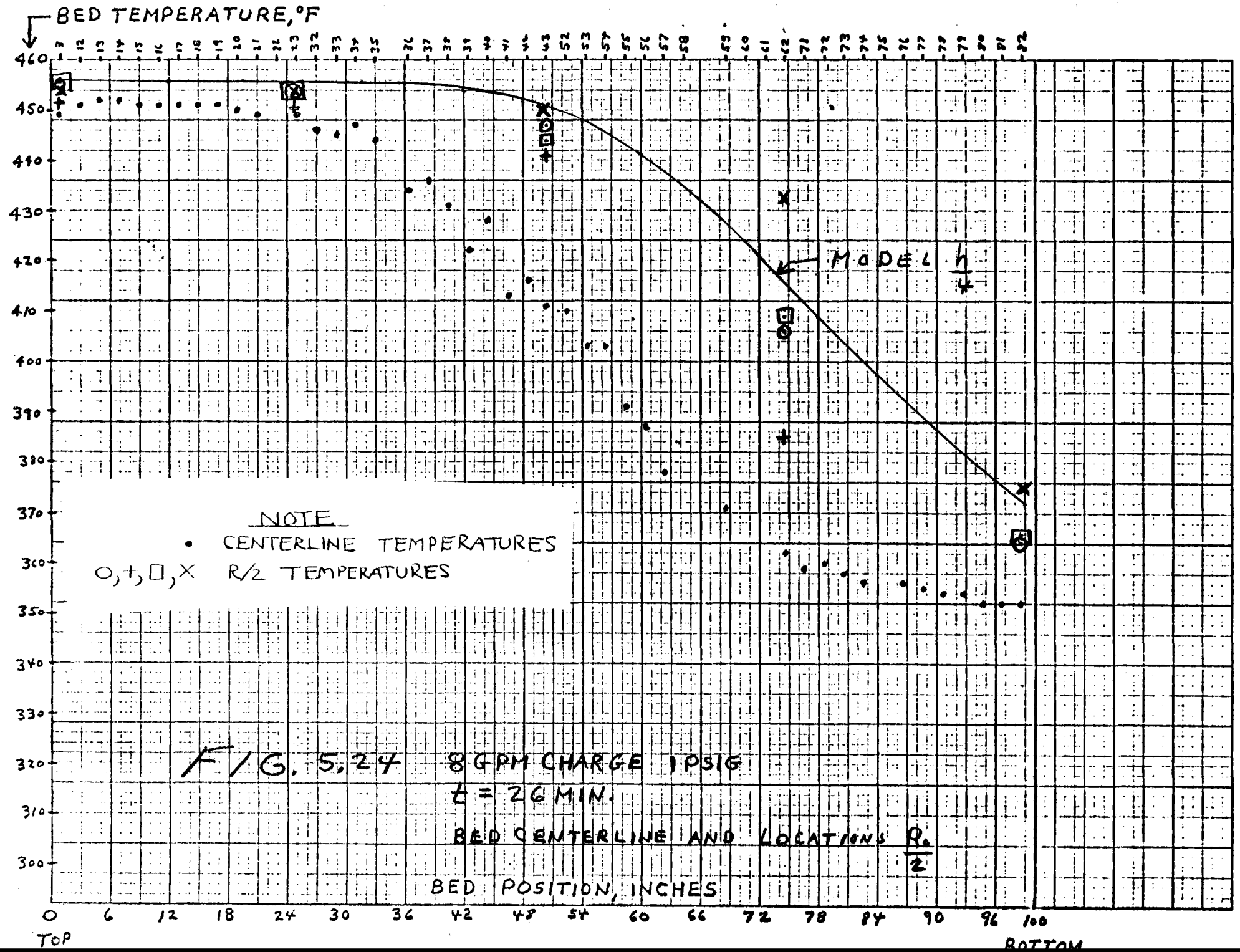
BED TEMPERATURE, °F
460
450
440
430
420
410
400
390
380
370
360
350
340
330
320
310
300
MODEL h/t
NOTE
• CENTERLINE TEMPERATURES
○, +, □, × R/2 TEMPERATURES
FIG. 5.24 8 GPM CHARGE 1 PSIG
t = 26 MIN.
BED CENTERLINE AND LOCATIONS Ro/2
BED POSITION, INCHES
0 TOP
6
12
18
24
30
36
42
48
54
60
66
72
78
84
90
96
100 BOTTOM

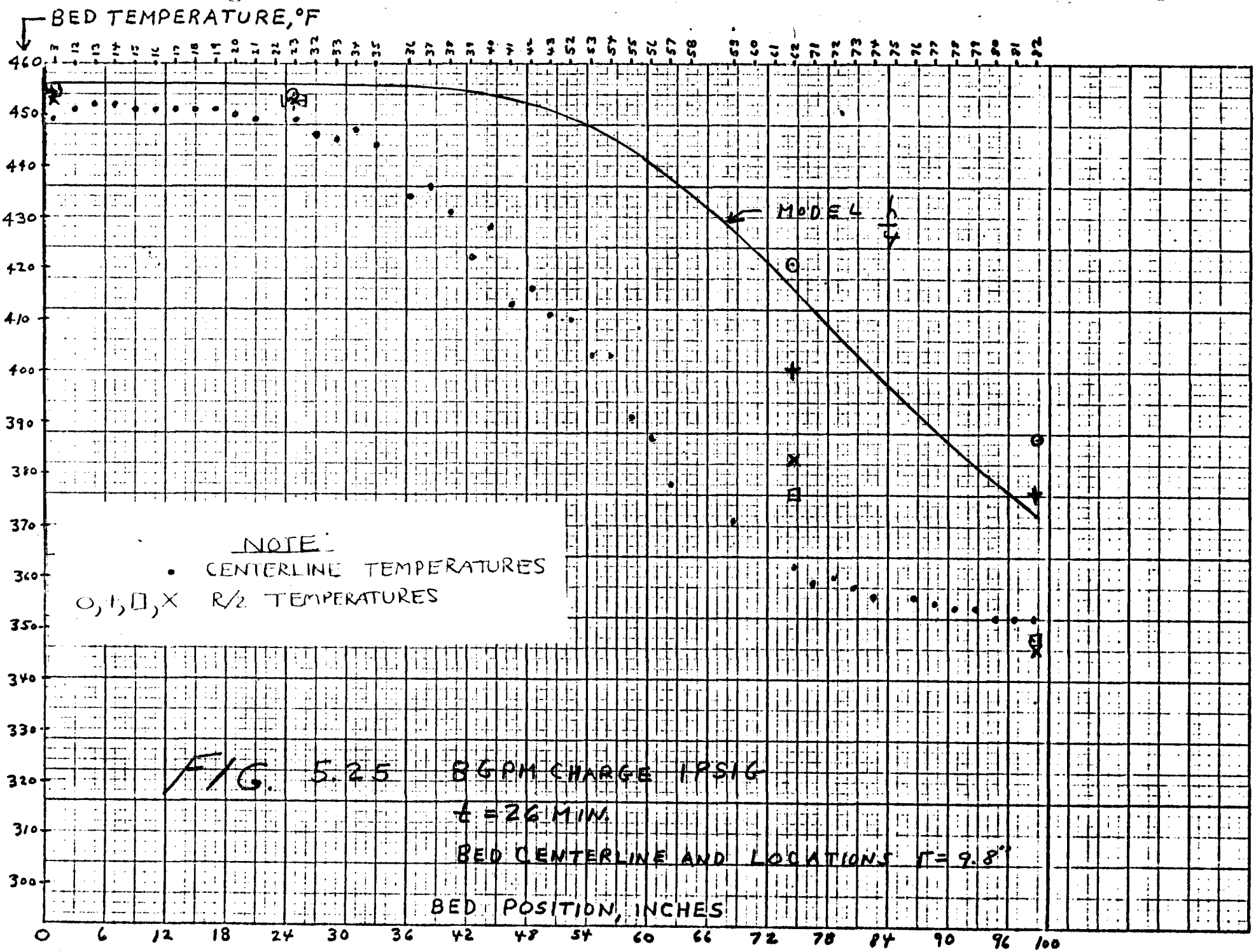

FIG. 5.25 8 GPM CHARGE 1 PSIG
$t = 26$ MIN.
BED CENTERLINE AND LOCATIONS $r = 9.8"$

FIG. 5.26

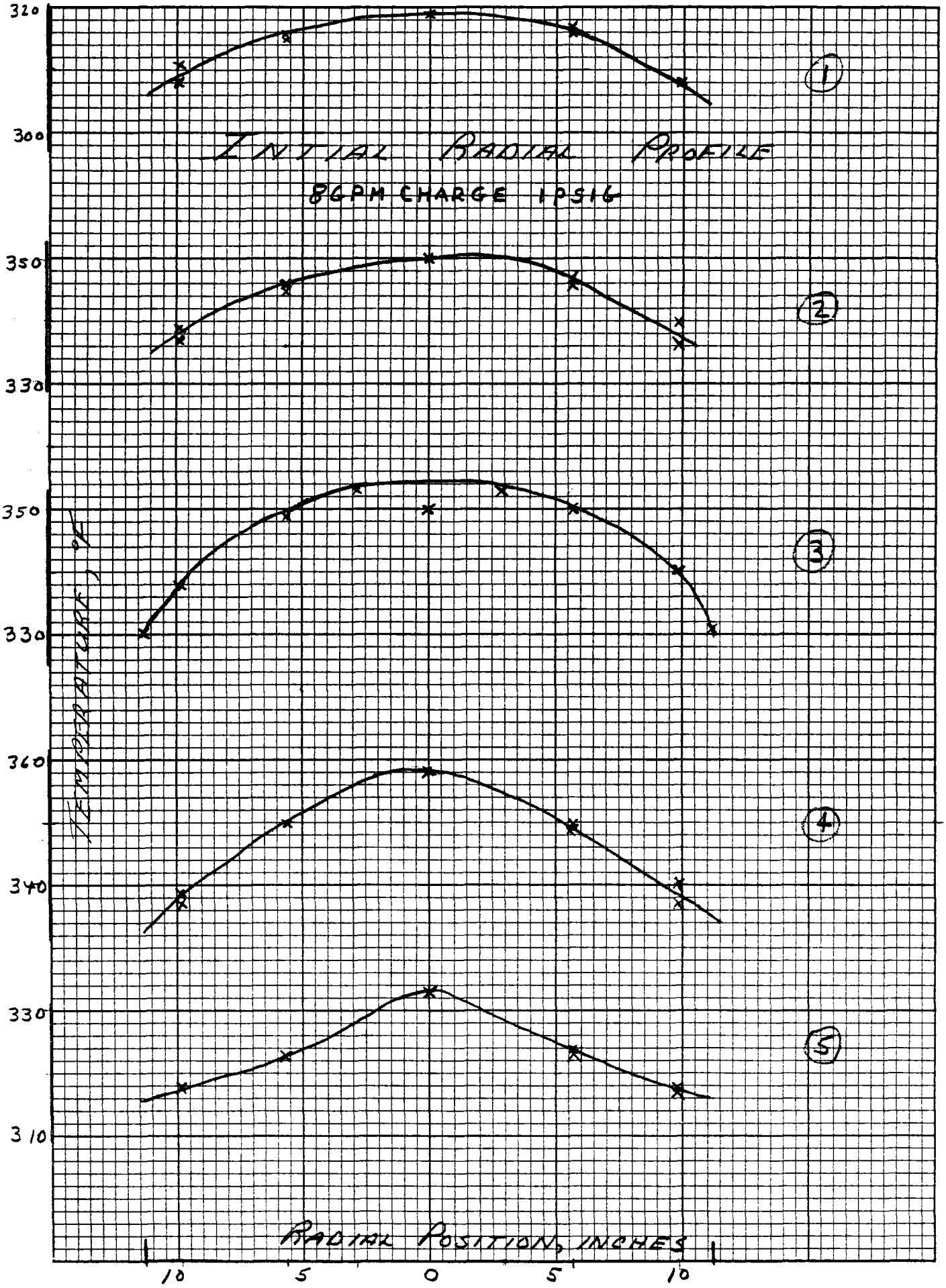
320
300
350
330
350
330
360
340
330
310
INITIAL RADIAL PROFILE
80PM CHARGE 1PSIG
TEMPERATURE °F
RADIAL POSITION, INCHES
10
5
0
5
10
1
2
3
4
5

FIG. 5.27

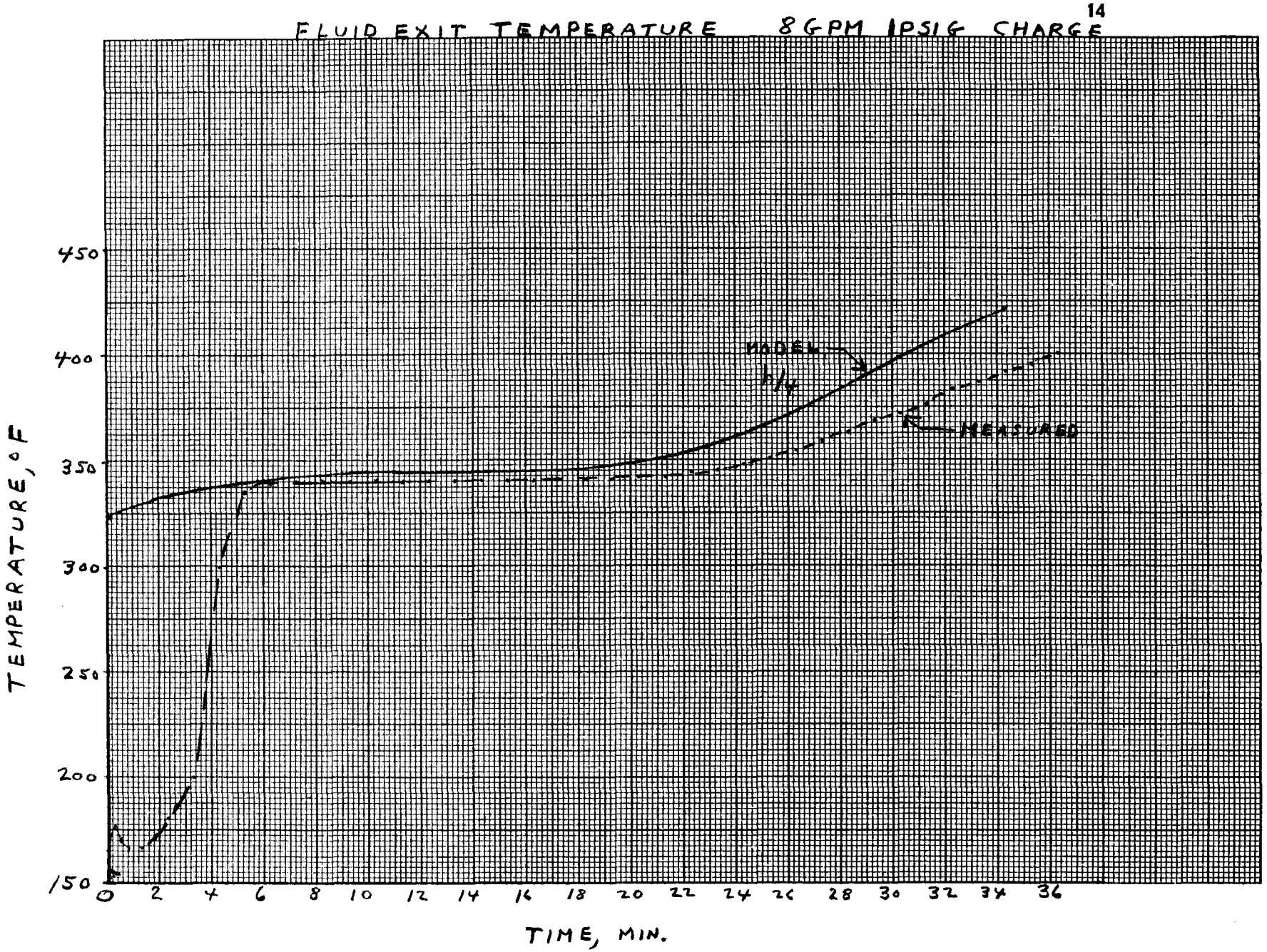
FLUID EXIT TEMPERATURE 8 GPM 14 PSIG CHARGE
450
400
350
300
250
200
150
TEMPERATURE, °F
MODEL
MEASURED
0
2
4
6
8
10
12
14
16
18
20
22
24
26
28
30
32
34
36
TIME, MIN.

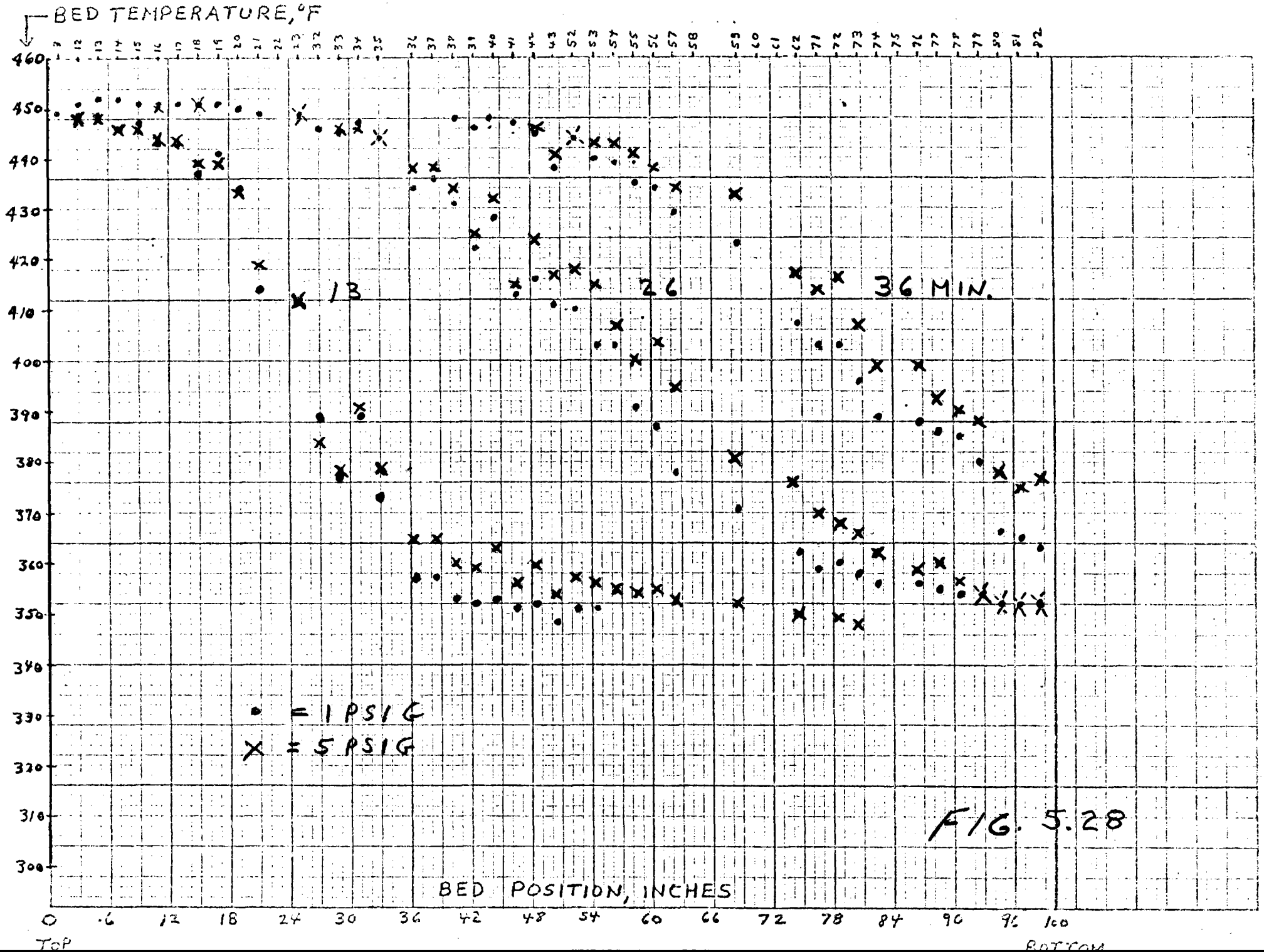
BED TEMPERATURE, °F
460
450
440
430
420
410
400
390
380
370
360
350
340
330
320
310
300
1B
2C
36 MIN.
• = 1 PSIG
X = 5 PSIG
BED POSITION, INCHES
0
6
12
18
24
30
36
42
48
54
60
66
72
78
84
90
96
100
TOP
BOTTOM

FIG. 5.28

5.1.3 4 GPM Charge

Figure 5.29 shows the initial centerline profile and the profiles at 15, 47 and 72 minutes. The initial radial profiles and the integrated average axial profiles are shown in figures 5.30 and 5.31 respectively. The temperatures from figure 5.31 and the fluid inlet temperature* histories were used as inputs to the model.

Figures 5.32 and 5.33 show the model results in comparison to the measured profiles at $\frac{Ro}{2}$ and near the wall along with the measured centerline profiles. At this flow rate, the effects of fluid mal-distribution are becoming evident. Here the centerline slope is showing the effect of lean direct flow with considerable flow inward and cooler fluid reaching the centerline. The model and measured slopes are in better agreement at the $\frac{Ro}{2}$ and near wall position.

5.1.3.1 Fluid Exit Temperature

Figure 5.34 shows the measured and radial fluid exit temperatures. The agreement is poorer at this flow rate primarily due to the greater heat loss in the tank bottom and exit line due to the previously mentioned pump coolant effect. At this flow rate there is a 5 minute residence time in the tank bottom (capacity~ 20 gallons).

*The fluid inlet temperature for this test was 430°F.

FIG. 5.29

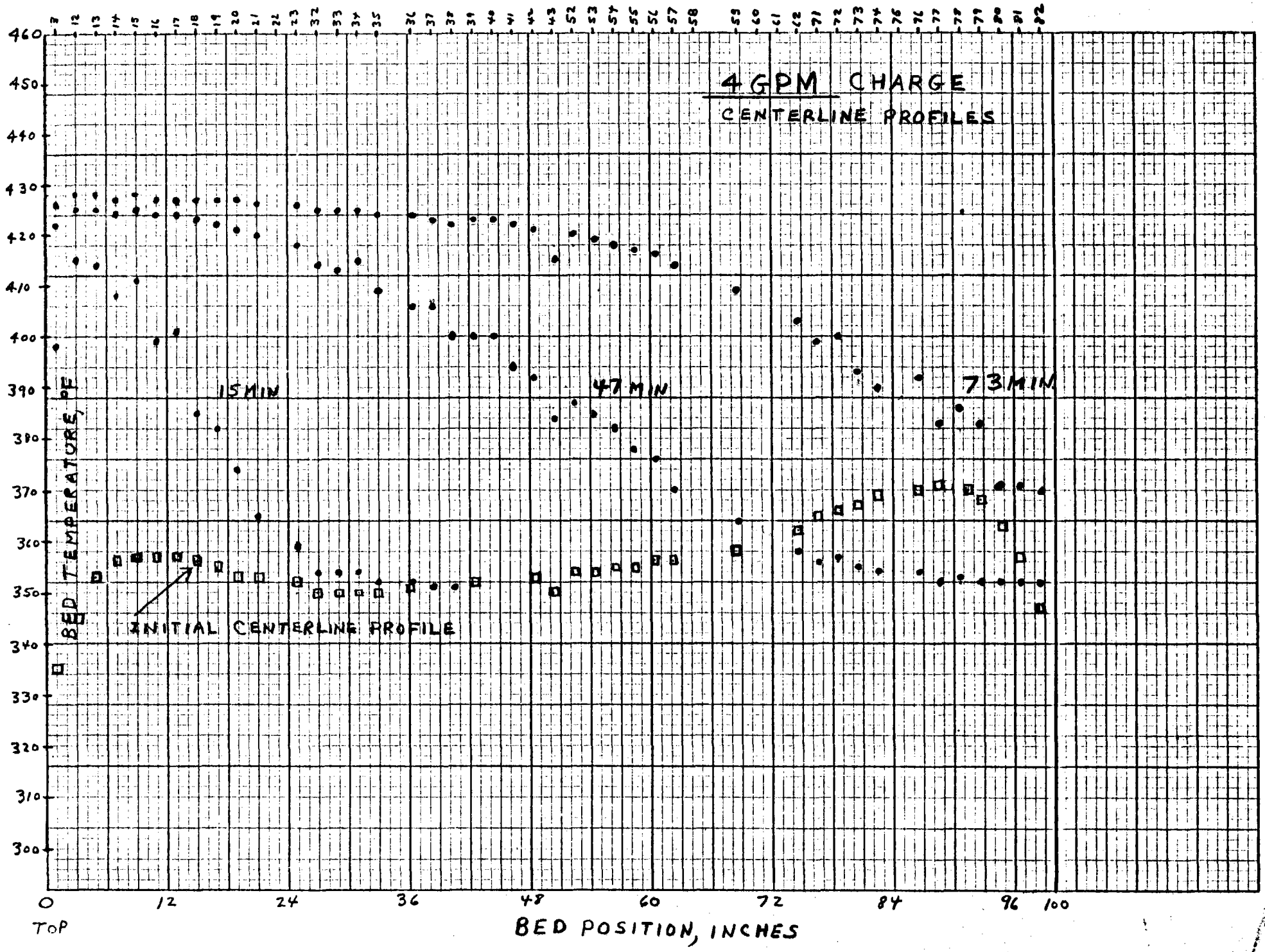

FIG. 5.30

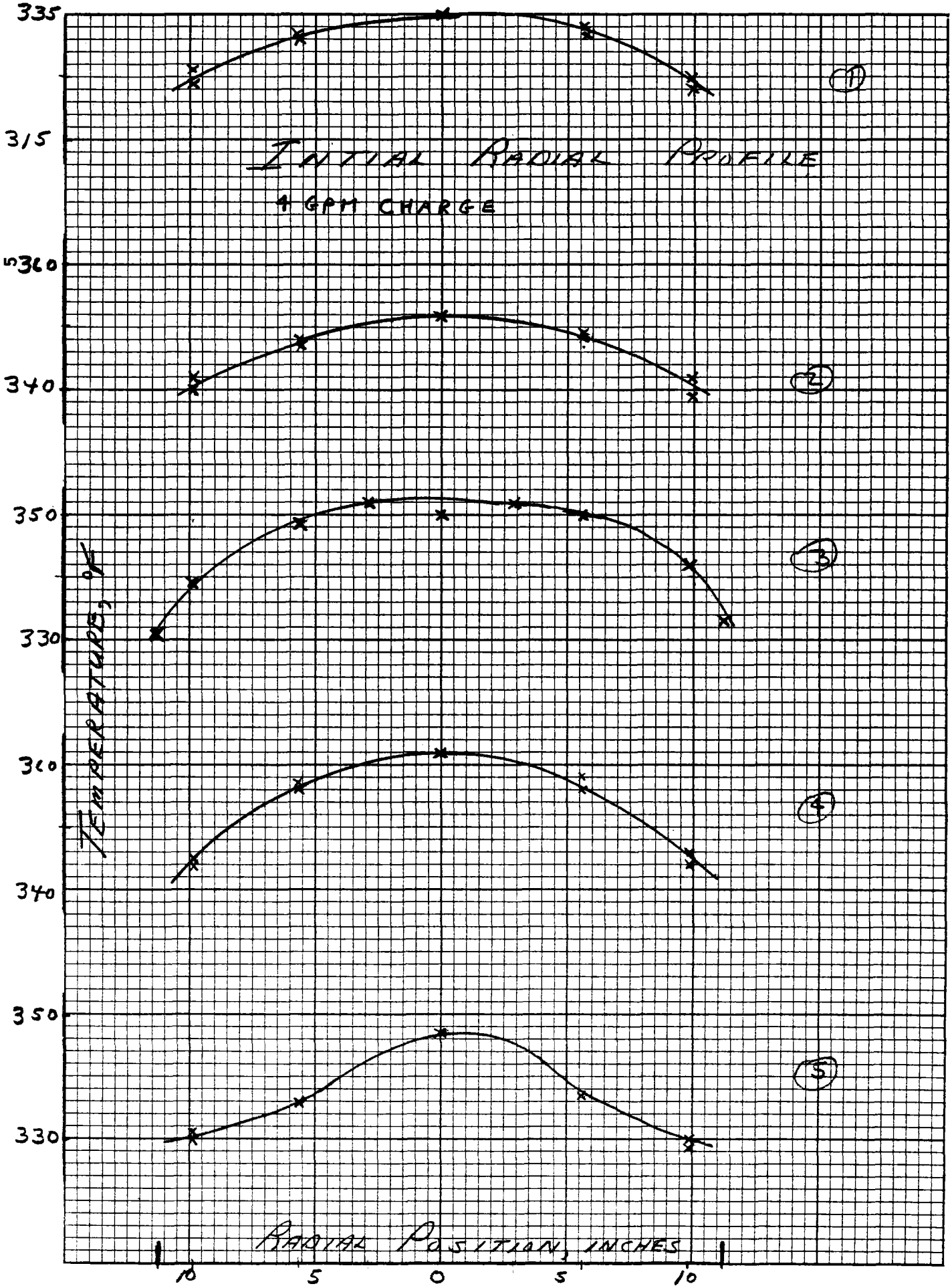
INITIAL RADIAL PROFILE
4 GPM CHARGE
335
315
360
340
350
330
360
340
350
330
TEMPERATURE, °F
1
2
3
4
5
10
5
0
5
10
RADIAL POSITION, INCHES

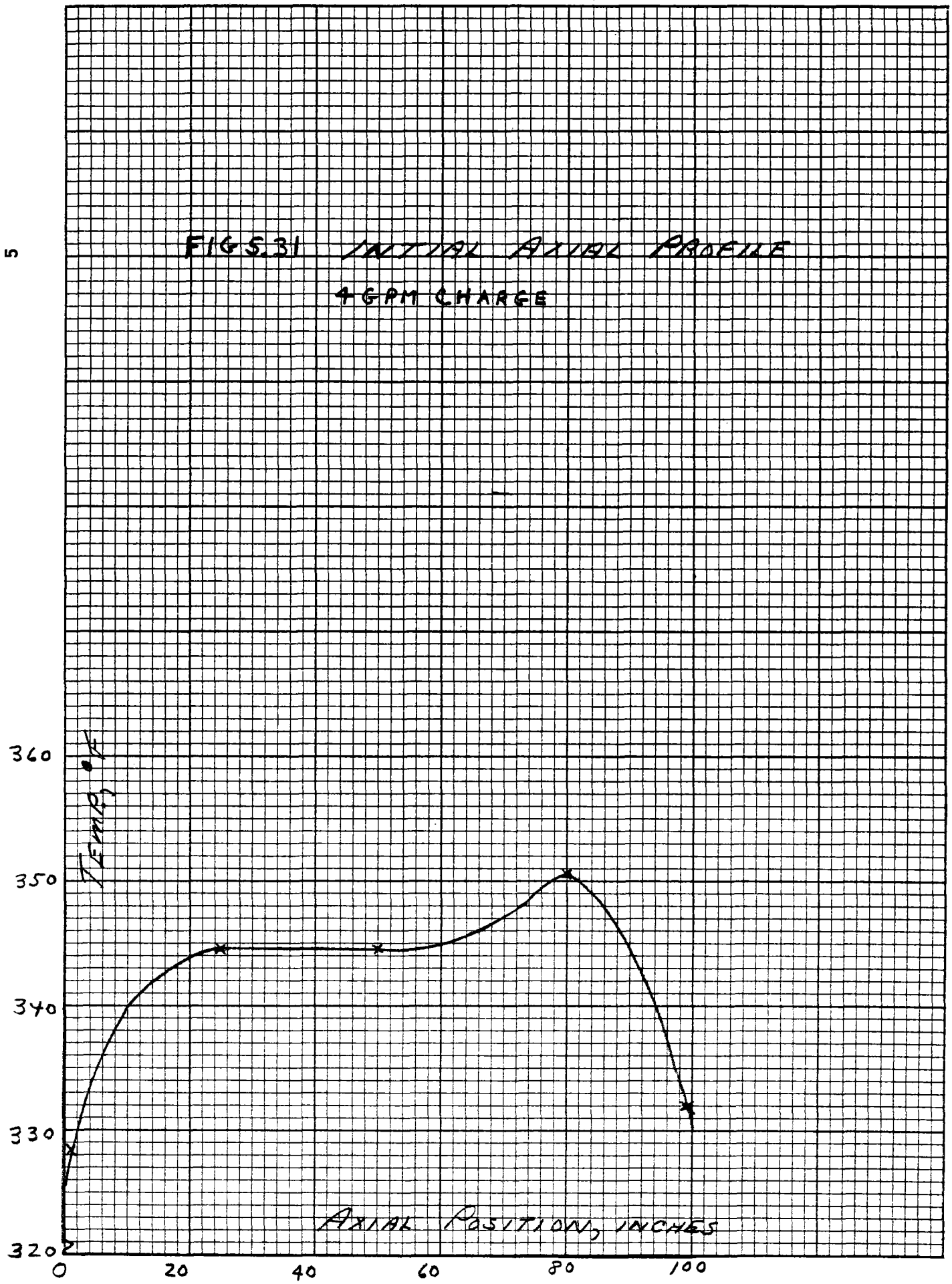
FIG 5.31 INITIAL AXIAL PROFILE
4 GPM CHARGE
360
350
340
330
320
TEMP, °F
0
20
40
60
80
100
AXIAL POSITION, INCHES

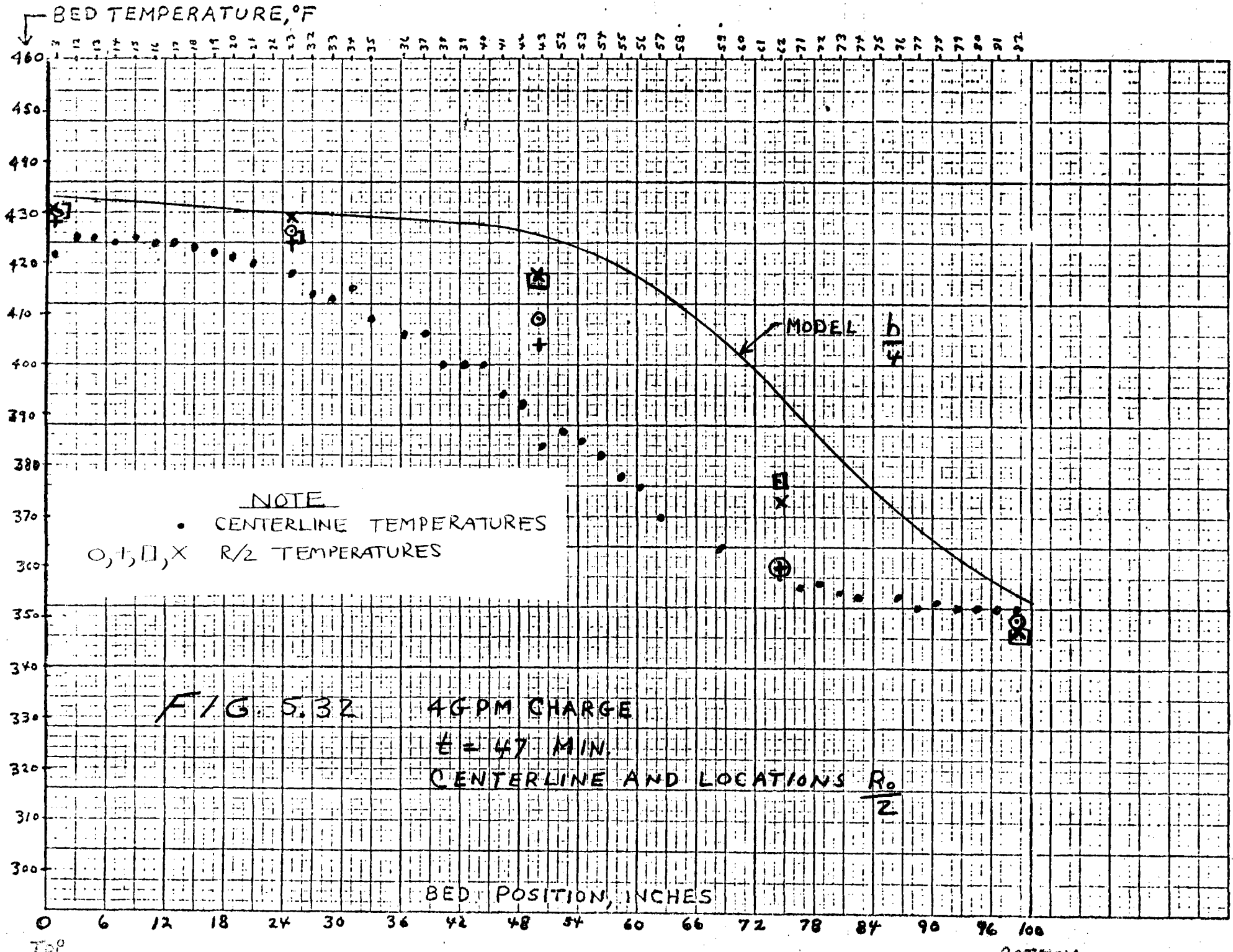
BED TEMPERATURE, °F
460
450
440
430
420
410
400
390
380
370
360
350
340
330
320
310
300
MODEL h/4
NOTE
• CENTERLINE TEMPERATURES
○, +, □, X R/2 TEMPERATURES
FIG. 5.32 46 PM CHARGE
t = 47 MIN.
CENTERLINE AND LOCATIONS Ro/2
BED POSITION, INCHES
0
6
12
18
24
30
36
42
48
54
60
66
72
78
84
90
96
100
TOP
BOTTOM

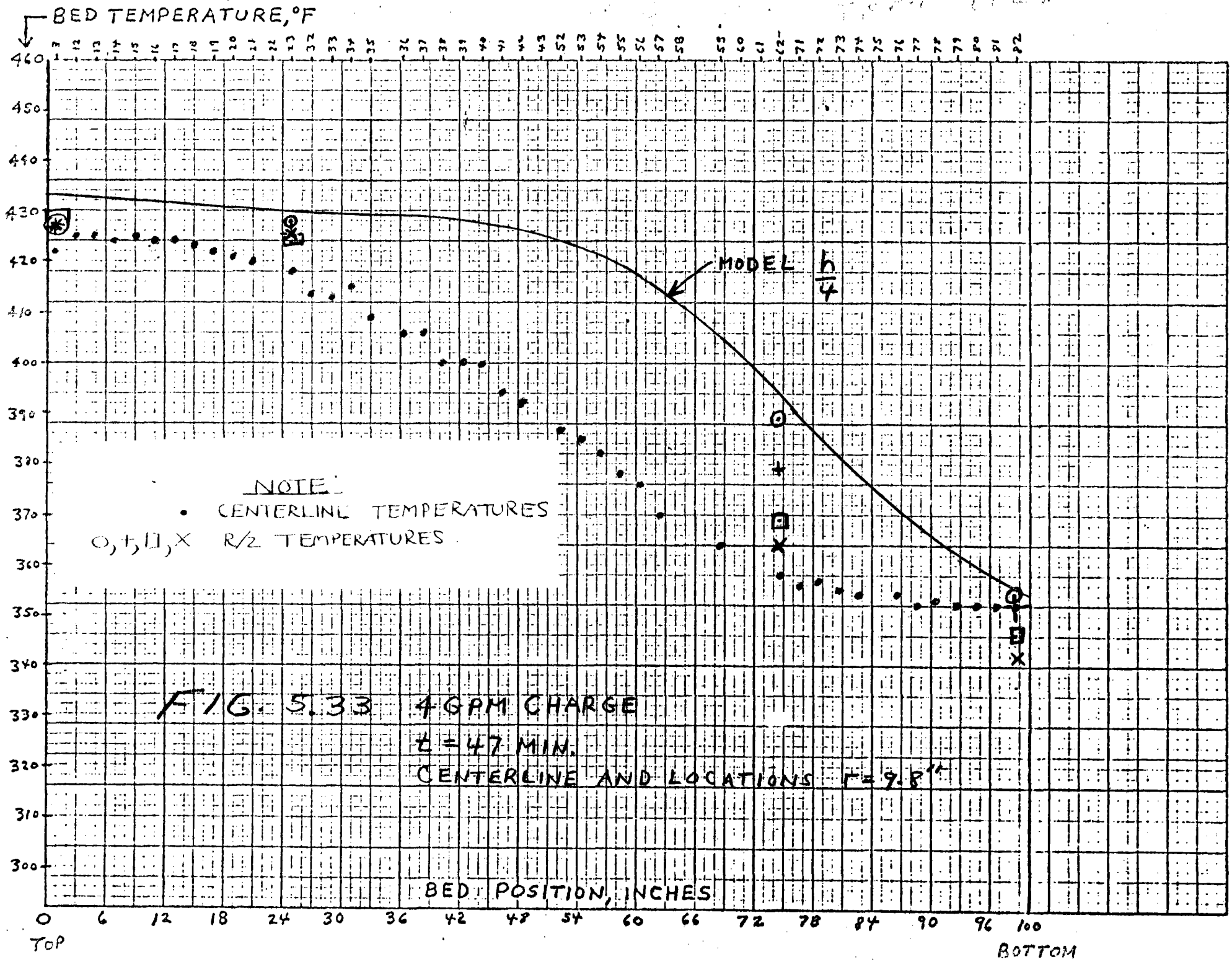
BED TEMPERATURE, °F
460
450
440
430
420
410
400
390
380
370
360
350
340
330
320
310
300
MODEL h/4
NOTE:
• CENTERLINE TEMPERATURES
○, +, □, X R/2 TEMPERATURES
FIG. 5.33 4 GPM CHARGE
t = 47 MIN.
CENTERLINE AND LOCATIONS r = 9.8"
BED POSITION, INCHES
0 6 12 18 24 30 36 42 48 54 60 66 72 78 84 90 96 100
TOP
BOTTOM

FIG. 5.34

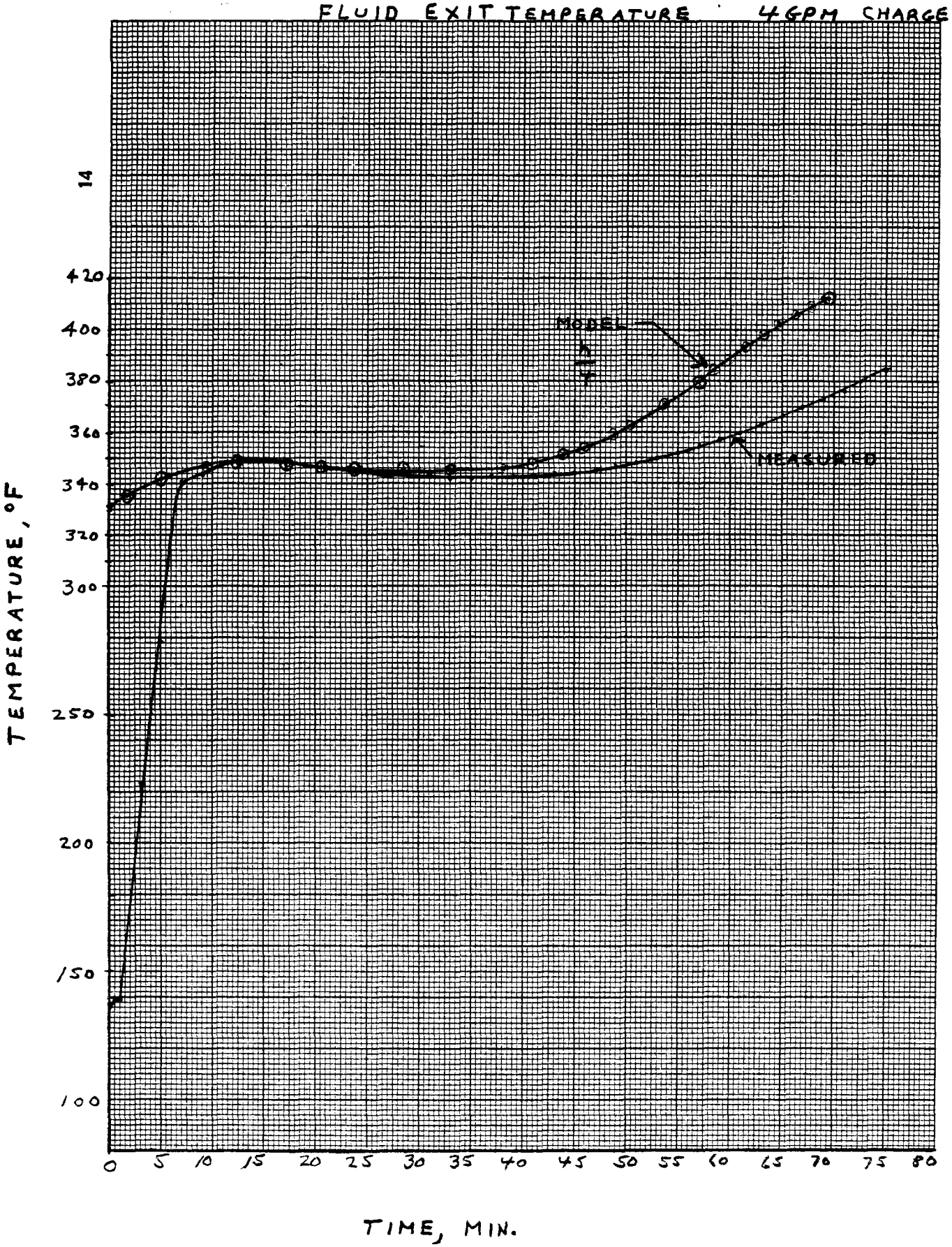
FLUID EXIT TEMPERATURE 4 GPM CHARGE
14
420
400
380
360
340
320
300
250
200
150
100
MODEL
MEASURED
TEMPERATURE, °F
0 5 10 15 20 25 30 35 40 45 50 55 60 65 70 75 80
TIME, MIN.

5.1.4 1 GPM Charge

At a flow rate of 1 GPM it was not possible to charge the bed uniformly. The preferential flow to the outer ring(s) (see Section 5.6) was so great that the bed temperature profiles shown in figure 5.35 resulted. It is seen that after 5 hours the bed centerline temperature had risen only a few degrees in the top half of the bed, and the temperatures at $\frac{Ro}{2}$ and near the wall are progressively higher in the higher flow regions. Visual observation through the view port at the top of the tank confirmed that flow was from the outer periphery though it was not possible to discern whether the flow was through the outer ring only or the outer two rings. Assuming predominant flow in the outer ring, the test shows that the space between fluid outlet ports must be considerably less than 20 inches at this flow rate (140 lbs/ft^2hr) The test was not repeated because of lack of funding and the judgement that very little charging would be done at this very low flow rate in the actual system.

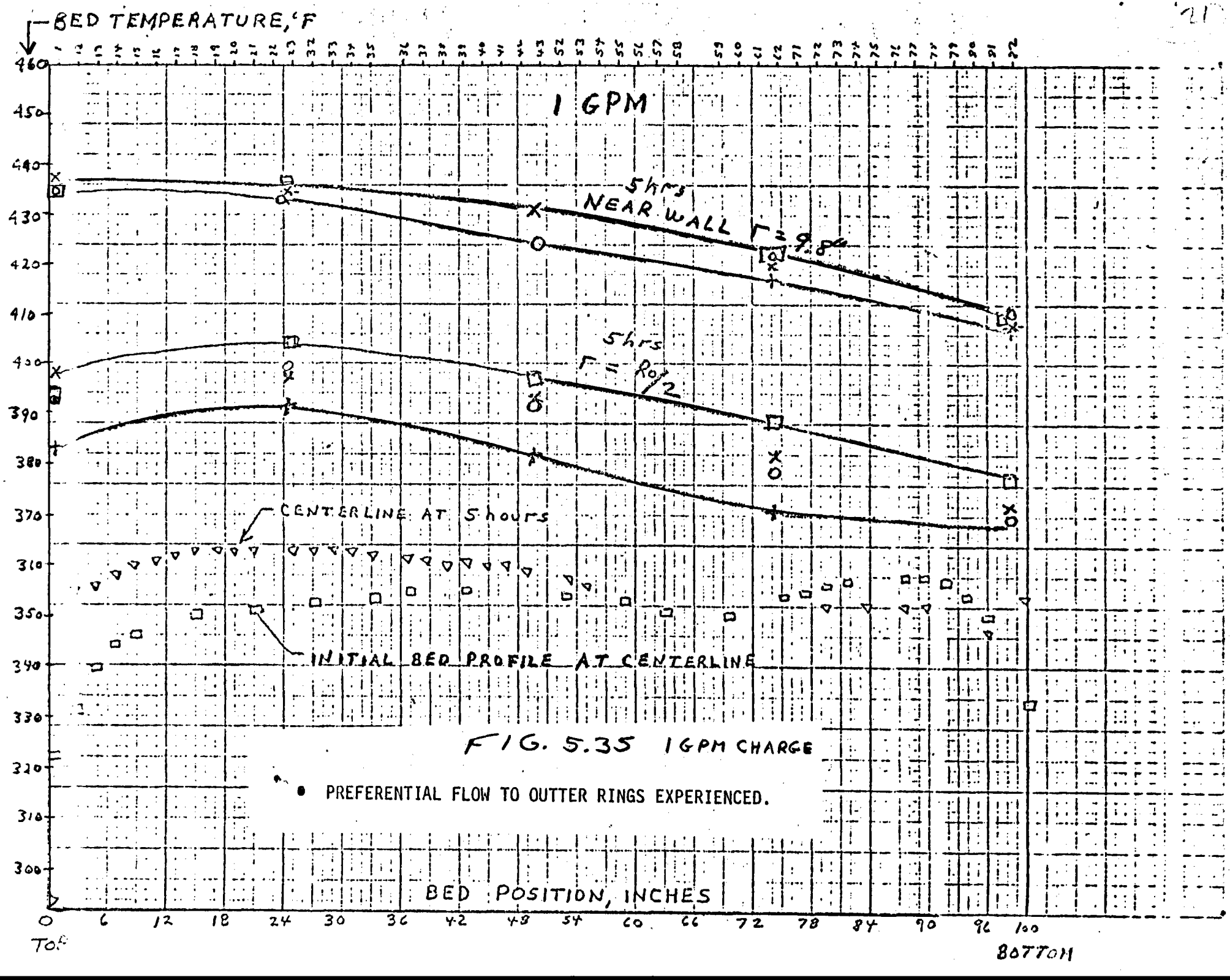

FIG. 5.35 1 GPM CHARGE

• PREFERENTIAL FLOW TO OUTTER RINGS EXPERIENCED.

DISCHARGING TESTS

5.2 Discharging Tests

Discharge tests were run at 4.0 and 9.6 GPM. The planned discharge test at 1 GPM was not run because of the failure to charge the bed at 1 GPM due to the fluid distributor problem. The 9.6 GPM discharges were performed following the 17.2 GPM charge, and the two 8 GPM charges at 5 psig and 1 psig.

5.2.1 9.6 GPM Discharge Following 8 GPM Charge at 5 psig

Figures 5.36 and 5.37 show the initial bed centerline profile and the temperatures measured at $\frac{Ro}{2}$ and r=9.8 inches, respectively. Figure 5.38 is a plot of the radial distribution in the 5 planes at t=o. Figure 5.39 shows three centerline thermoclines at 12, 16, and 20 minutes. The model fit for t=20 minutes is shown in figures 5.40 and 5.41 for $\frac{Ro}{2}$ and r=9.8 inches. It is seen in discharging as in charging that the centerline temperature lags the temperature at $\frac{Ro}{2}$ and r=9.8 due to the outer ring preferential flow. The slope of the $\frac{h}{4}$ curve is seen to be a reasonable fit to data. It is also seen, as in the charging mode, that large radial gradients do not persist but are washed out as discharging proceeds.

5.2.1.1 Fluid Exit Temperature

Figure 5.42 shows the model and measured fluid exit temperature profiles. The model was run using the measured centerline temperature and the fluid inlet temperature history. The effect of using the integrated average temperature profile would be to lower the model temperature level but not change the slope. This is shown in section 5.2.3 where both temperature profiles were used.

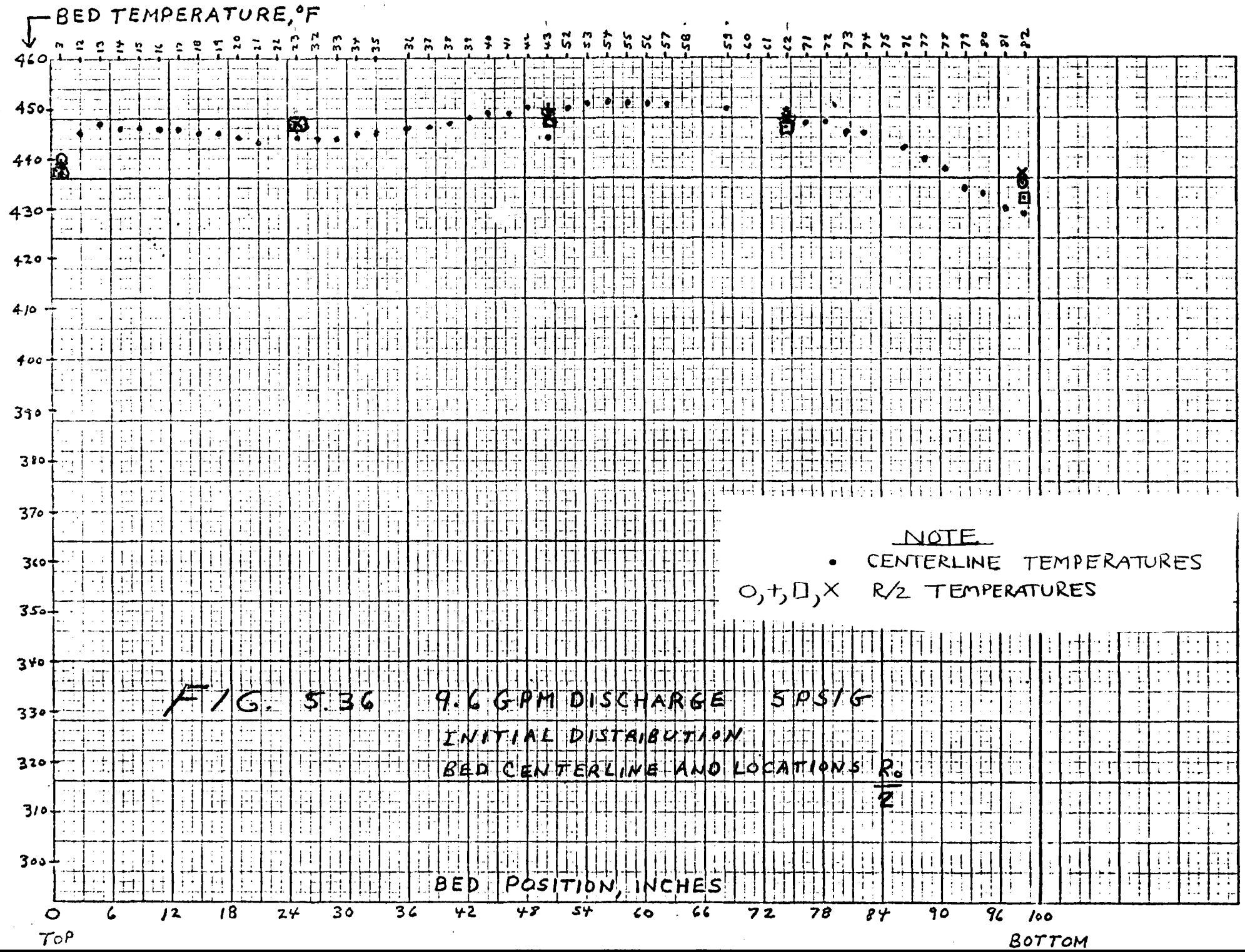
BED TEMPERATURE, °F
460
450
440
430
420
410
400
390
380
370
360
350
340
330
320
310
300
NOTE
• CENTERLINE TEMPERATURES
O, +, □, X R/2 TEMPERATURES
FIG. 5.36 9.6 GPM DISCHARGE 5 PSIG
INITIAL DISTRIBUTION
BED CENTERLINE AND LOCATIONS R₀/2
BED POSITION, INCHES
0 6 12 18 24 30 36 42 48 54 60 66 72 78 84 90 96 100
TOP
BOTTOM

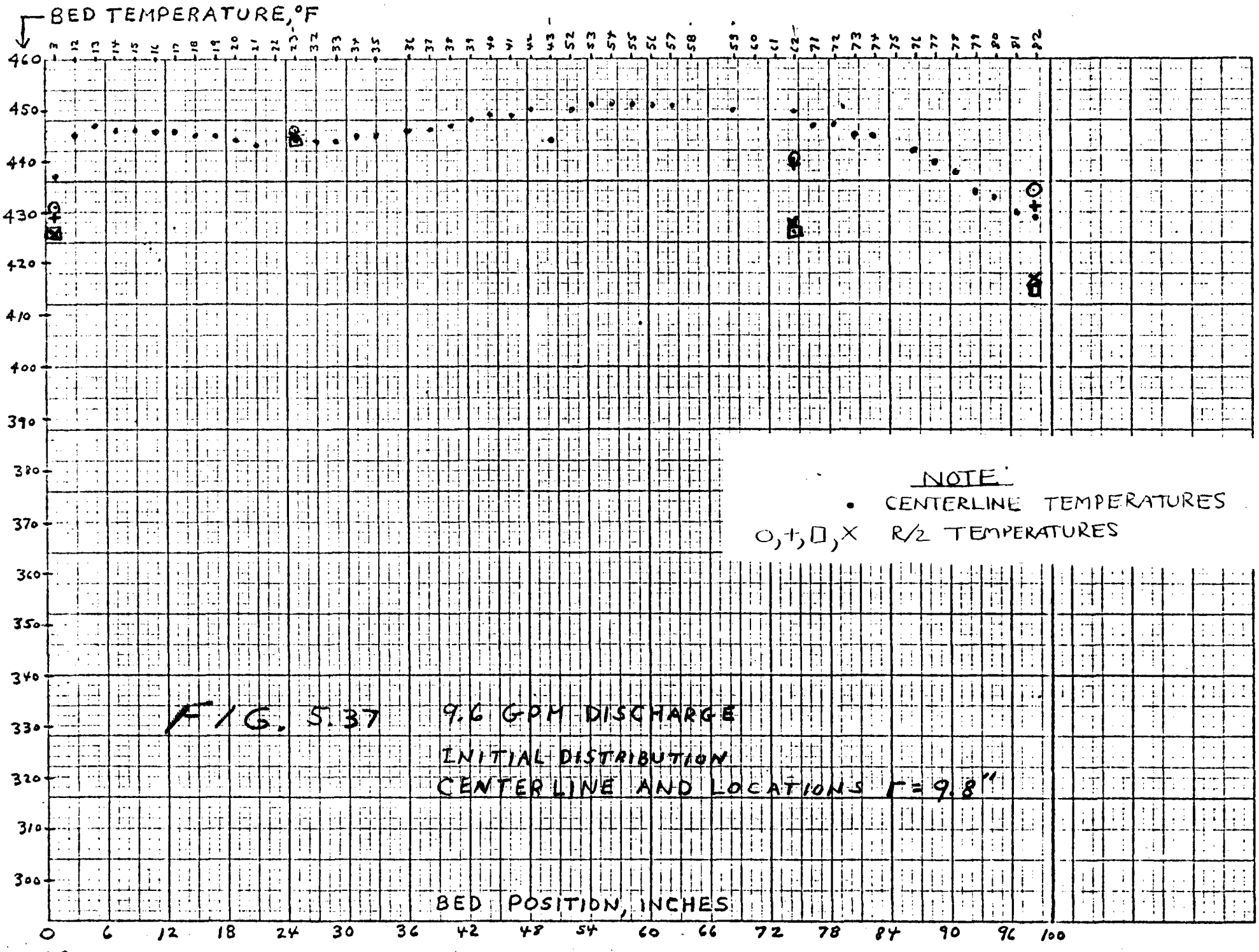
BED TEMPERATURE, °F
460
450
440
430
420
410
400
390
380
370
360
350
340
330
320
310
300
NOTE
• CENTERLINE TEMPERATURES
O, +, □, X R/2 TEMPERATURES
FIG. 5.37 9.6 GPM DISCHARGE
INITIAL DISTRIBUTION
CENTER LINE AND LOCATIONS t = 9.8'
BED POSITION, INCHES
0 6 12 18 24 30 36 42 48 54 60 66 72 78 84 90 96 100
TOP
BOTTOM

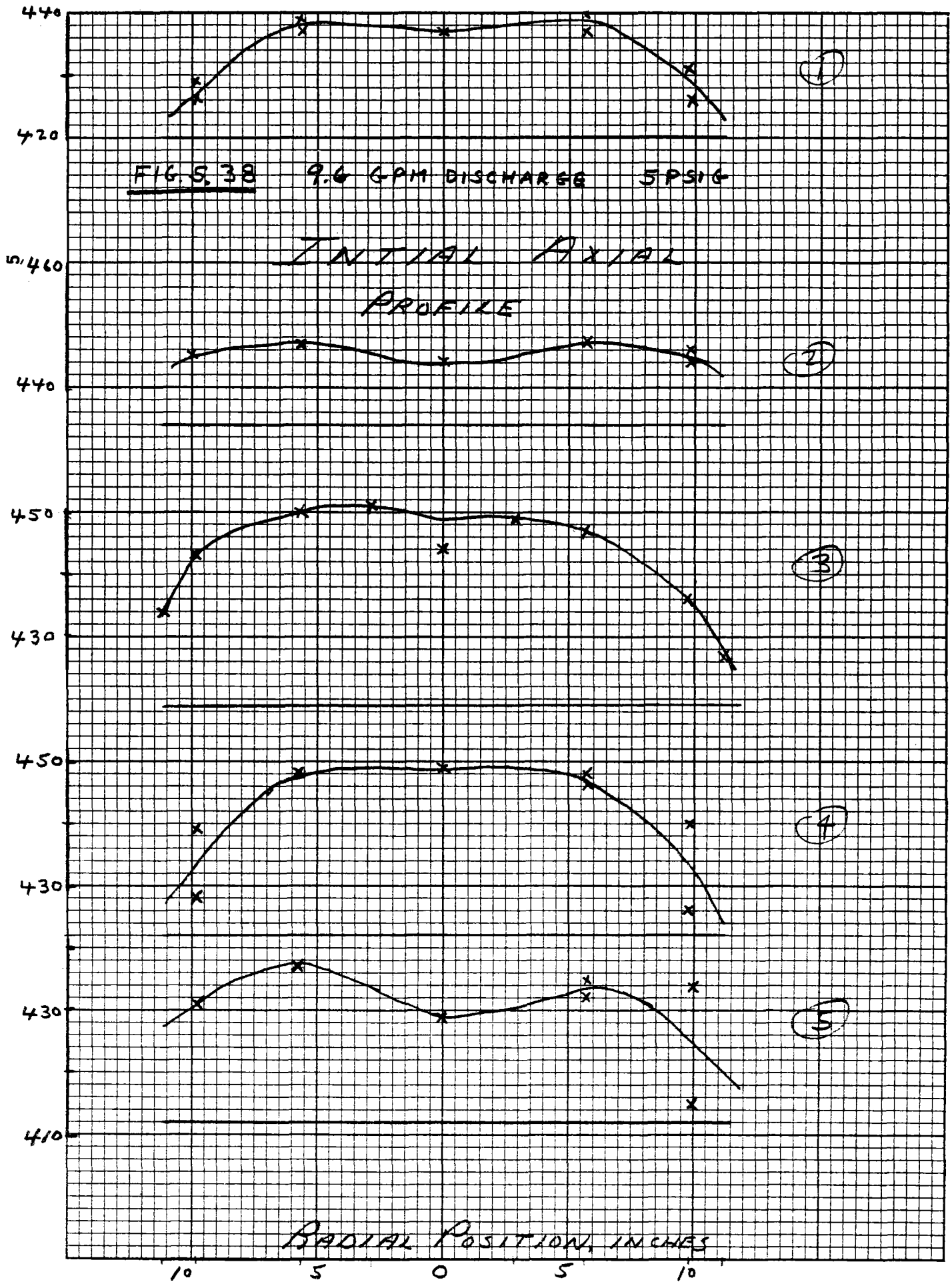
FIG. 5.38 9.6 GPM DISCHARGE 5PSIG
INITIAL AXIAL PROFILE
440
420
460
440
450
430
450
430
430
410
1
2
3
4
5
10
5
0
5
10
RADIAL POSITION, INCHES

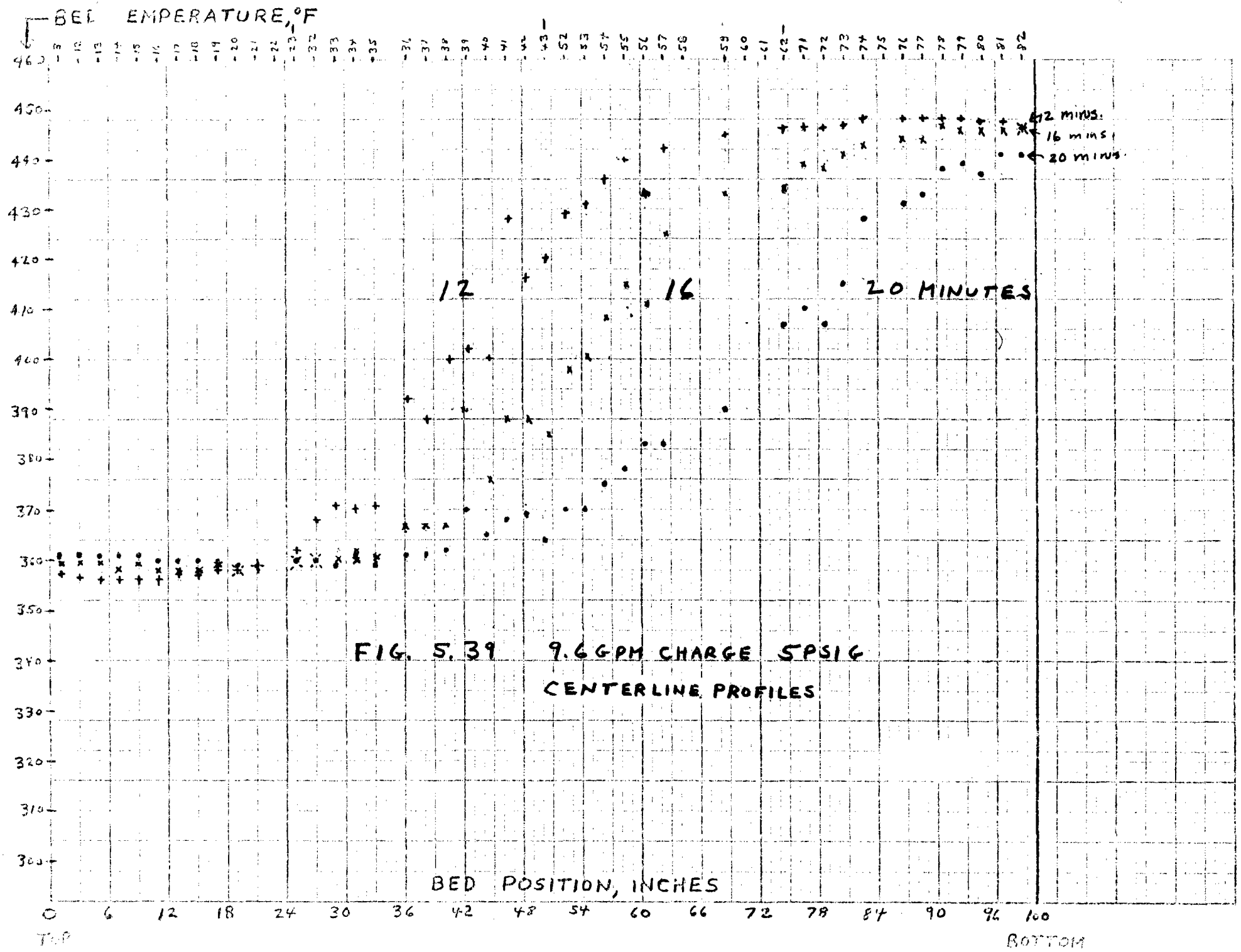

FIG. 5.39 9.6 GPM CHARGE 5 PSIG
CENTERLINE PROFILES

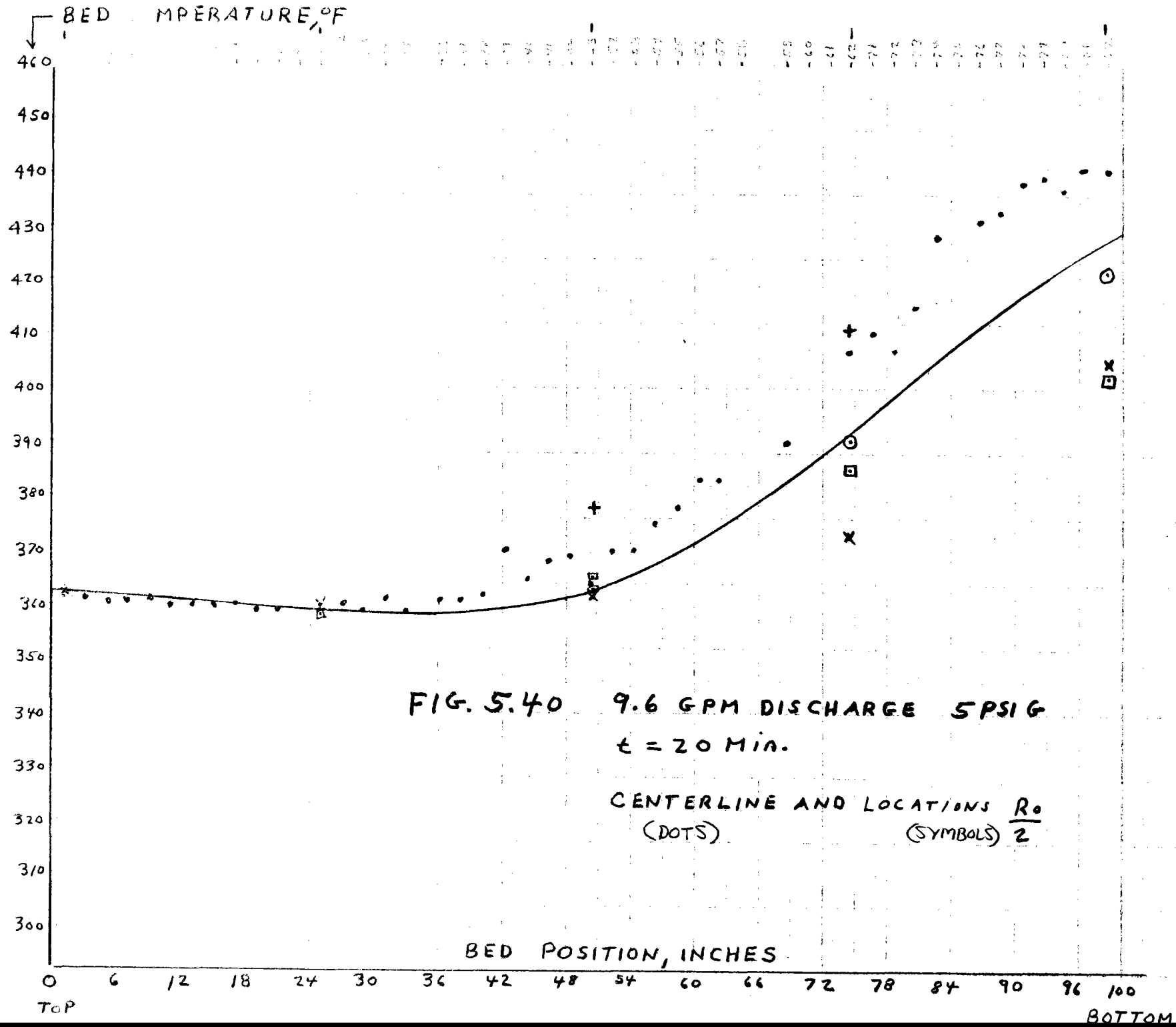

FIG. 5.40 9.6 GPM DISCHARGE 5 PSIG
$t = 20$ Min.

CENTERLINE AND LOCATIONS $\frac{R_o}{2}$
(DOTS) (SYMBOLS)

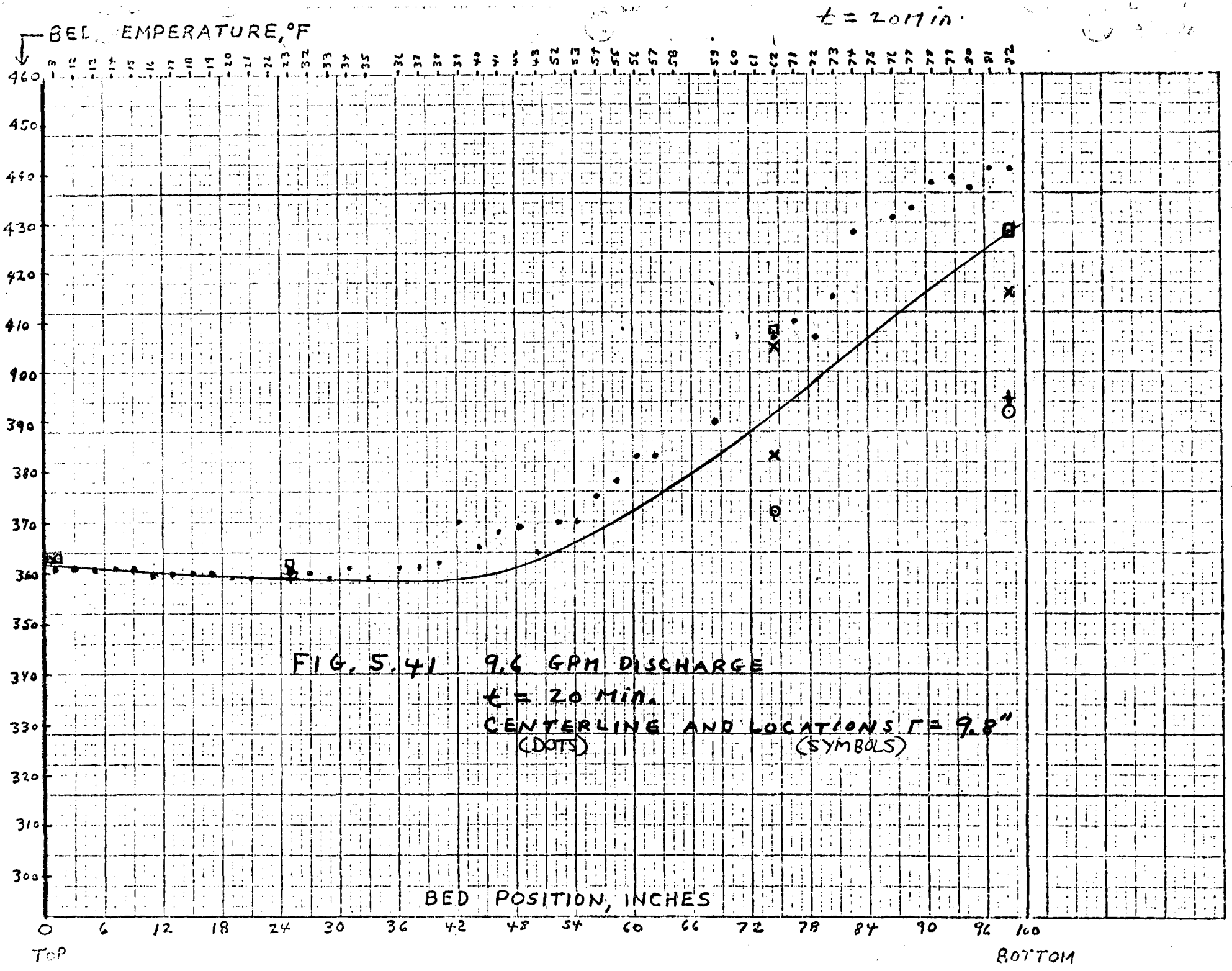

FIG. 5.41 9.6 GPM DISCHARGE
$t = 20$ MIN.
CENTERLINE AND LOCATIONS $r = 9.8$"
(DOTS) (SYMBOLS)

FIG. 5.42 9.6 GPM DISCHARGE 5 PSIG FLUID EXIT TEMP.

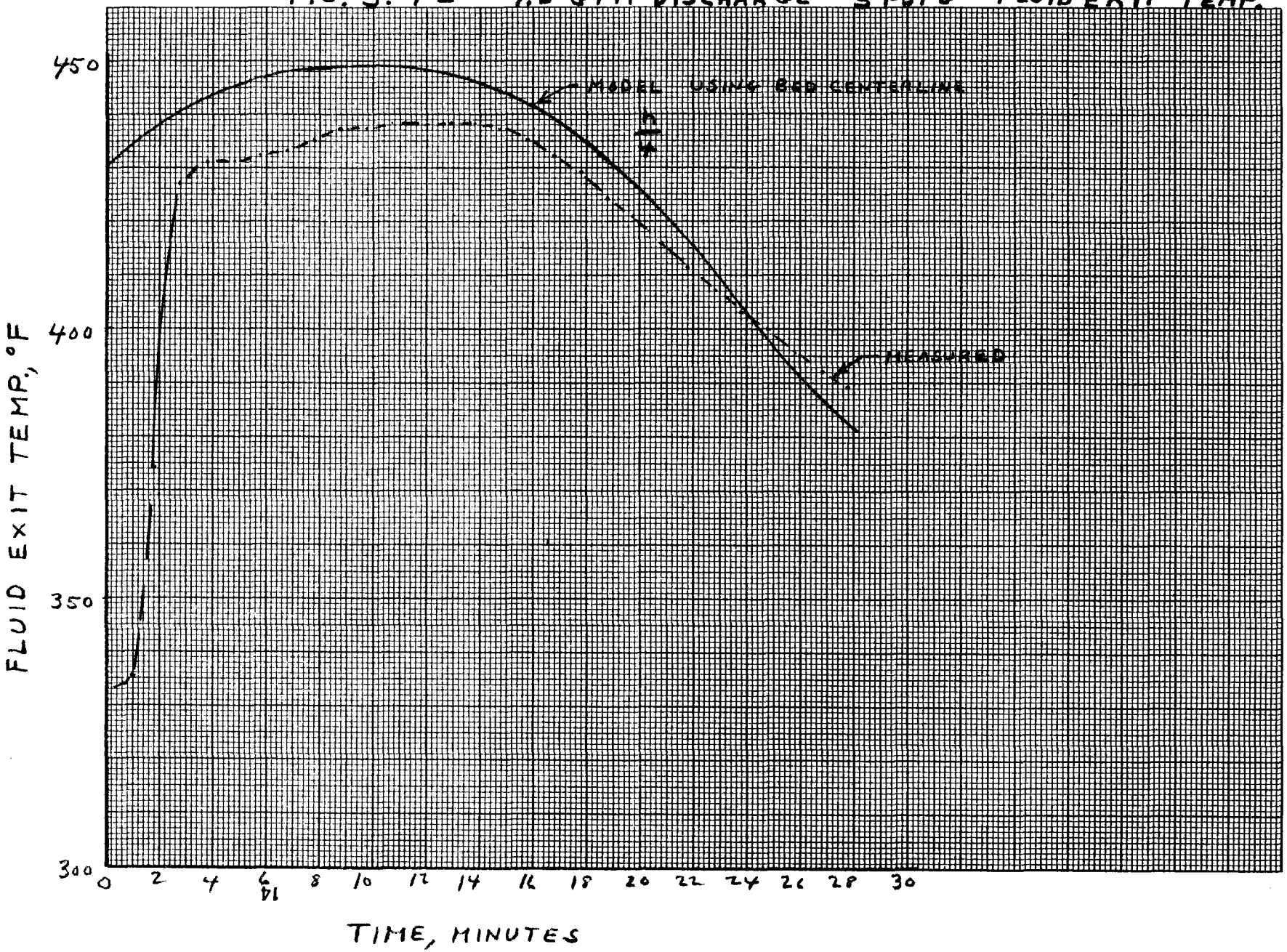

5.2.2 9.6 GPM Discharge Following 8 GPM Charge at 1 psig

Figures 5.43 and 5.44 show the initial bed centerline temperature profile and the temperatures measured at $\frac{Ro}{2}$ and r=9.8", respectively. Figure 5.45 shows the radial temperature distribution in the 5 planes at t=o. Figure 5.46 shows the centerline profiles measured at 12, 16 and 20 minutes. The model fit for t=20 minutes is shown in figures 5.47 and 5.48 for $\frac{Ro}{2}$ and r=9.8 inches. The model slope and the measured slopes are in good agreement and the steep radial gradients are again washed out as discharging proceeds.

5.2.2.1 Fluid Exit Temperatures

The measured and model fluid exit temperatures are shown in figure 5.49. The same comments apply as given in section 5.2.1.1.

5.2.2.2 Thermocline Comparison at 1 and 5 psig

Figure 5.50 shows the measured thermocline at the centerline for both pressures. There is no significant difference in the slopes of the curves.

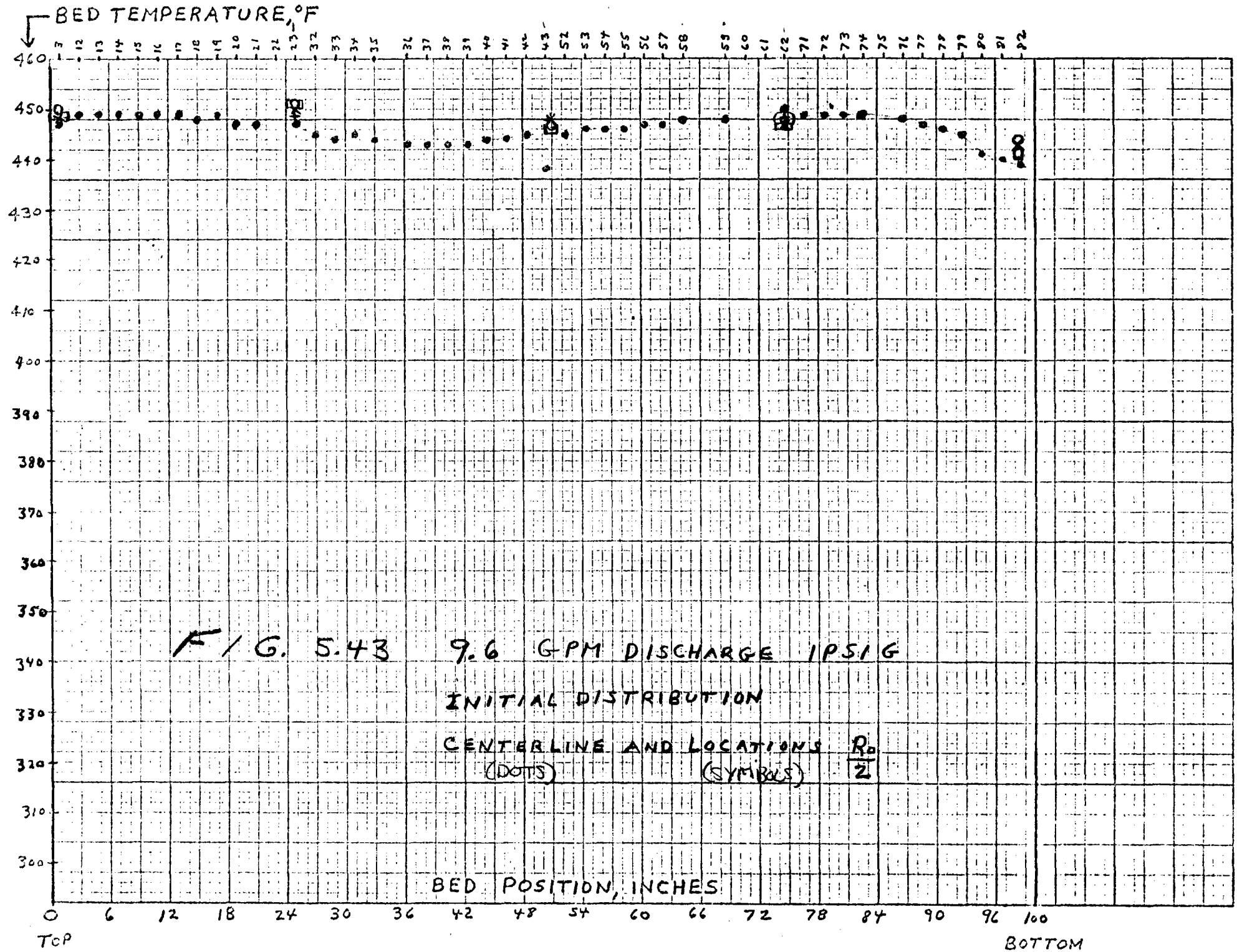
BED TEMPERATURE, °F
460
450
440
430
420
410
400
390
380
370
360
350
340
330
320
310
300
3 12 13 14 15 16 17 18 19 20 21 22 23 32 33 34 35 36 37 39 39 40 41 42 43 52 53 54 55 56 57 58 59 60 61 62 71 72 73 74 75 76 77 78 79 80 81 82
FIG. 5.43 9.6 GPM DISCHARGE IPSIG
INITIAL DISTRIBUTION
CENTERLINE AND LOCATIONS $\frac{R_o}{2}$
(DOTS) (SYMBOLS)
BED POSITION, INCHES
0 6 12 18 24 30 36 42 48 54 60 66 72 78 84 90 96 100
TOP
BOTTOM

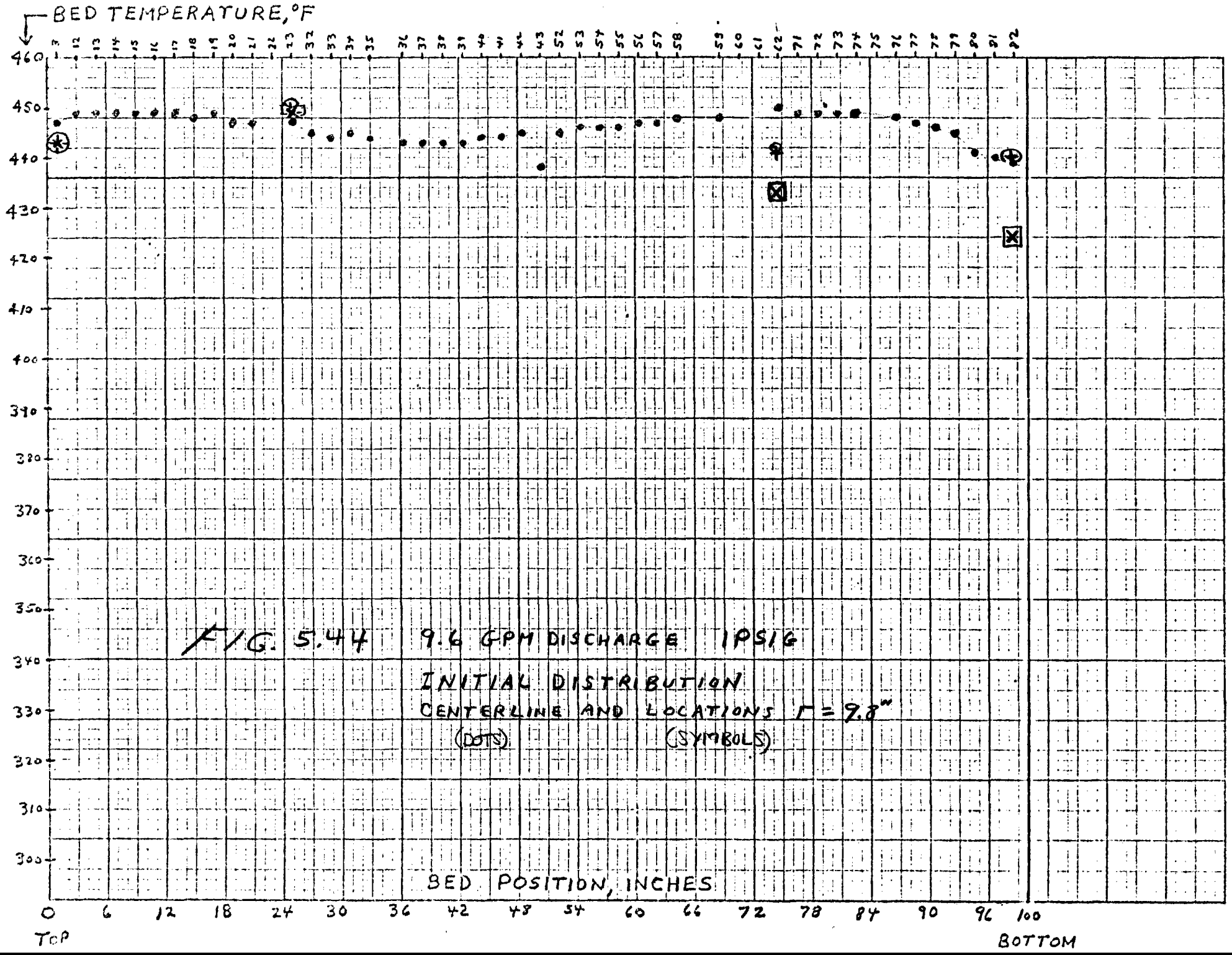
BED TEMPERATURE, °F
460
450
440
430
420
410
400
390
380
370
360
350
340
330
320
310
300
0
6
12
18
24
30
36
42
48
54
60
66
72
78
84
90
96
100
TOP
BOTTOM
BED POSITION, INCHES
FIG. 5.44 9.6 GPM DISCHARGE 1PSIG
INITIAL DISTRIBUTION
CENTERLINE AND LOCATIONS r = 9.8"
(DOTS)
(SYMBOLS)

FIG. 5.45 9.6 GPM DISCHARGE 1PSIG

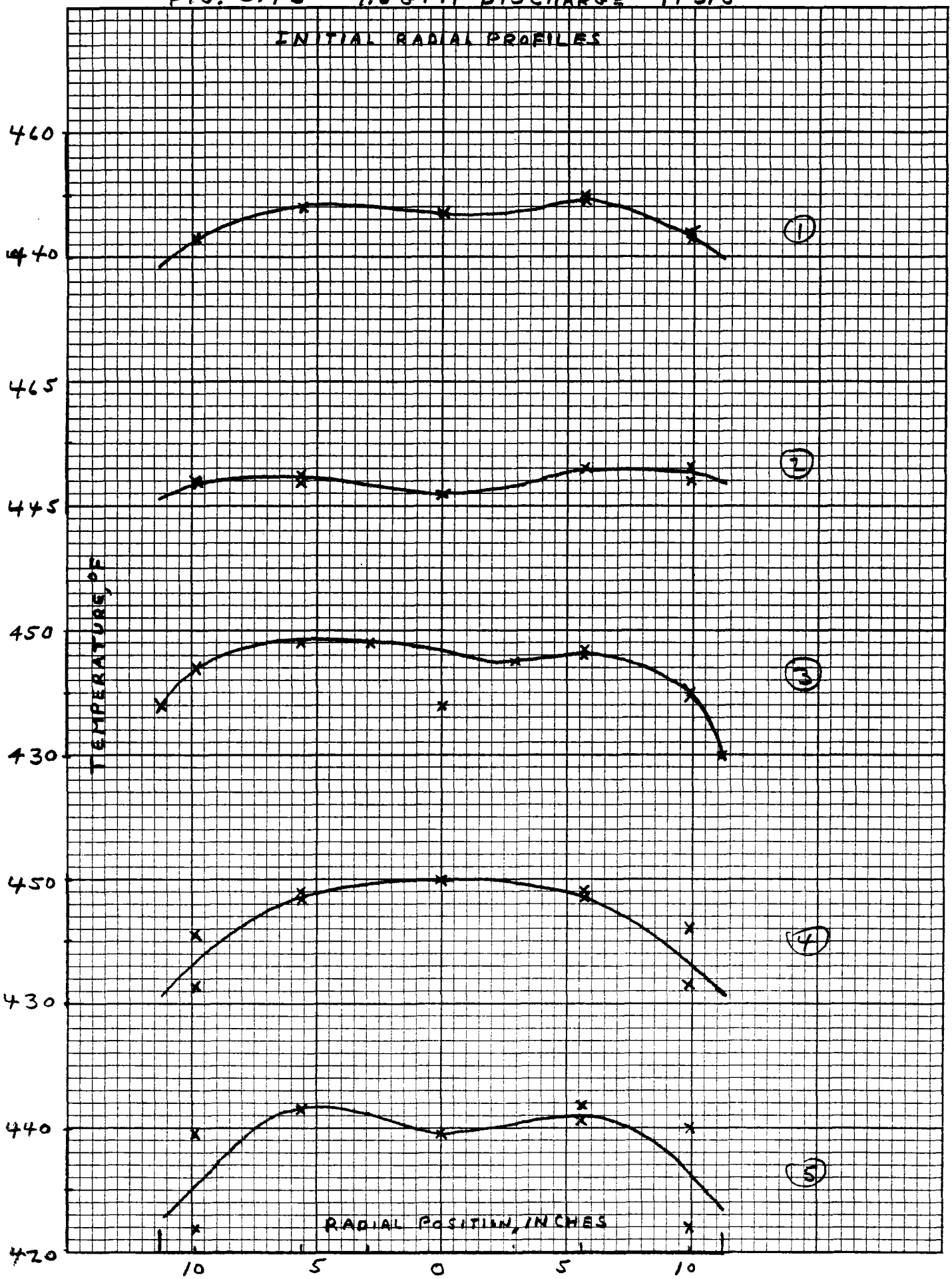

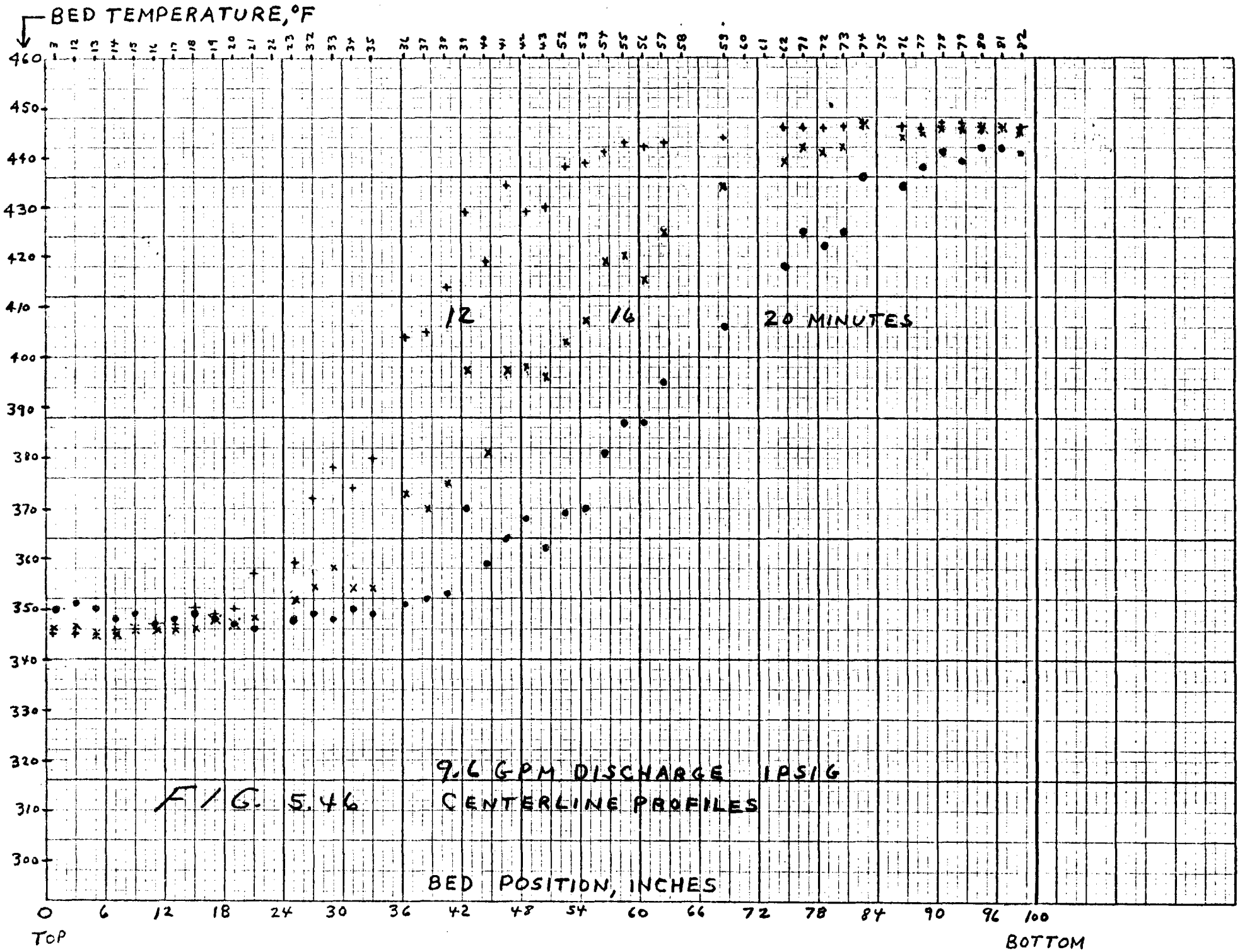
BED TEMPERATURE, °F
460
450
440
430
420
410
400
390
380
370
360
350
340
330
320
310
300
12
16
20 MINUTES
9.6 GPM DISCHARGE 1PSIG
CENTERLINE PROFILES
BED POSITION, INCHES
0
6
12
18
24
30
36
42
48
54
60
66
72
78
84
90
96
100
TOP
BOTTOM

FIG. 5.46

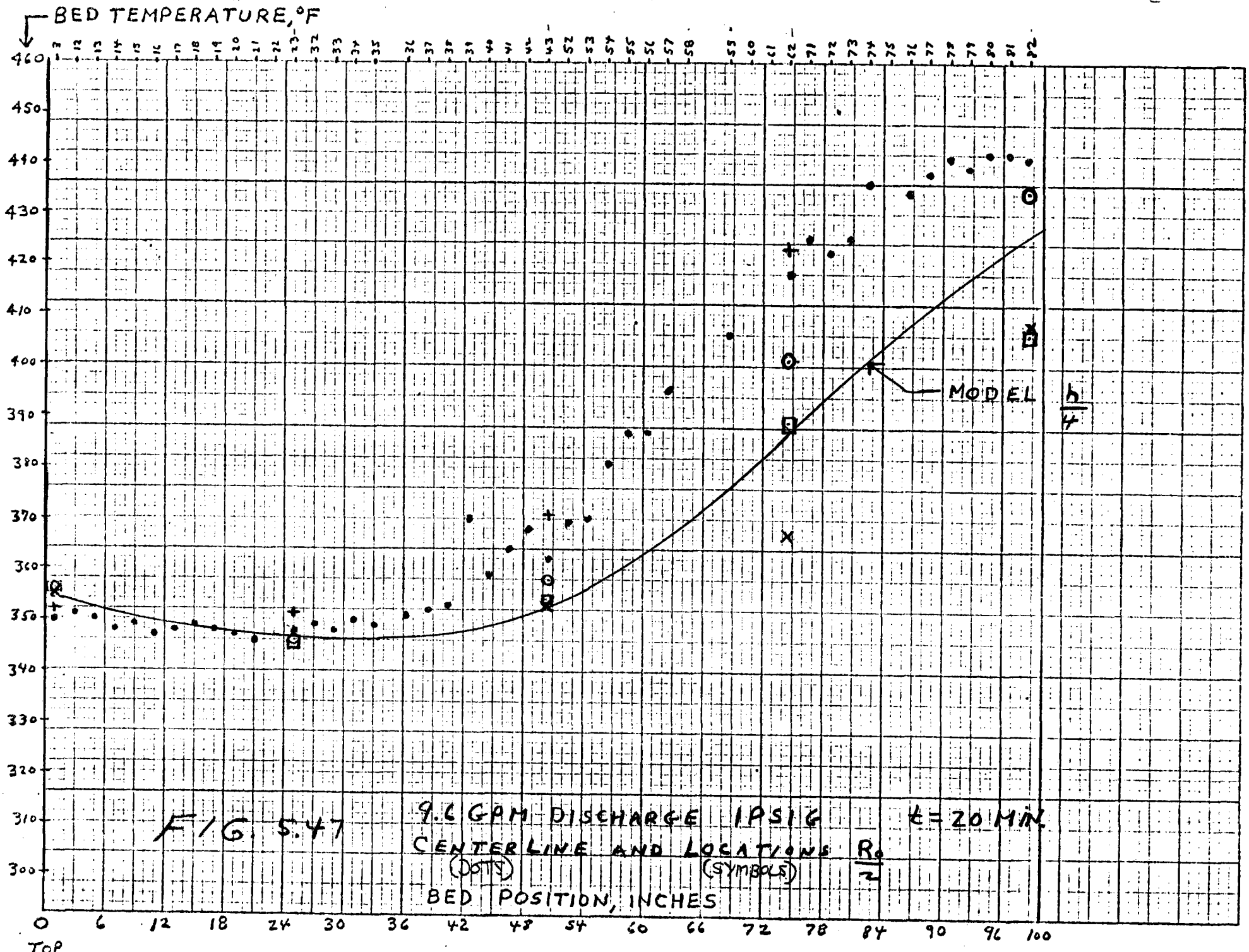

FIG. 5.47 9.6 GPM DISCHARGE 1 PSIG t = 20 MIN.
CENTERLINE AND LOCATIONS $\frac{R_o}{2}$
(DOTS) (SYMBOLS)

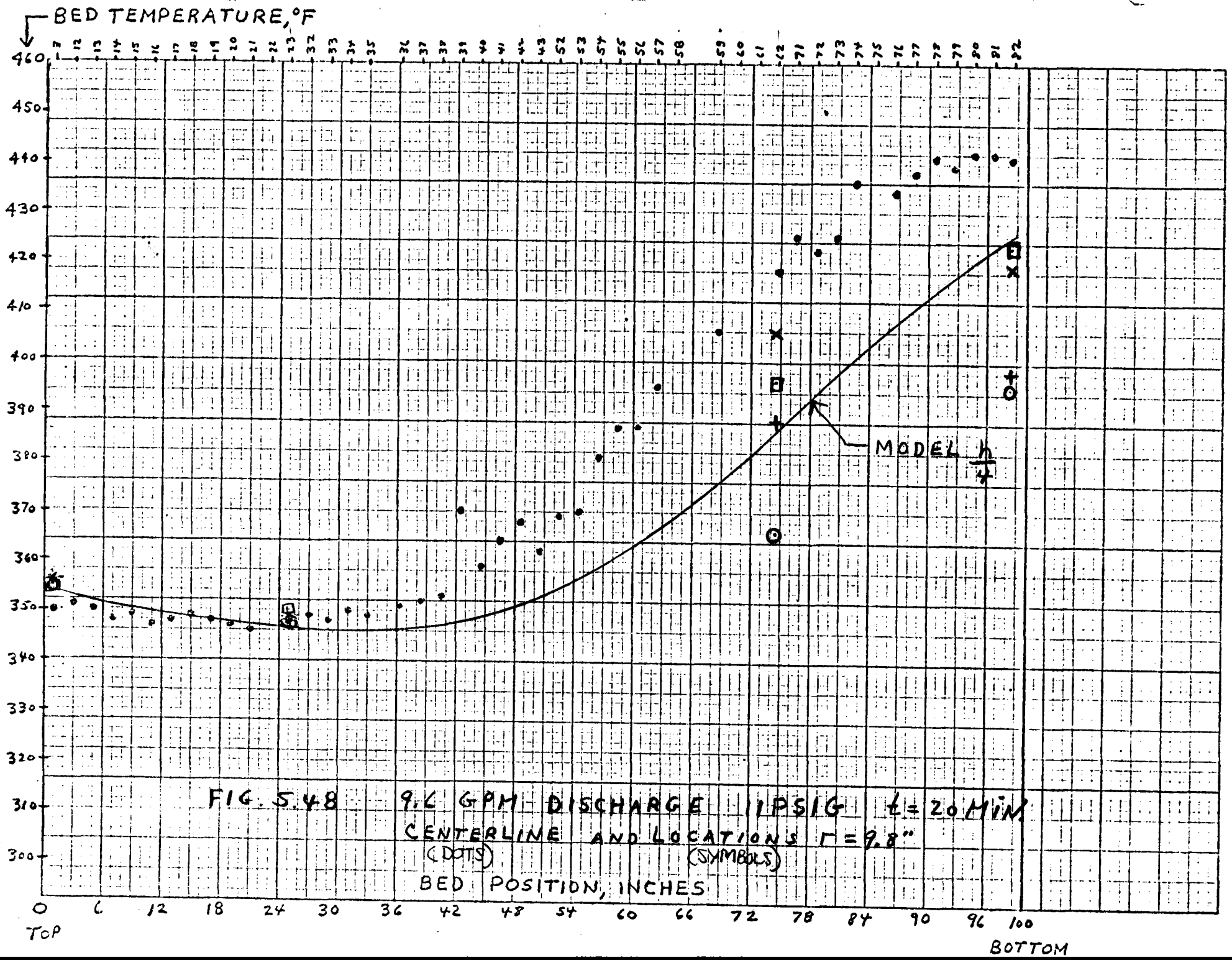

FIG. 5.48 9.6 GPM DISCHARGE 11 PSIG $t = 20$ MIN.
CENTERLINE AND LOCATIONS $r = 9.8$"
(DOTS) (SYMBOLS)

FIG. 5.49 9.6 GPM DISCHARGE 1PSIG FLUID EXIT TEMPERATURE

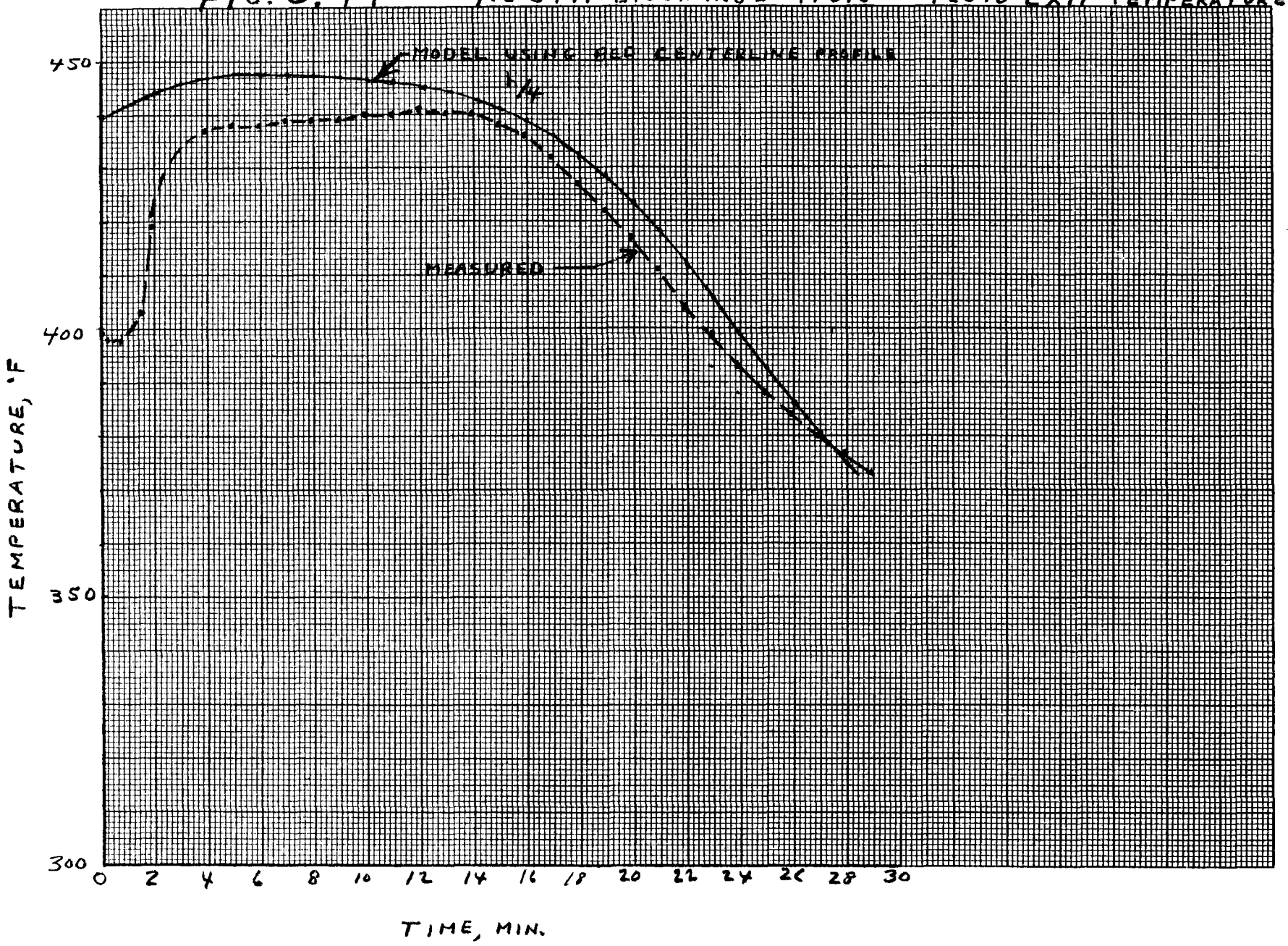

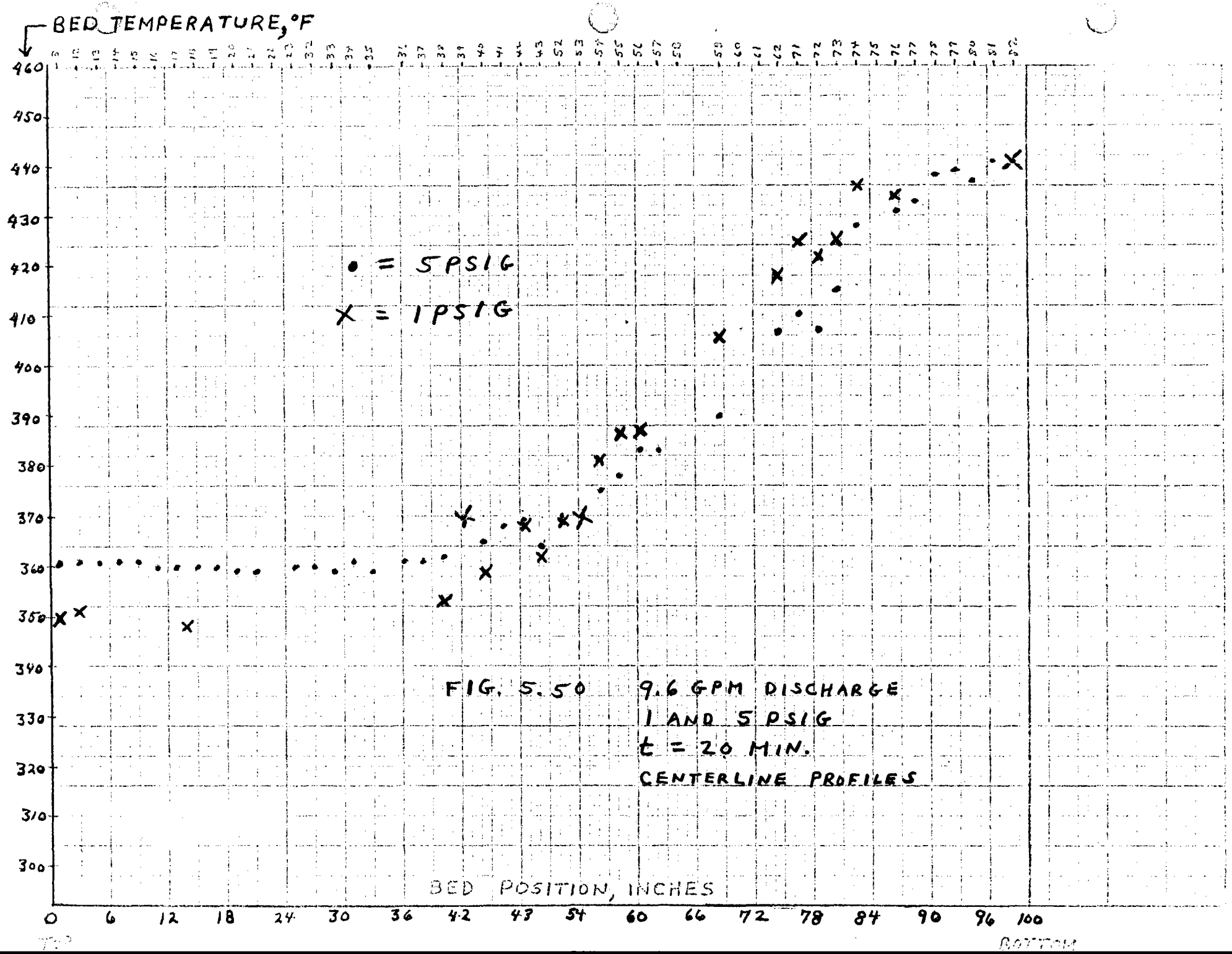

FIG. 5.50 9.6 GPM DISCHARGE
1 AND 5 PSIG
t = 20 MIN.
CENTERLINE PROFILES

5.2.3 9.6 GPM Discharge Following 17.2 GPM Charge

Prior to this discharge test, the bed was charged at 17.2 GPM. It was then held for 5½ hours, and discharged.

Figures 5.51 and 5.52 show the centerline and radial temperature distributions at $\frac{Ro}{2}$ and r=9.8" at the beginning of the discharge test as a function of axial position. Figure 5.53 shows the radial distribution in the 5 planes. From these profiles, the area weighted average temperature was calculated for each plane as plotted in figure 5.54. This profile was used as the initial condition in the model.

The model results and the measured data are shown in Figures 5.55 and 5.56 for t=16 minutes. As usual the centerline lags the outer temperatures. The slope of the model, however, is in good agreement with the off centerline profiles.

5.2.3.1 Fluid Exit Temperature

The measured and model fluid exit temperature are shown in figure 5.57. Model profiles are shown for two initial bed temperature profiles, one, the radial area weighted profile of figure 5.54 and the other, the bed centerline profile.

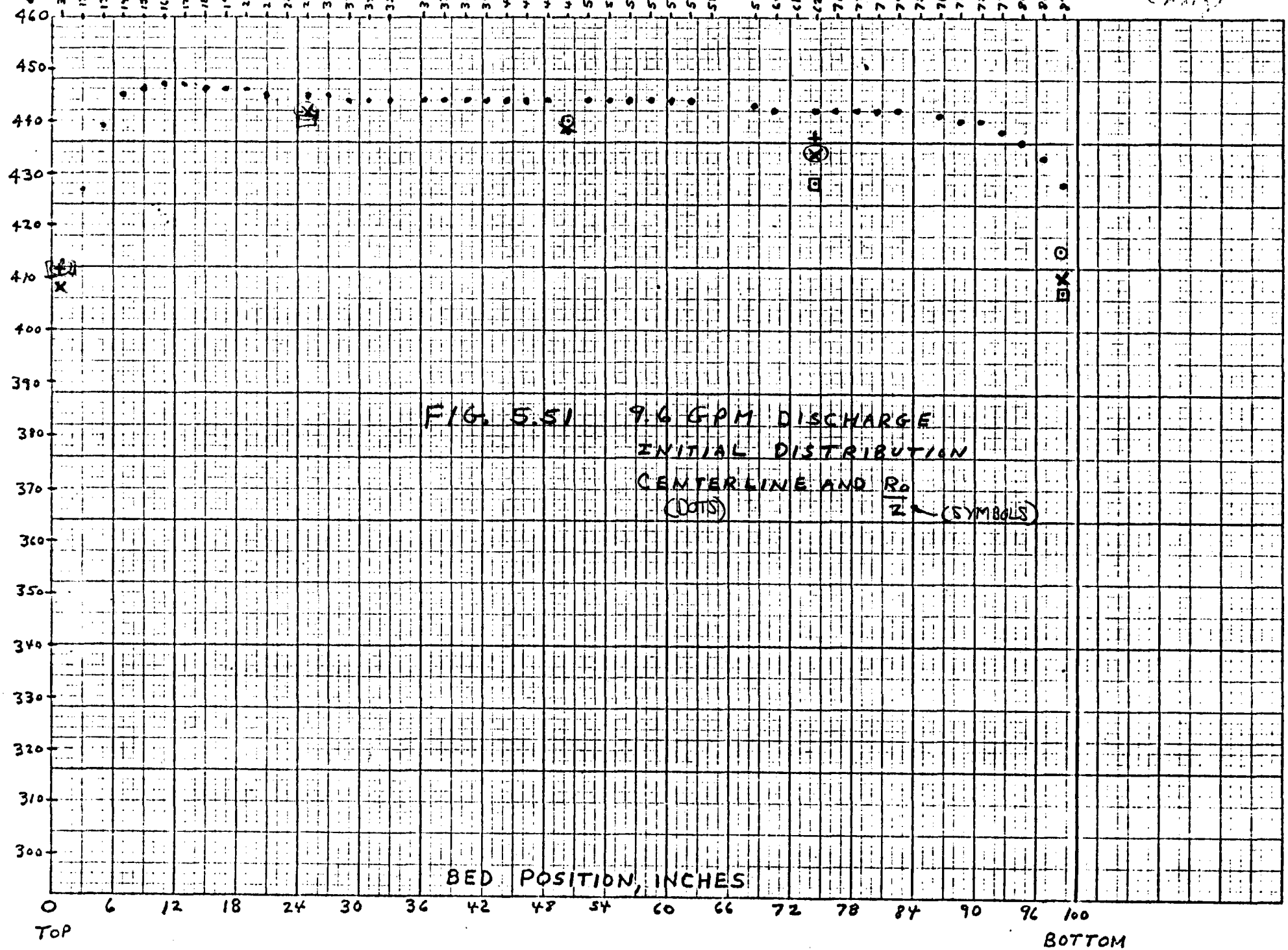
BED TEMPERATURE, °F
460
450
440
430
420
410
400
390
380
370
360
350
340
330
320
310
300
FIG. 5.51 9.6 GPM DISCHARGE
INITIAL DISTRIBUTION
CENTERLINE AND RO
(DOTS)
(SYMBOLS)
BED POSITION, INCHES
0
6
12
18
24
30
36
42
48
54
60
66
72
78
84
90
96
100
TOP
BOTTOM

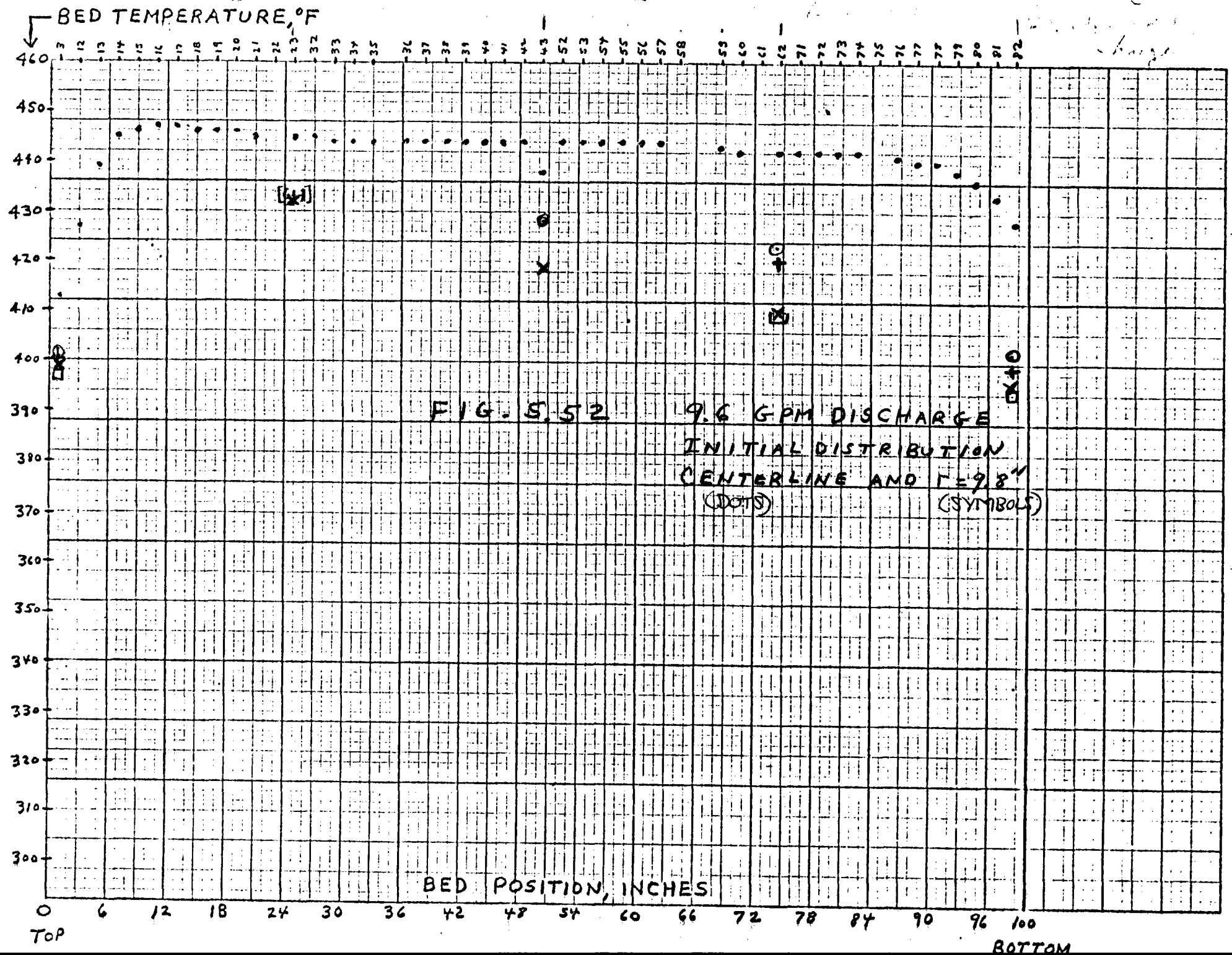
BED TEMPERATURE, °F
460
450
440
430
420
410
400
390
380
370
360
350
340
330
320
310
300
FIG. 5.52
9.6 GPM DISCHARGE
INITIAL DISTRIBUTION
CENTERLINE AND r=9.8"
(DOTS)
(SYMBOLS)
BED POSITION, INCHES
0
6
12
18
24
30
36
42
48
54
60
66
72
78
84
90
96
100
TOP
BOTTOM

FIG. 5.53

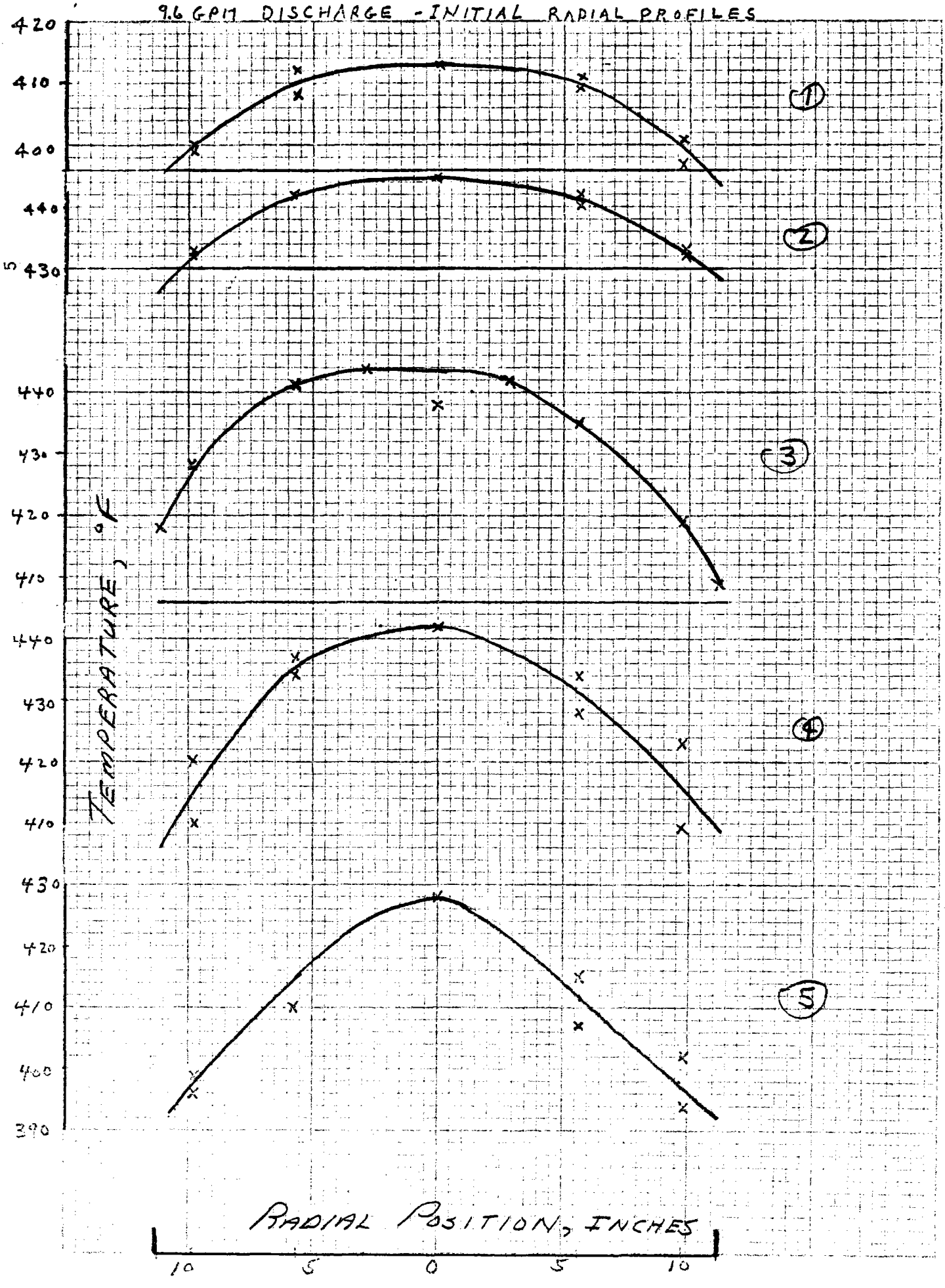
9.6 GPM DISCHARGE - INITIAL RADIAL PROFILES
420
410
400
440
430
440
430
420
410
440
430
420
410
430
420
410
400
390
1
2
3
4
5
TEMPERATURE, °F
RADIAL POSITION, INCHES
10
5
0
5
10

9.6 GPM DISCHARGE - INITIAL AVERAGE TEMPERATURES

FIG. 5.54

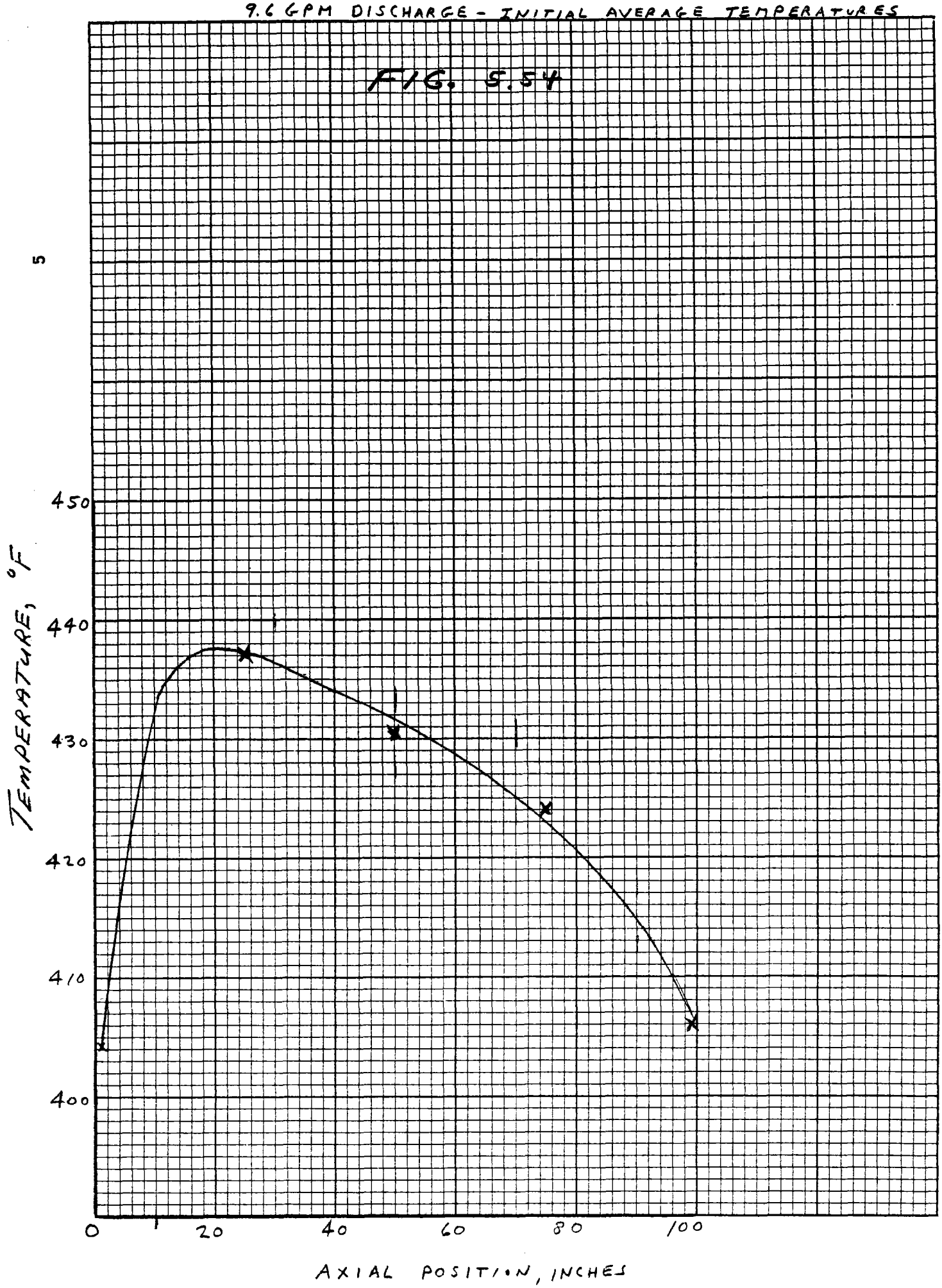

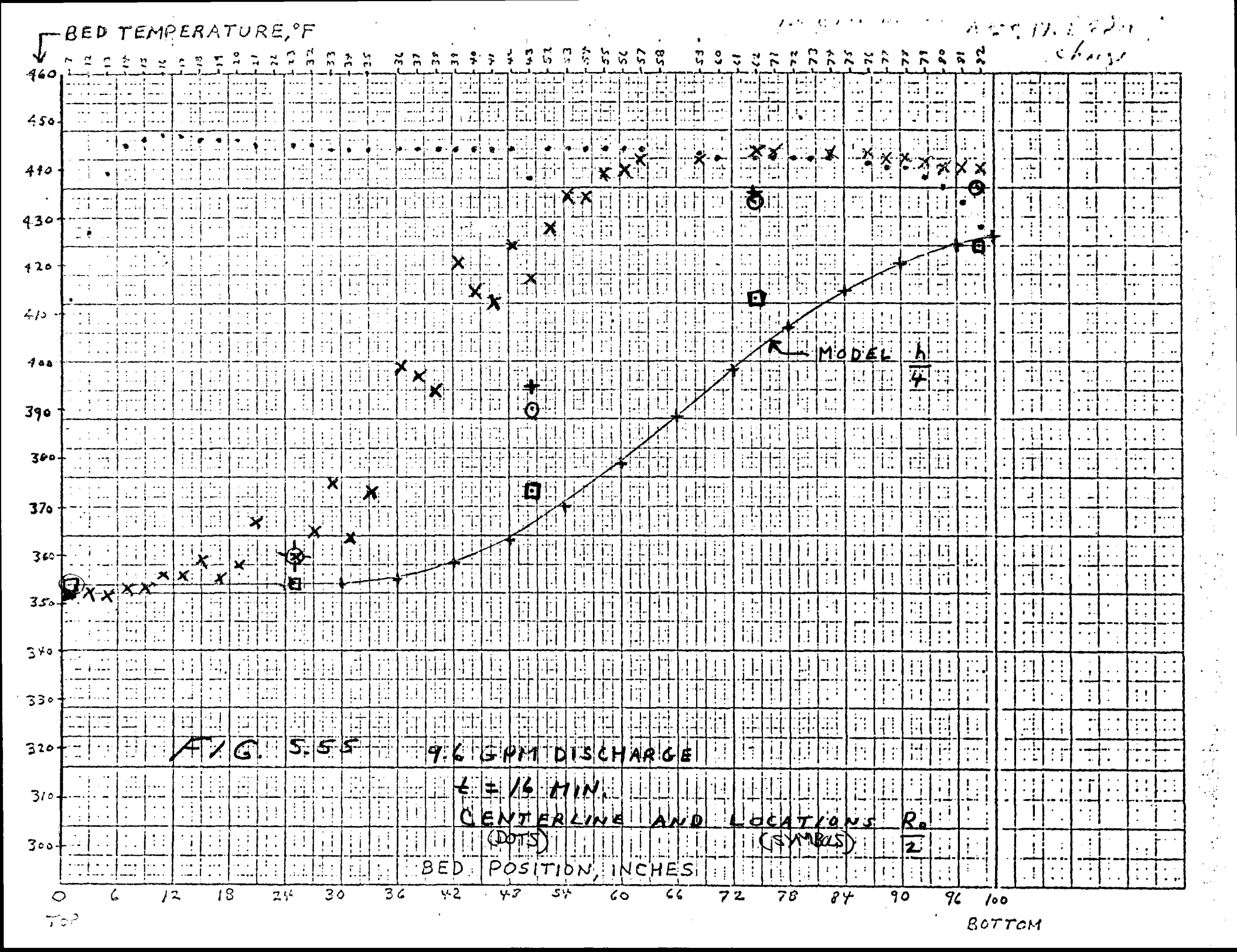
BED TEMPERATURE, °F
460
450
440
430
420
410
400
390
380
370
360
350
340
330
320
310
300
MODEL h/4
FIG. 5.55 9.6 GPM DISCHARGE
t = 16 MIN.
CENTERLINE AND LOCATIONS R₀/2
(DOTS) (SYMBOLS)
BED POSITION, INCHES
0 6 12 18 24 30 36 42 48 54 60 66 72 78 84 90 96 100
TOP
BOTTOM

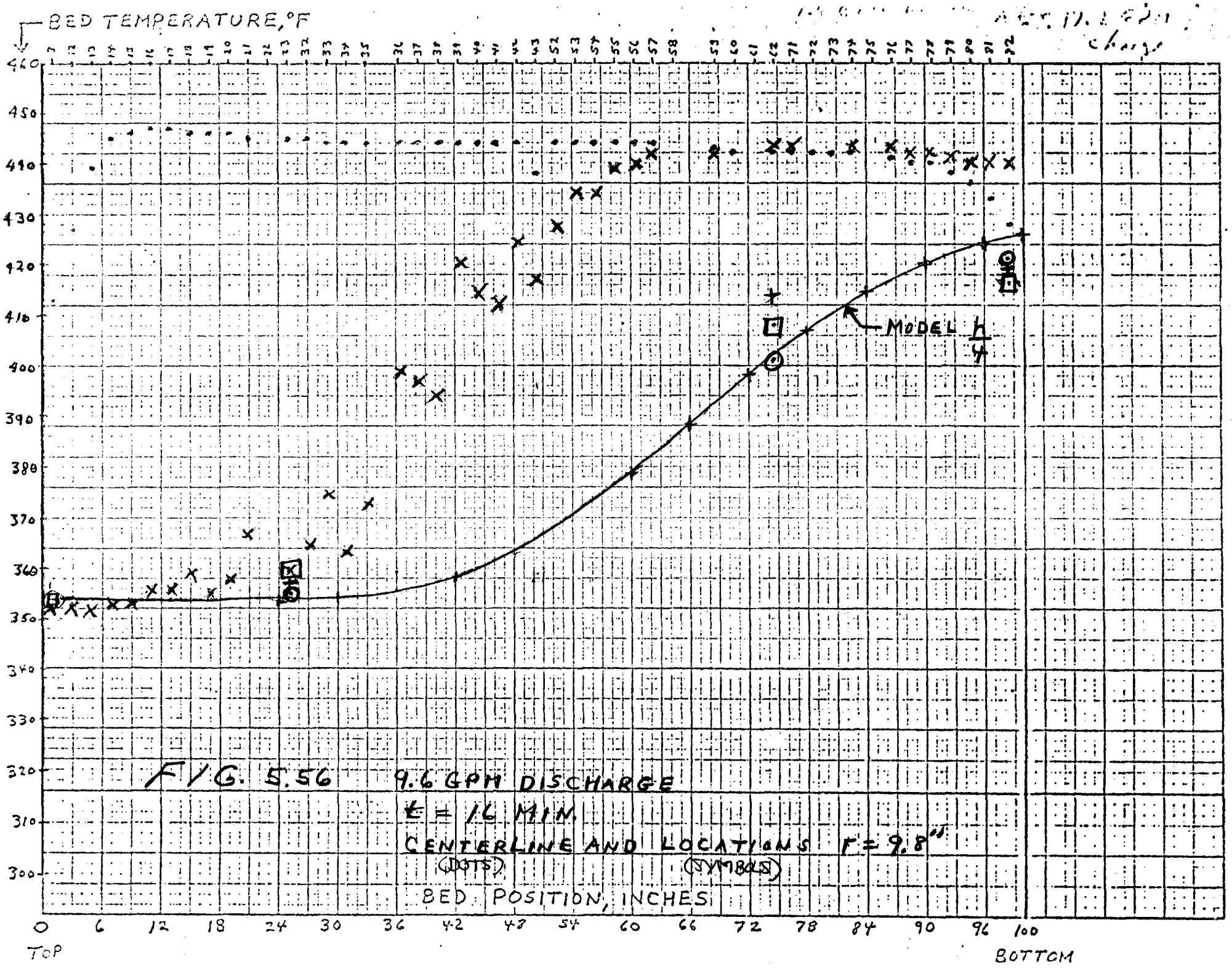

FIG. 5.56 9.6 GPM DISCHARGE

ϵ = 16 MIN.

CENTERLINE AND LOCATIONS (DOTS) (SYMBOLS) $r = 9.8''$

FIG

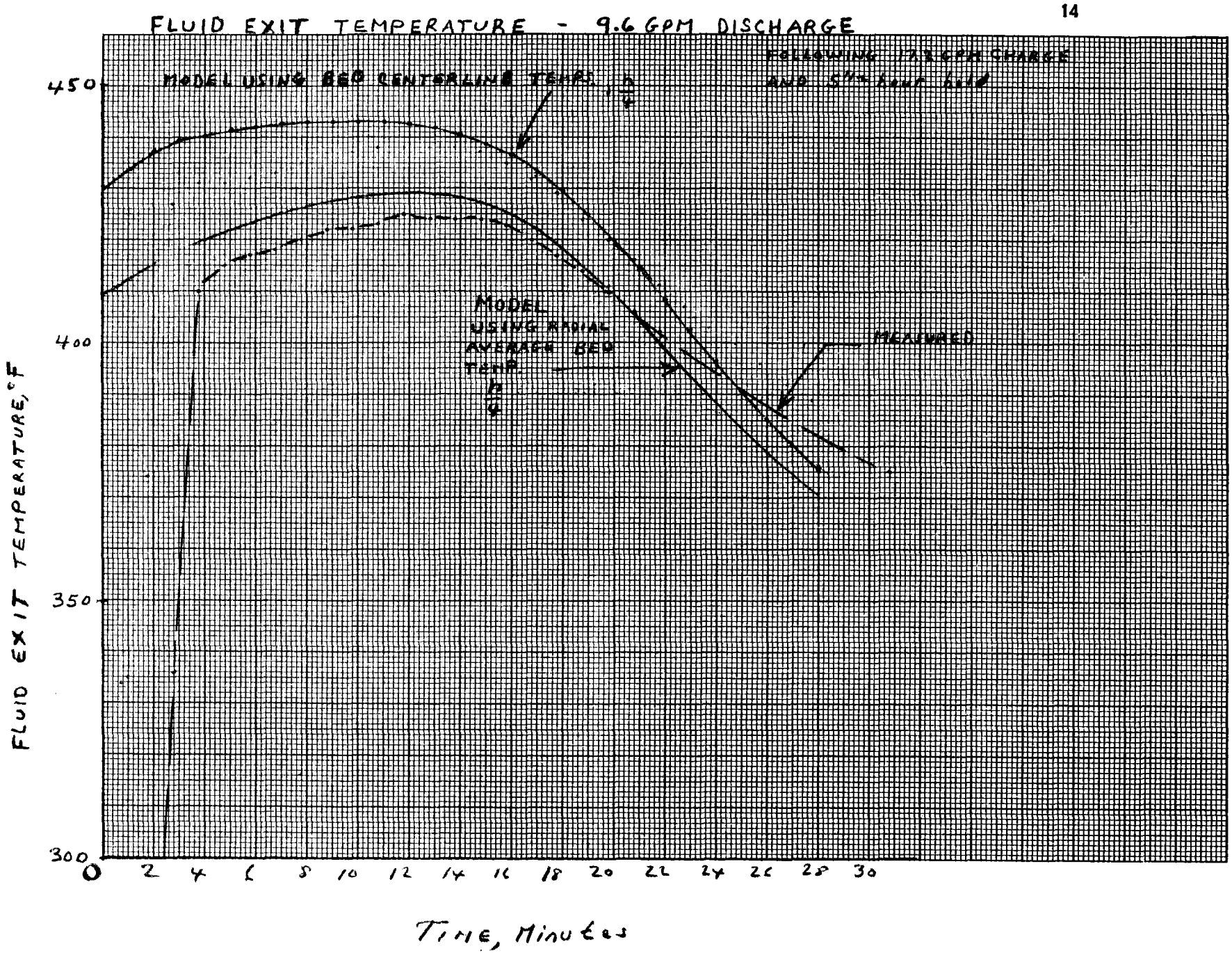
FLUID EXIT TEMPERATURE - 9.6 GPM DISCHARGE
FOLLOWING 17.5 GPM CHARGE AND 5 1/2 HOUR RELIEF
MODEL USING BED CENTERLINE TEMPS. 1 hr
MODEL USING RADIAL AVERAGE BED TEMP. 1 hr
MEASURED
FLUID EXIT TEMPERATURE, °F
450
400
350
300
0
2
4
6
8
10
12
14
16
18
20
22
24
26
28
30
TIME, Minutes

5.2.3 4 GPM Discharge

Figures 5.58 and 5.59 show the initial centerline and temperatures at $\frac{Ro}{2}$, and near the wall. Figure 5.60 is a plot of initial temperature versus radial position. The integrated average profile was not calculated. The bed centerline temperature and inlet fluid temperature history was used as input to the model.

Figure 5.61 shows the measured centerline profiles at 16, 30, 46, and 60 minutes. Figure 5.62 shows the 46 minute profile in comparison with the model at the centerline and $\frac{Ro}{2}$. Figure 5.63 shows the near wall profiles. It is seen that the slopes are generally in good agreement with the model. This was not the case in the 4 GPM charge mode, indicating that the maldistribution effect is more severe in the charge mode.

4 GPM Fluid Exit Temperature

The measured and model fluid exit temperatures are shown in figure 5.64. As in the 4 GPM charge the slope of the fluid temperature charge is less steep than the model.

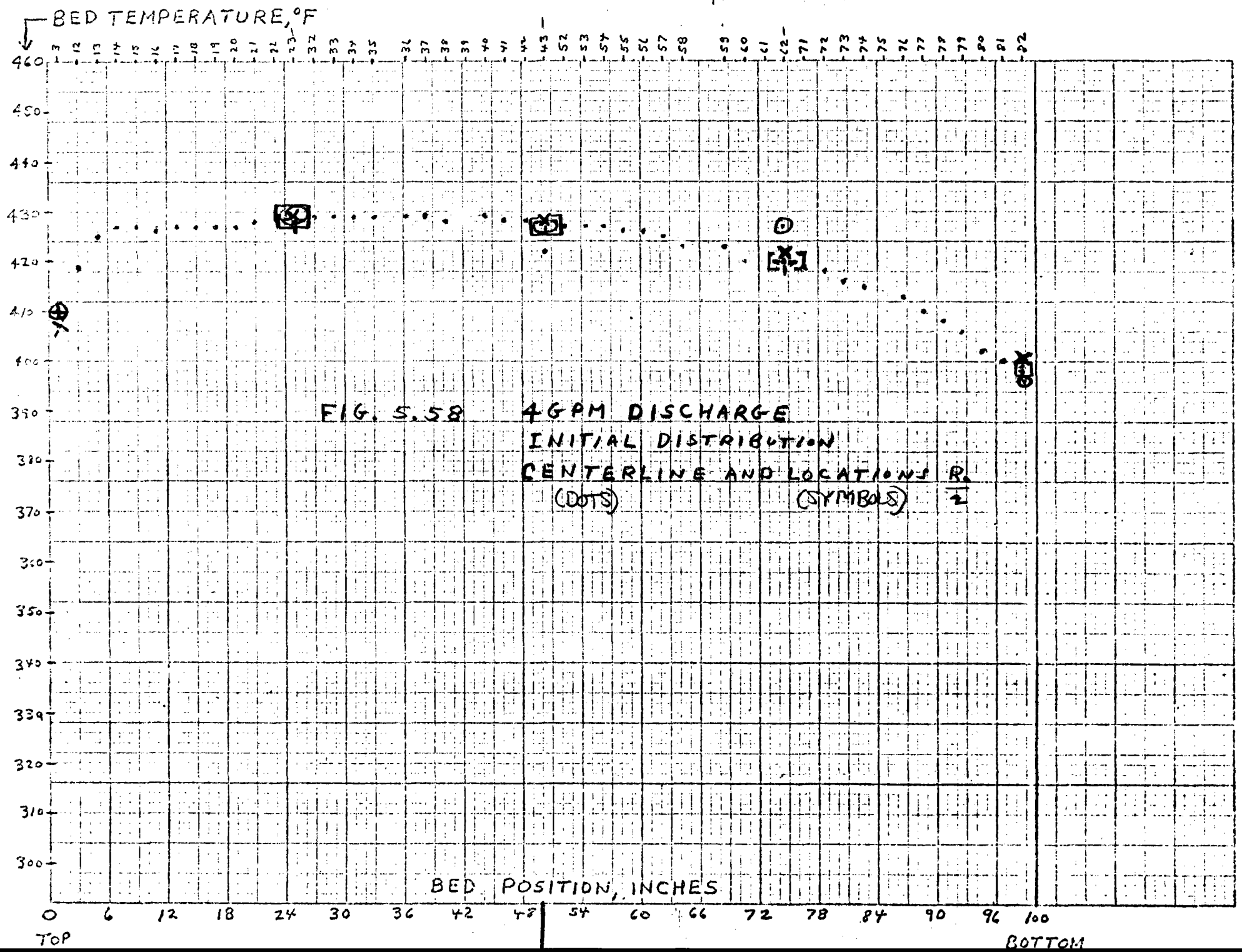

FIG. 5.58 4 GPM DISCHARGE
INITIAL DISTRIBUTION
CENTERLINE AND LOCATIONS R/2
(DOTS) (SYMBOLS)

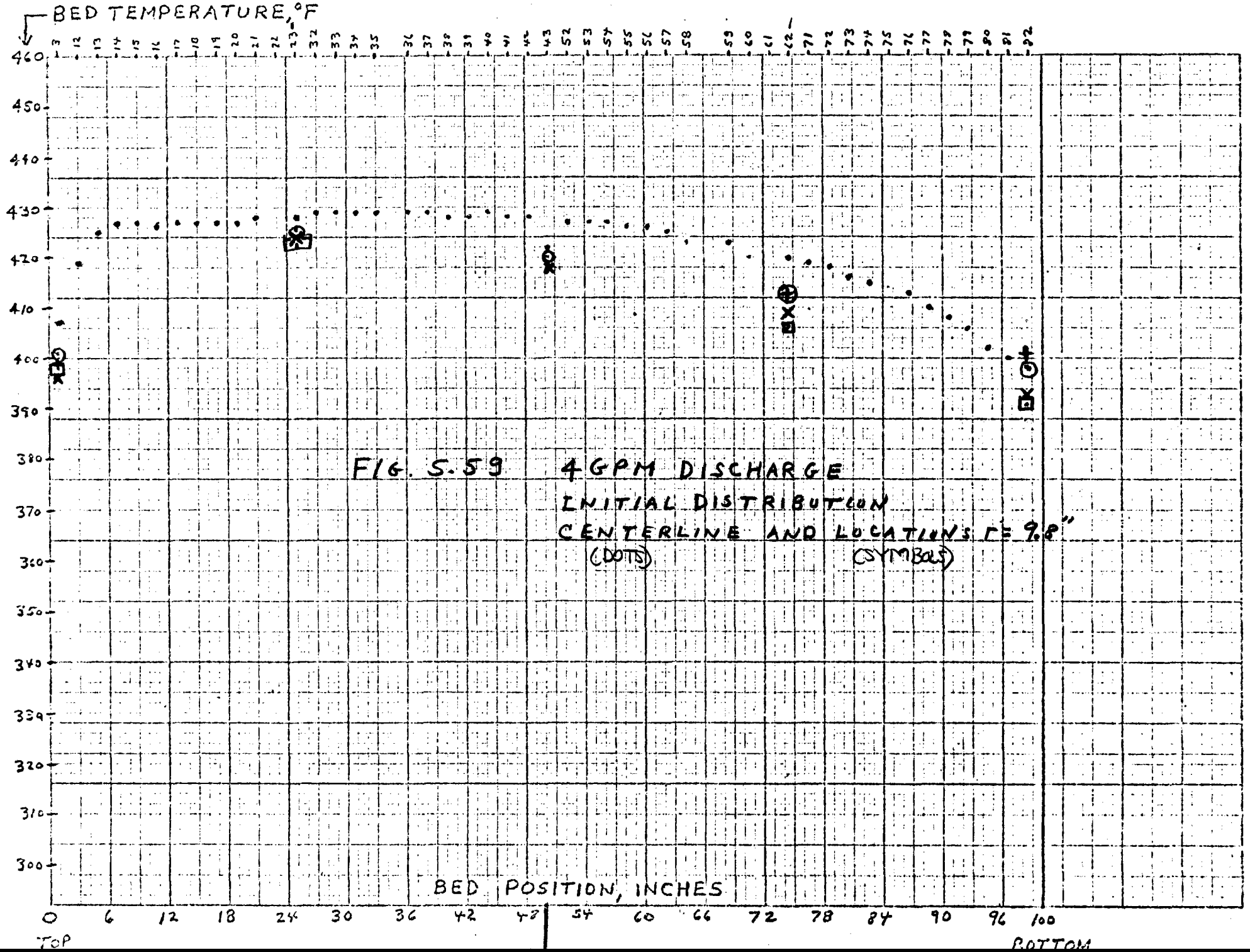

FIG. 5.59 4 GPM DISCHARGE
INITIAL DISTRIBUTION
CENTERLINE AND LOCATIONS: r = 9.8"
(DOTS) (SYMBOLS)

FIG. 5.60 4 GPM DISCHARGE - INITIAL TEMPERATURE

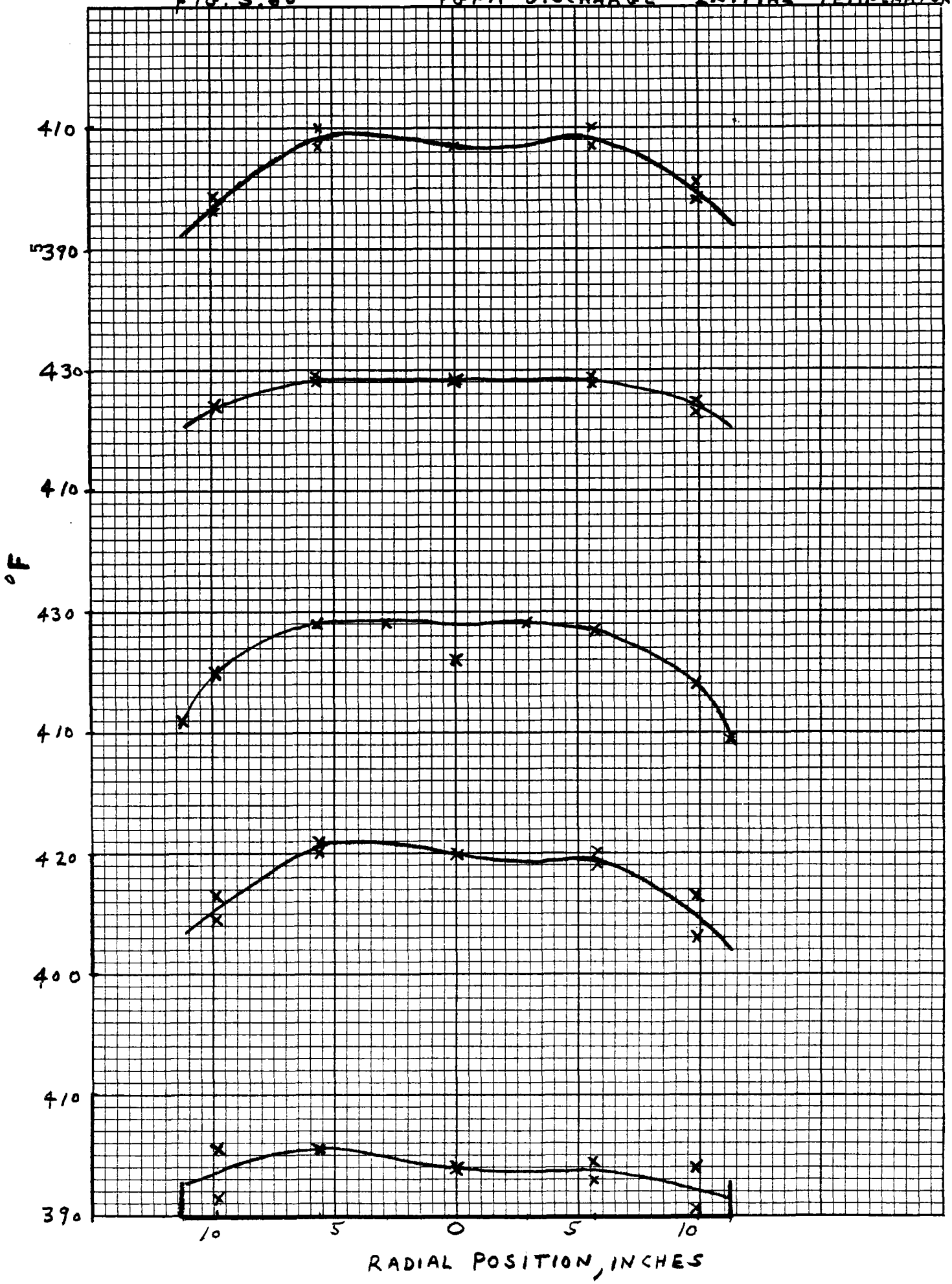

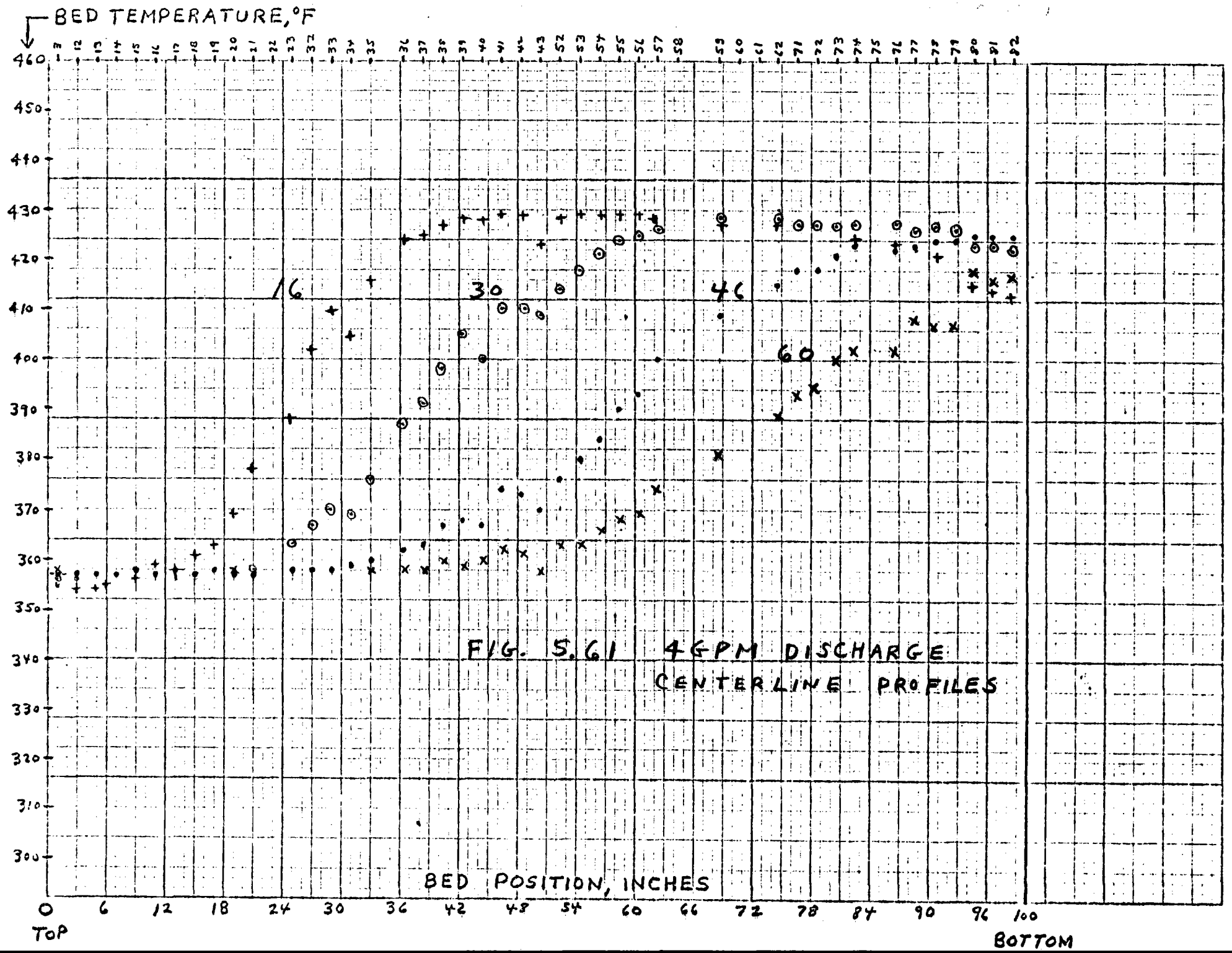

FIG. 5.61 4 GPM DISCHARGE
CENTERLINE PROFILES

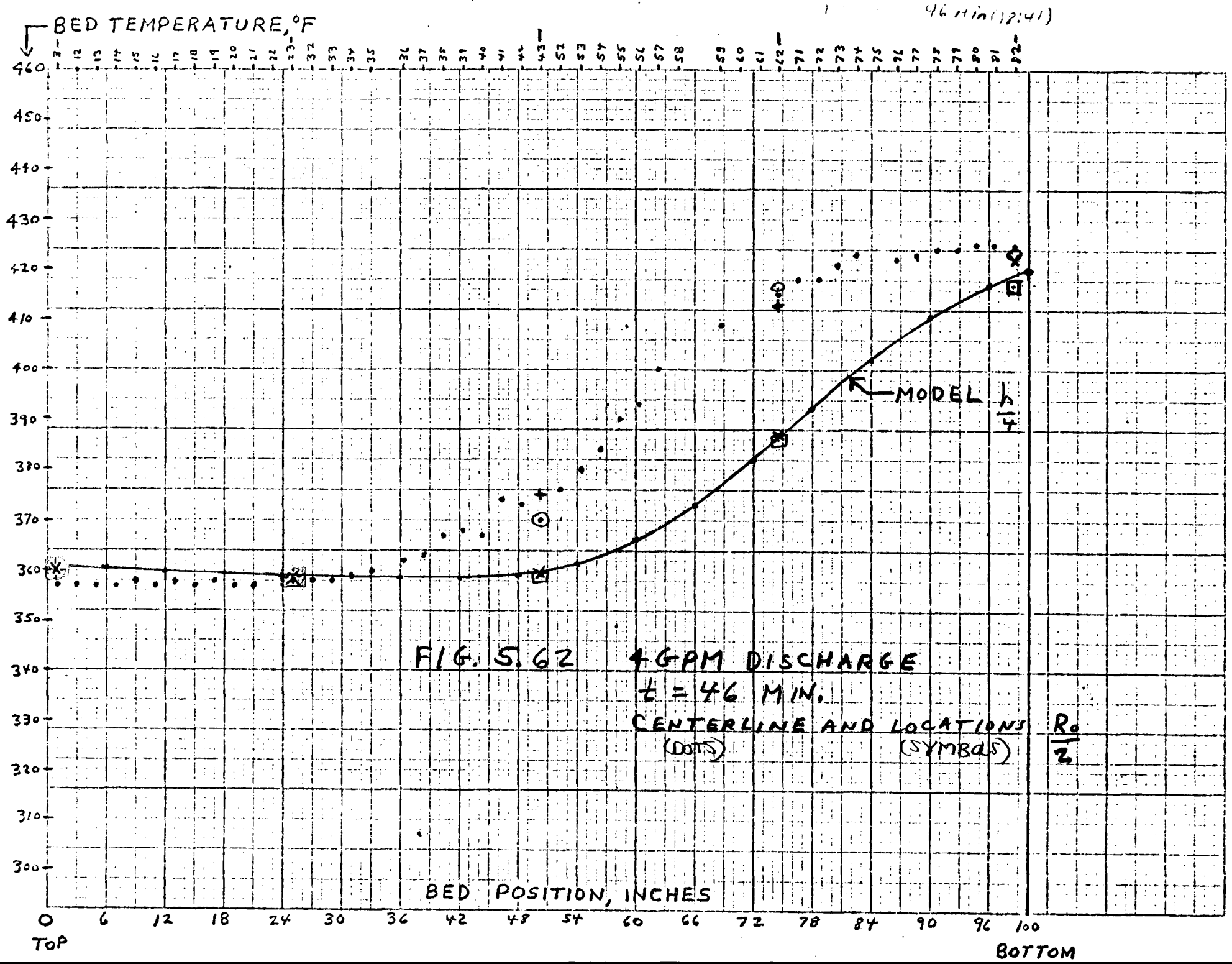
46 min (12:41)
BED TEMPERATURE, °F
460
450
440
430
420
410
400
390
380
370
360
350
340
330
320
310
300
MODEL
BED POSITION, INCHES
0
6
12
18
24
30
36
42
48
54
60
66
72
78
84
90
96
100
TOP
BOTTOM
FIG. 5.62 4 GPM DISCHARGE
t = 46 MIN.
CENTERLINE AND LOCATIONS
(DOTS)
(SYMBOLS)
R₀/2

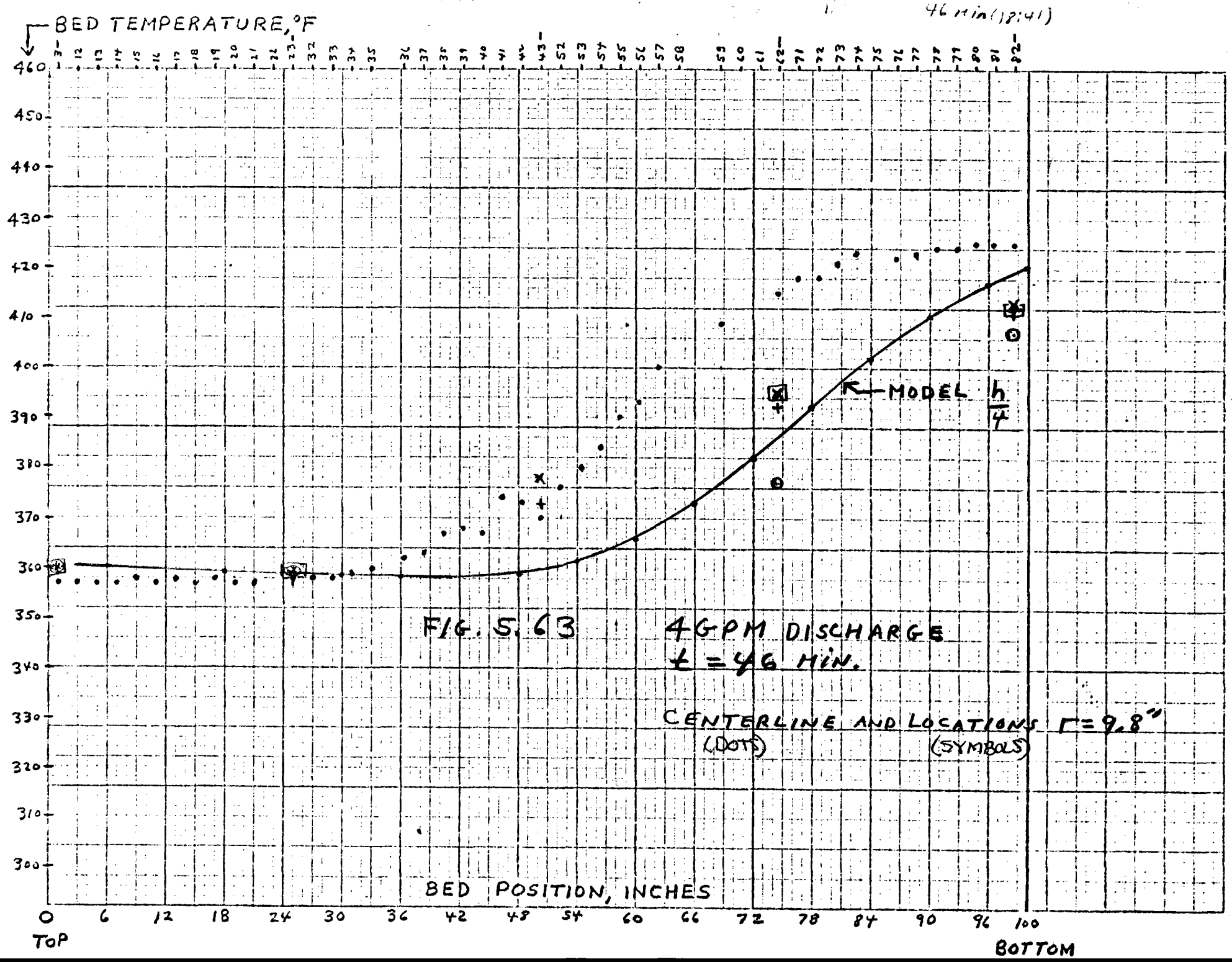

FIG. 5.63 4 GPM DISCHARGE
$t = 46$ MIN.

CENTERLINE AND LOCATIONS $r = 9.8''$
(DOTS) (SYMBOLS)

FIG. 5.64 FLUID EXIT TEMPERATURE
4 GPM DISCHARGE

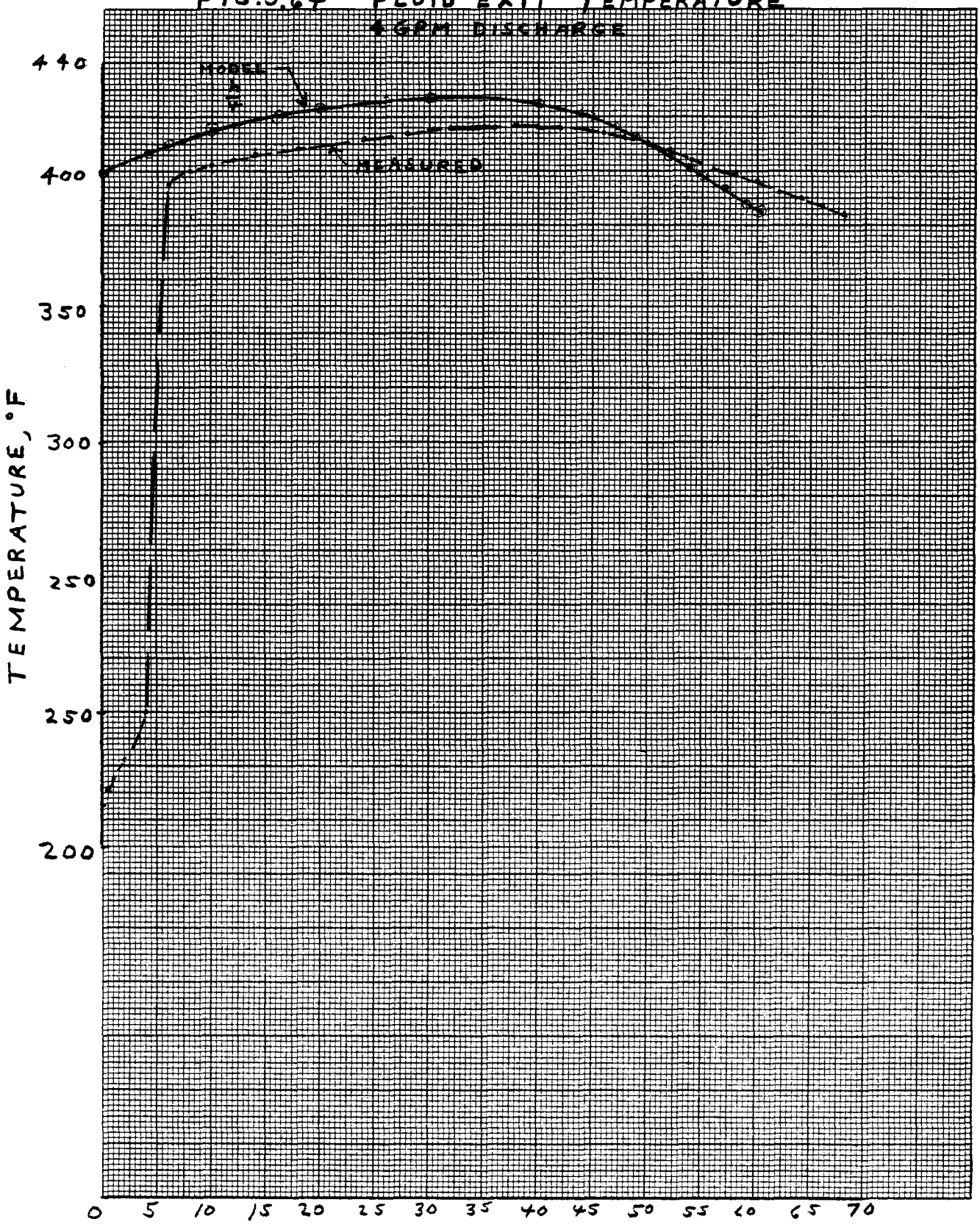

HOLDING TESTS

5.3 Holding Tests

Two holding tests were run to observe the charges in the bed temperature profiles. The first test consisted of partially charging the bed at a 3.5 GPM flow rate, then holding for 11 hours.

In the 2nd test the bed was partially discharged, then held for 10 hours.

5.3.1 1/2 Charge Hold

The centerline profiles are shown in figure H-1. It is seen that there is appreciable cooling only in the top 5 inches of the bed due to convective losses. t=o is defined as the time at which flow is stopped. Part of the rise in centerline temperature down the bed is due to the drainage of the dynamic holdup and in part due to radial inward conduction as well as axial conduction. All temperature levels drop as a function of time but even after 8 hours the thermocline shape is not significantly distorted. It is concluded that the bed thermal conductance in the full scale system will be sufficiently low that thermoclines will not be severly distorted and that the 14" of insulation will maintain heat losses at 4% over a 24 hour period. It is evident that radial conduction inward is occurring because the energy content at the centerline is greater after 6 hours than at t=o. The present bed model is one-dimensional; i.e., it handles only axial temperature variations. It is therefore not possible to separate the complex heat flow into components due to dynamic holdup drain, radial and axial conduction. Between 4 and 6 hours it is seen that there is very little temperature change in the bulk of the bed along the centerline. Beyond 6 hours all temperatures start to fall due to radial conduction outward, and axial conduction. The heat

flow pattern is seen by observing the radial temperature changes shown in figure H-2 and H-3. The centerline (439°F) is cooler than position $\frac{Ro}{2}$ and r=9.8", at t=o heat flows inward raising the centerline to a peak of 445°F which prevails till 8 hours where it drops to 444°F and then continues to drop slowly (441°F after 11 hrs.) During this time temperature at $\frac{Ro}{2}$ and r=9.8" are continually dropping.

The full scale system is 20Ft in diameter with 14" of insulation; the test is 2Ft in diameter with 8" of insulation. The ratio of $\left(\frac{T_{bed}-T_{ambient}}{L_{insulation}}\right)$ is the same for both, therefore, the surface heat flux is the same (insulation conductuity being equal). However, the area to volume ratio of the test is 7 times as large as the full scale system. Consequently, the observed drops in temperature are representative of less than the outer foot near the wall of the full scale system. Figure H-4 shows the axial profile at a location of $\frac{Ro}{2}$ as a function of time.

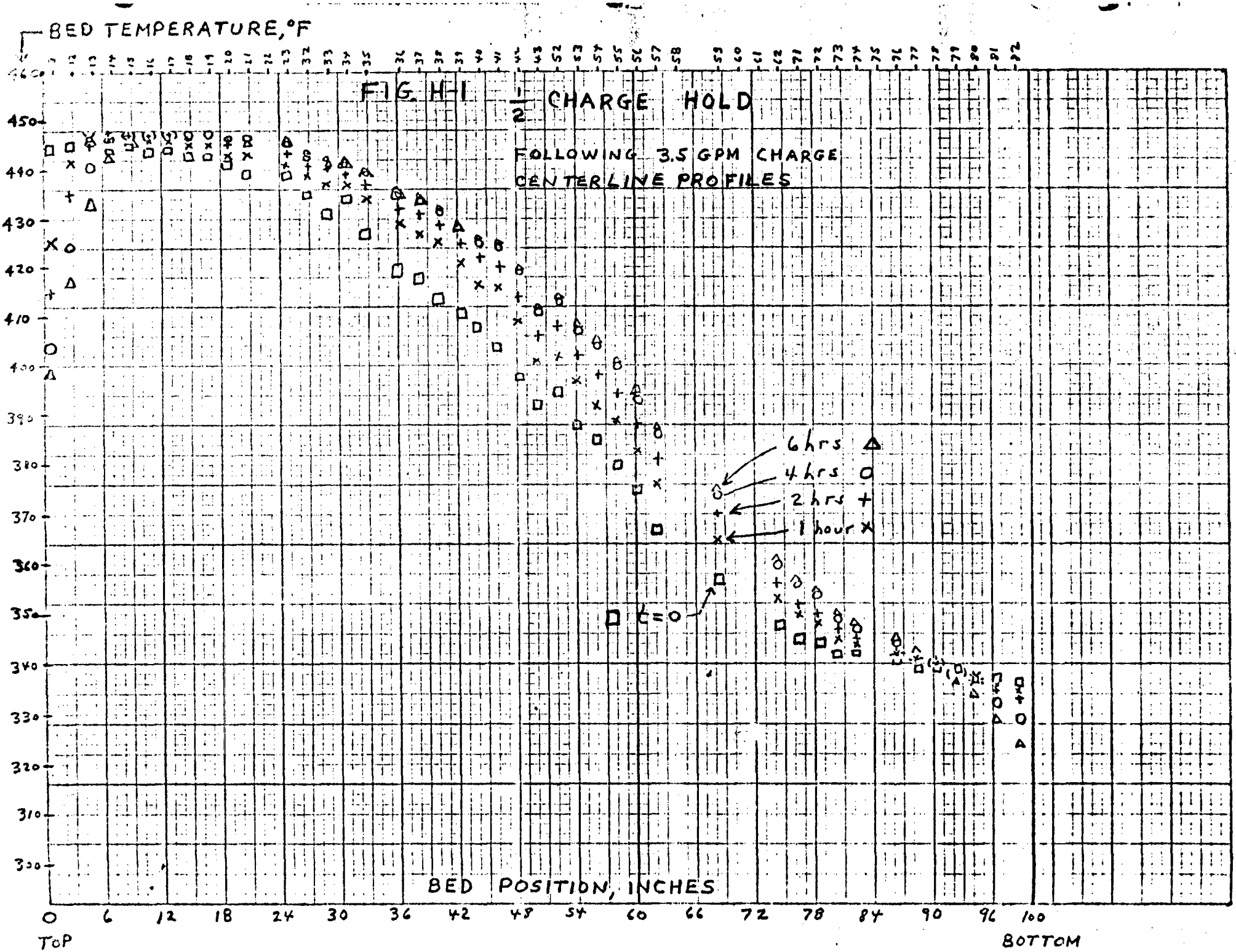
BED TEMPERATURE, °F
FIG. H-1
½ CHARGE HOLD
FOLLOWING 3.5 GPM CHARGE
CENTERLINE PROFILES
6 hrs
4 hrs
2 hrs
1 hour
t = 0
BED POSITION, INCHES
TOP
BOTTOM

FIG. H-2 1/2 Charge hold-radial profiles at

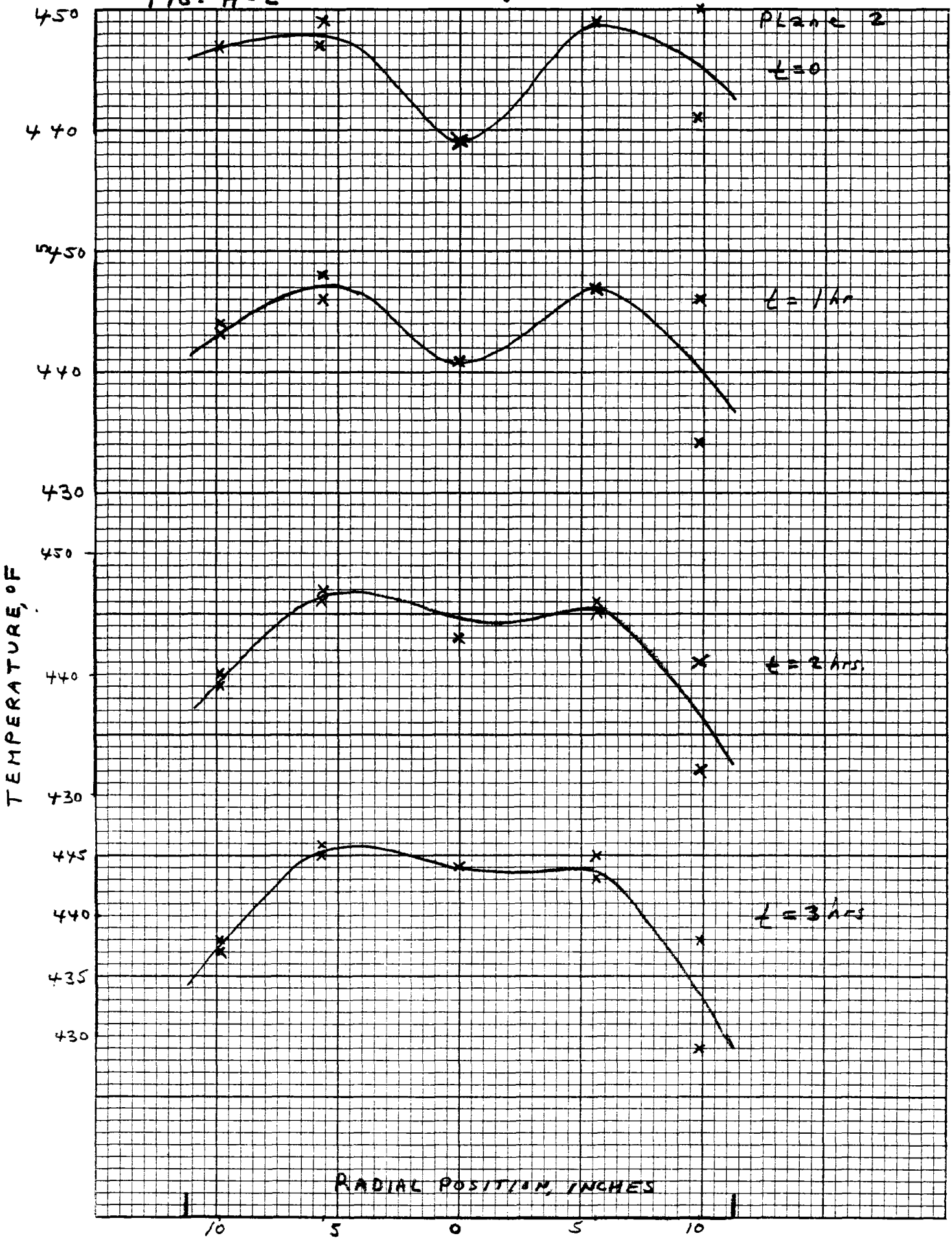

FIG. H-3 1/2 Charge hold - radial profiles at plane 2

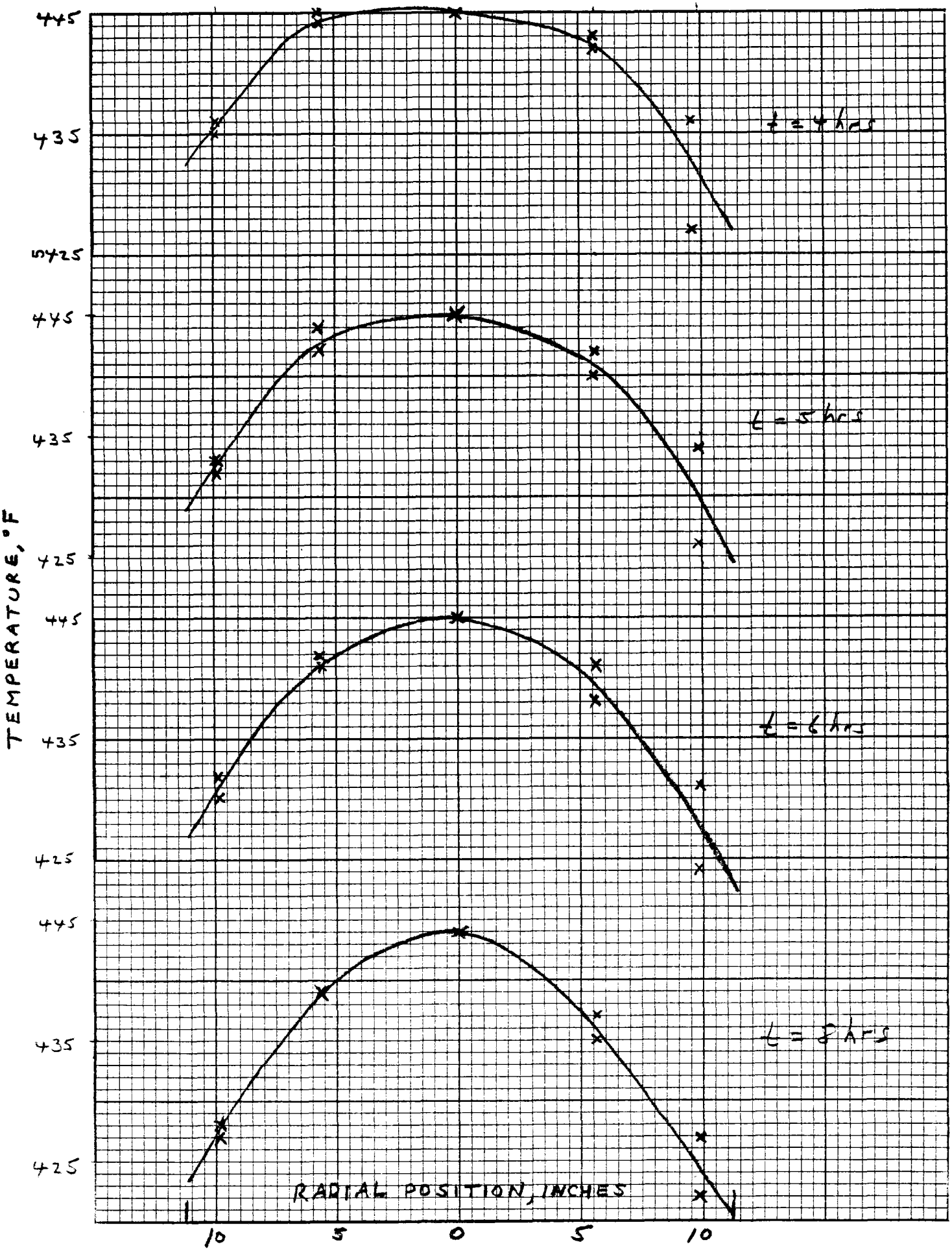

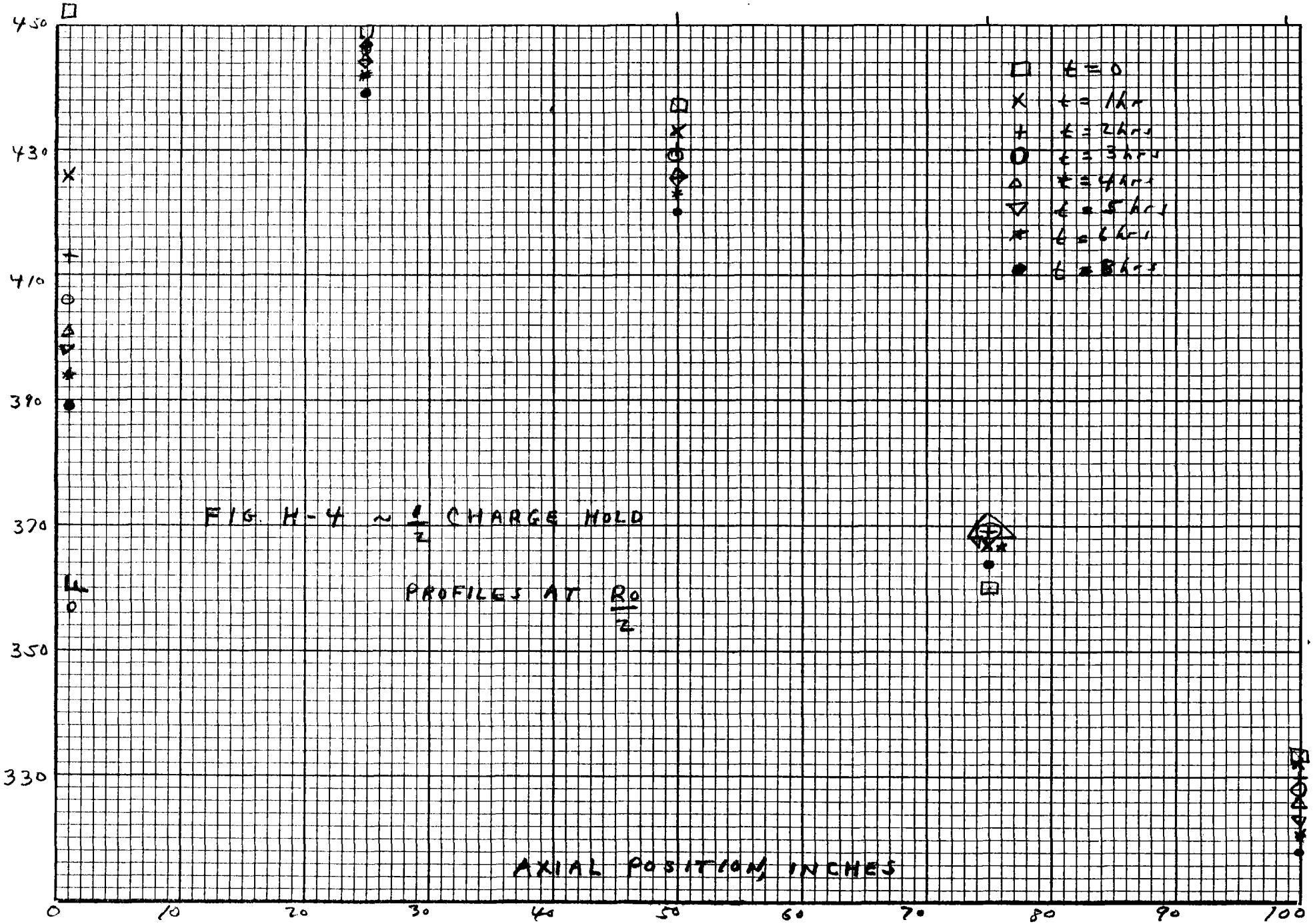

FIG. H-4 ~ $\frac{1}{2}$ CHARGE HOLD

PROFILES AT $\frac{R_0}{2}$

5.3.2 1/2 Discharge Hold

The centerline profiles are shown in figure H-5. In the discharge mode the centerline temperature was always hotter than the outer temperatures. Consequently, there is radially flow outward, as well as axial conduction upward and hot air convection currents upward. It was postulated that upward convection currents might be severe enough to flatten the thermocline. In the previous column test, run on a 2 foot long bed, these forces, combined with significant tank bottom heat losses, were large enough to drastically distort the thermocline as shown in figure H-6. In this 8 foot column test, the results clearly show that severe thermocline degradation will not occur.

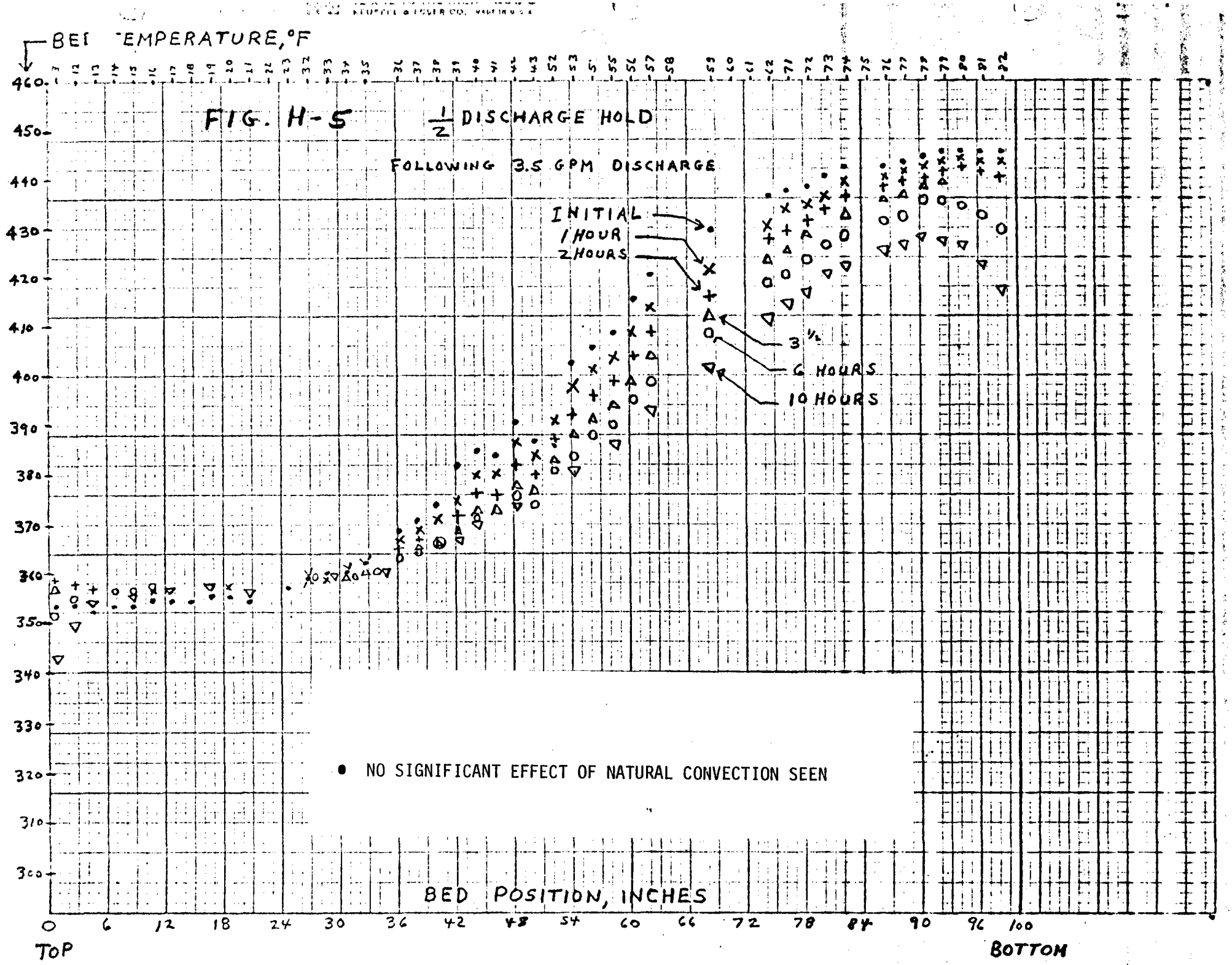
BED TEMPERATURE, °F
460
450
440
430
420
410
400
390
380
370
360
350
340
330
320
310
300
FIG. H-5
1/2 DISCHARGE HOLD
FOLLOWING 3.5 GPM DISCHARGE
INITIAL
1 HOUR
2 HOURS
3 1/2
6 HOURS
10 HOURS
• NO SIGNIFICANT EFFECT OF NATURAL CONVECTION SEEN
BED POSITION, INCHES
0
6
12
18
24
30
36
42
48
54
60
66
72
78
84
90
96
100
TOP
BOTTOM

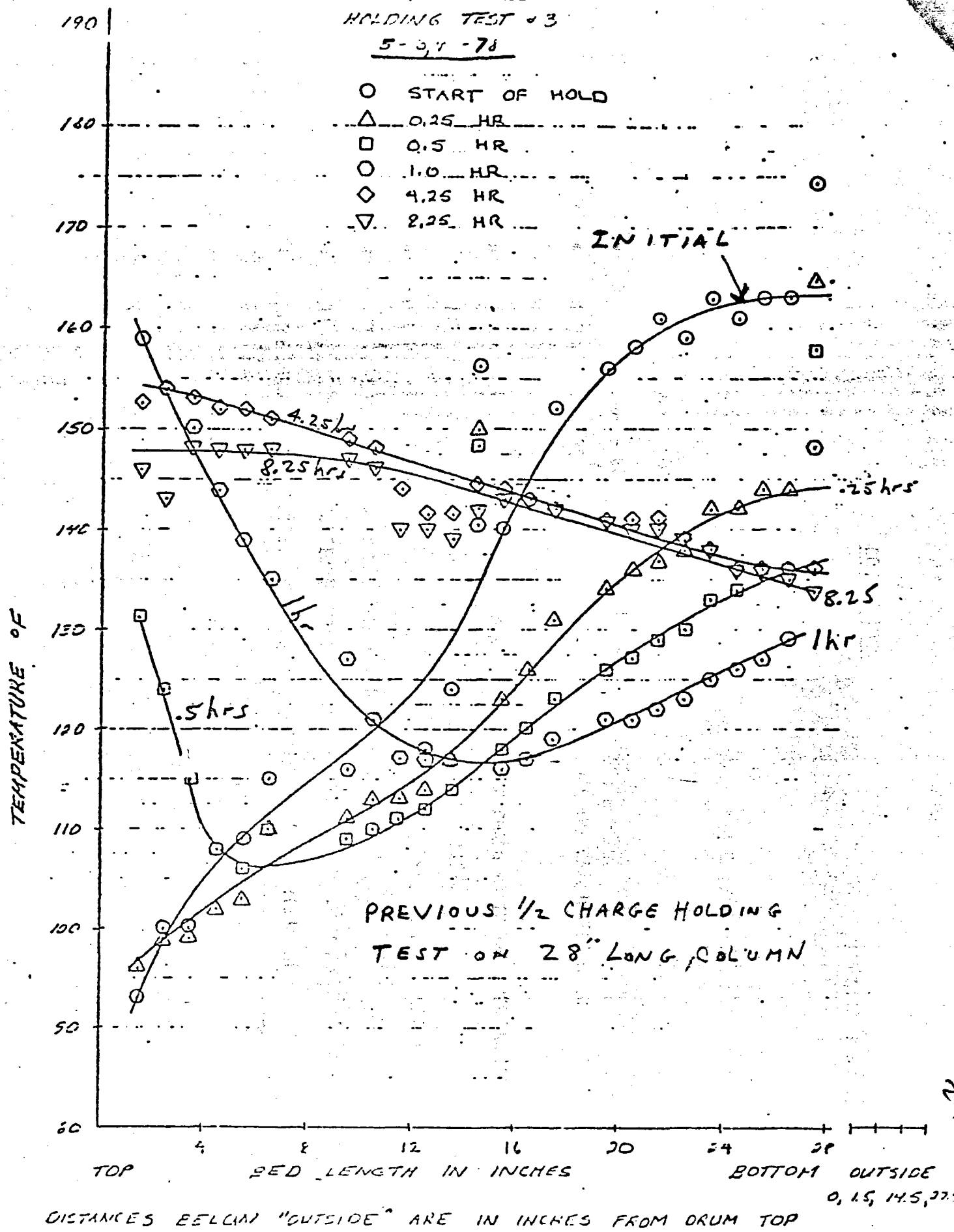

Figure 3.

ES 5/4/78

5.4 Inversion Test

Prior to inversion the bed was charged to approximately the 1/2 charge condition at a flow rate of 3.5 GPM. The bed centerline temperature at the end of charging is shown in figure I-1. Initial radial distributions in the five planes are shown in figure I-2. The area weighted average temperatures were calculated for the 5 planes resulting in the average plane temperature as a function of axial position shown in figure I-3. This profile was used as the initial bed condition in the model.

Figure I-4 shows the fluid exit temperature, which should equal the fluid inlet temperature, but is reduced by the heat loss in the tank exit line. (As previously mentioned this loss is primarily due to the water cooled exit pump.) The temperature loss is typically $10^{o}F$ between the exit and inlet. The present model cannot account for this loss and assumes that the inlet temperature is equal to the calculated exit temperature. Consequently, the agreement between model and measured performance would be expected to become increasingly poor with time as energy is drained from the system. This is shown in figures I-5 and I-6 at t=10 minutes, and 20 minutes. At 10 minutes the agreement between model and measured (measured is calculated from measured radial profile) is good except at the bed top, as here the temperatures are lower than predicted. As inversion progresses to the end, at 20 minutes, the agreement is poorer reflecting the energy loss; the top 2 feet of the bed being 15 to $20^{o}F$ cooler than predicted.

Considering the limitations of the model, and the heat loss problem, the only conclusion reached from test is that the inversion process appears feasible but only a re-test with minimal line losses could confirm this. Systems studies have shown that only a small fraction (10%) of the energy stored will require inversion, consequently the inversion process is of secondary importance.

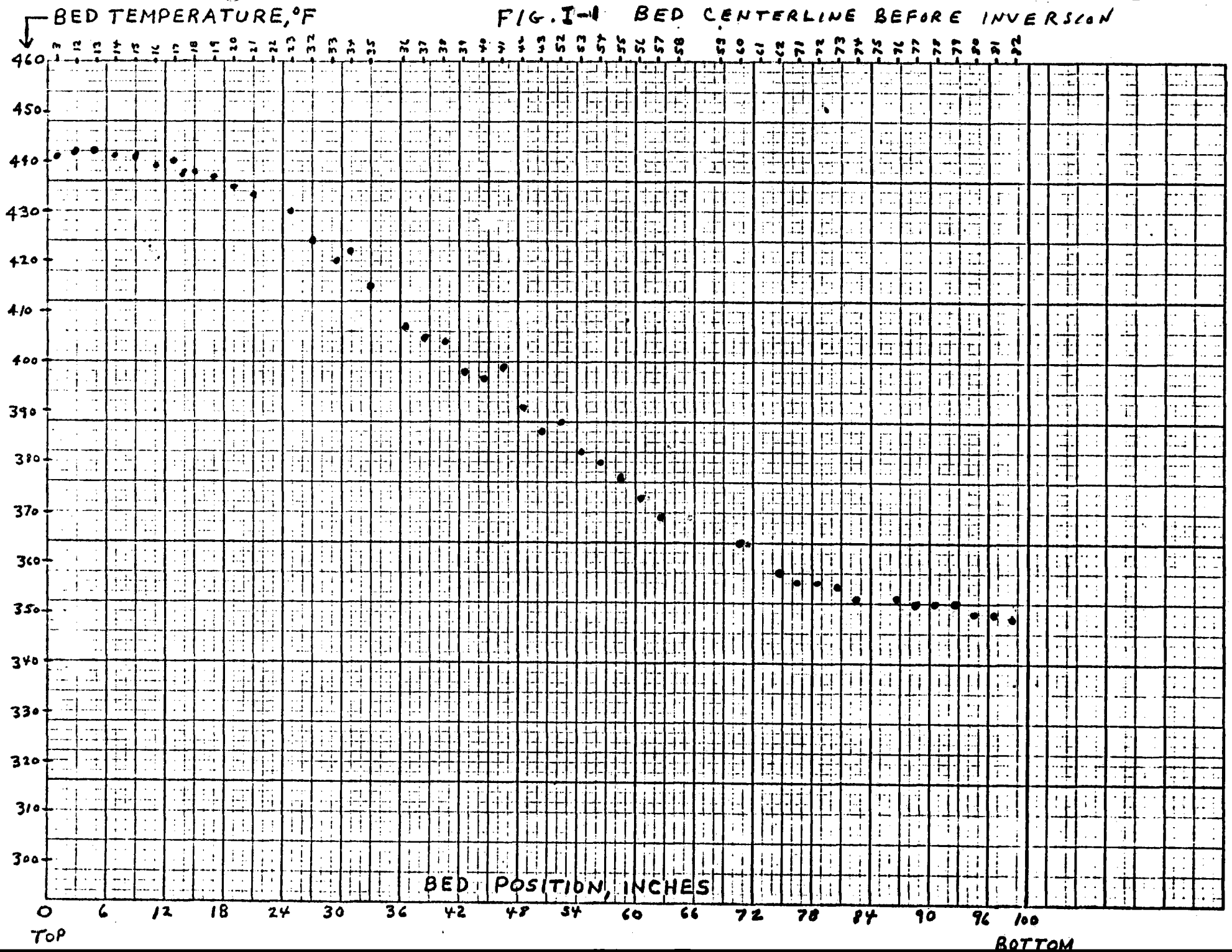
BED TEMPERATURE, °F
FIG. I-1 BED CENTERLINE BEFORE INVERSION
460
450
440
430
420
410
400
390
380
370
360
350
340
330
320
310
300
BED POSITION, INCHES
0
6
12
18
24
30
36
42
48
54
60
66
72
78
84
90
96
100
TOP
BOTTOM

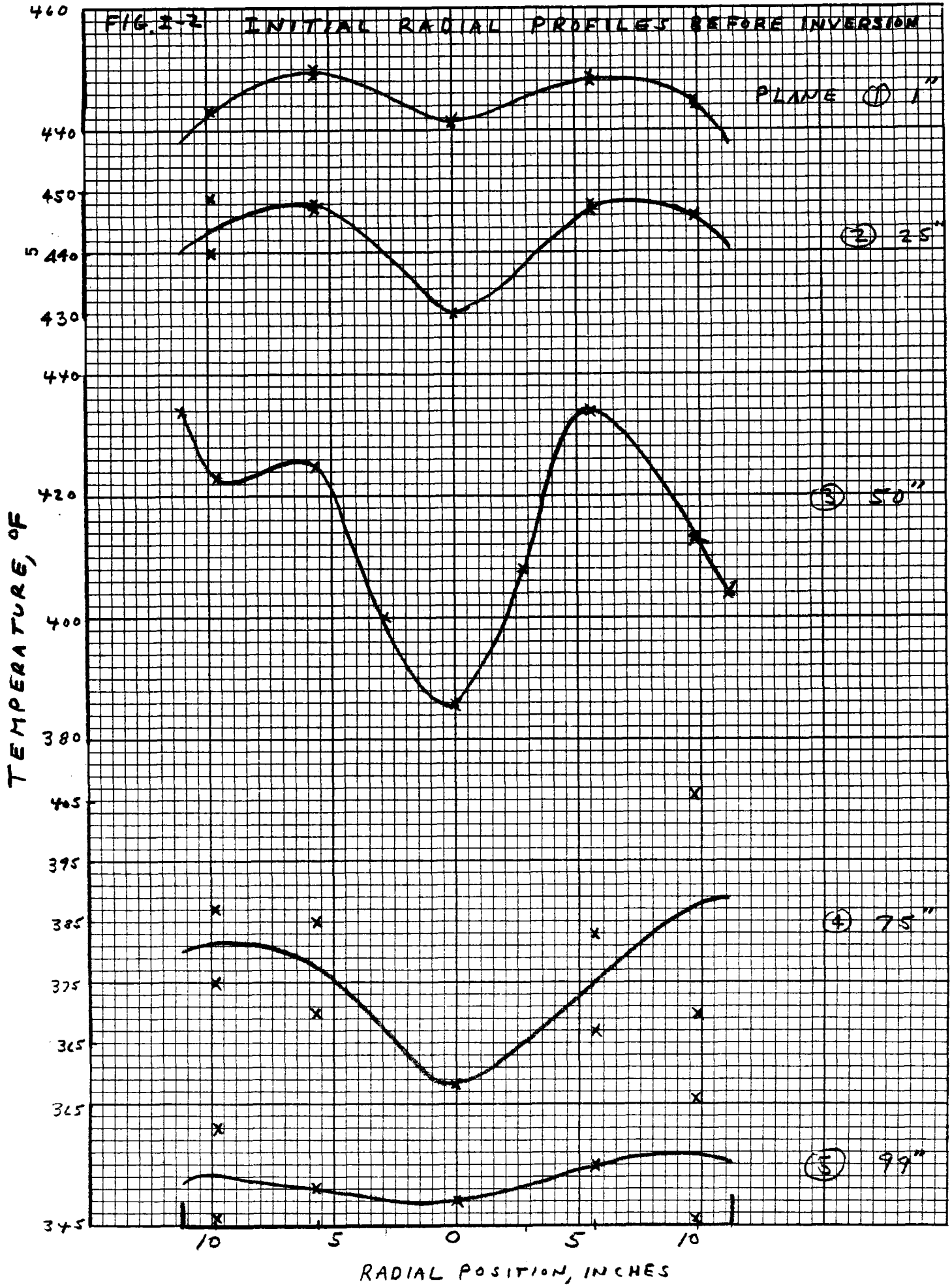
FIG. I-2 INITIAL RADIAL PROFILES BEFORE INVERSION
PLANE (1) 1"
(2) 25"
(3) 50"
(4) 75"
(5) 99"
TEMPERATURE, °F
460
440
450
440
430
440
420
400
380
405
395
385
375
365
345
10
5
0
5
10
RADIAL POSITION, INCHES

FIG. I-3

AXIAL PROFILE FROM RADIAL AVERAGE TEMPERATURES

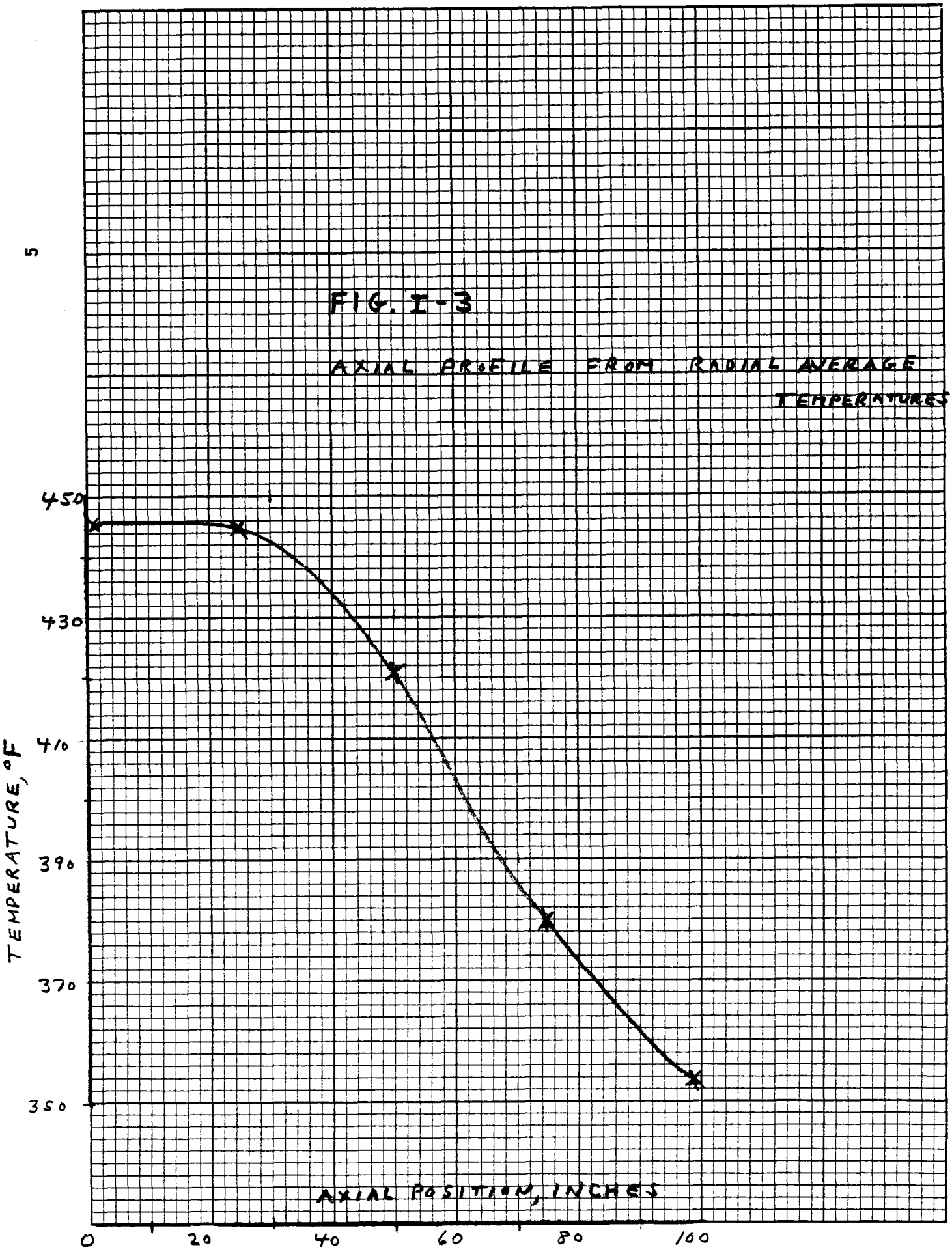

FIG. I-4 INVERSION TEST - FLUID INLET AND OUTLET TEMPERATURES

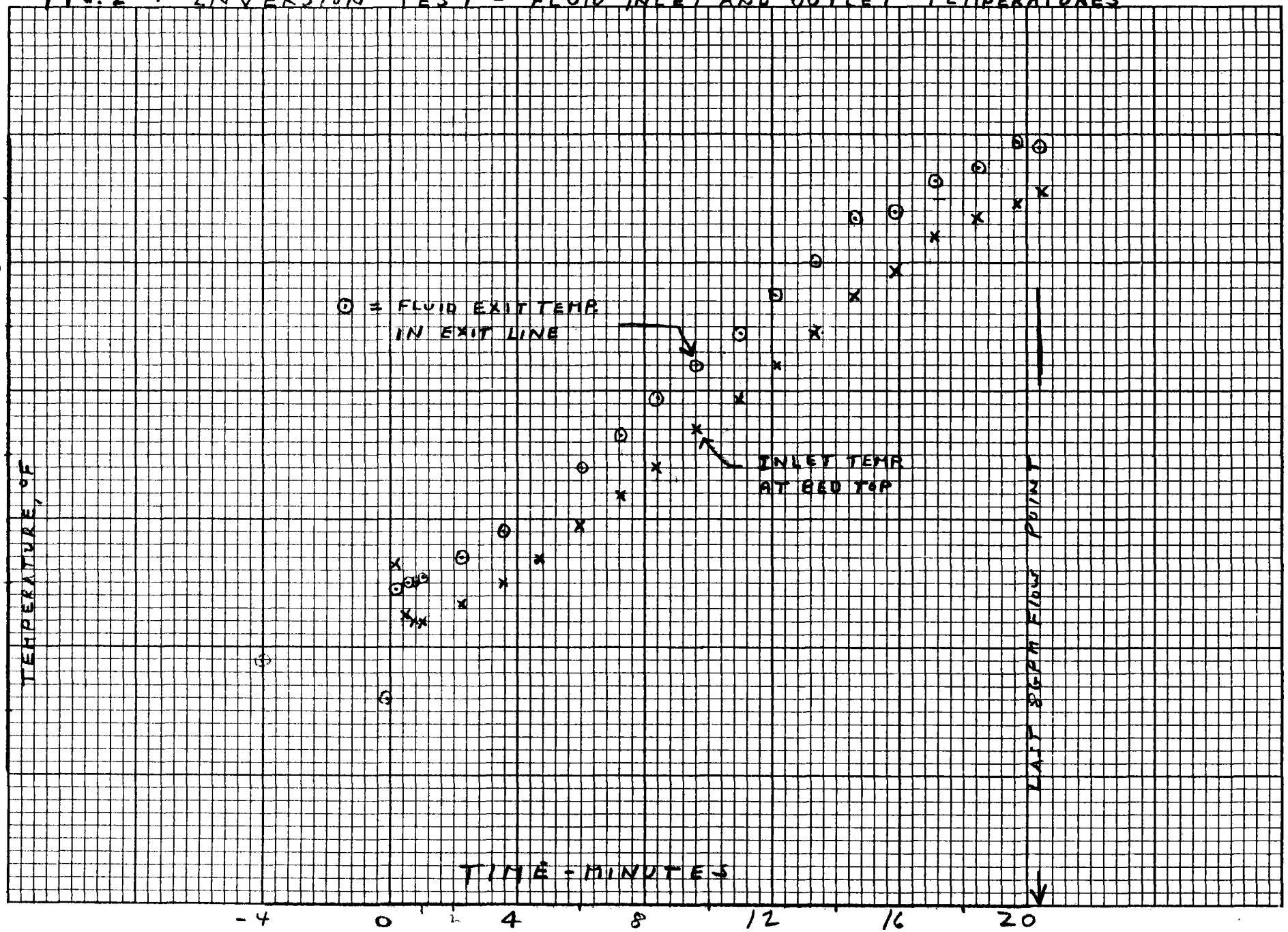

FIG. I-5 INVERSION PROCESS t = 10 MINUTES

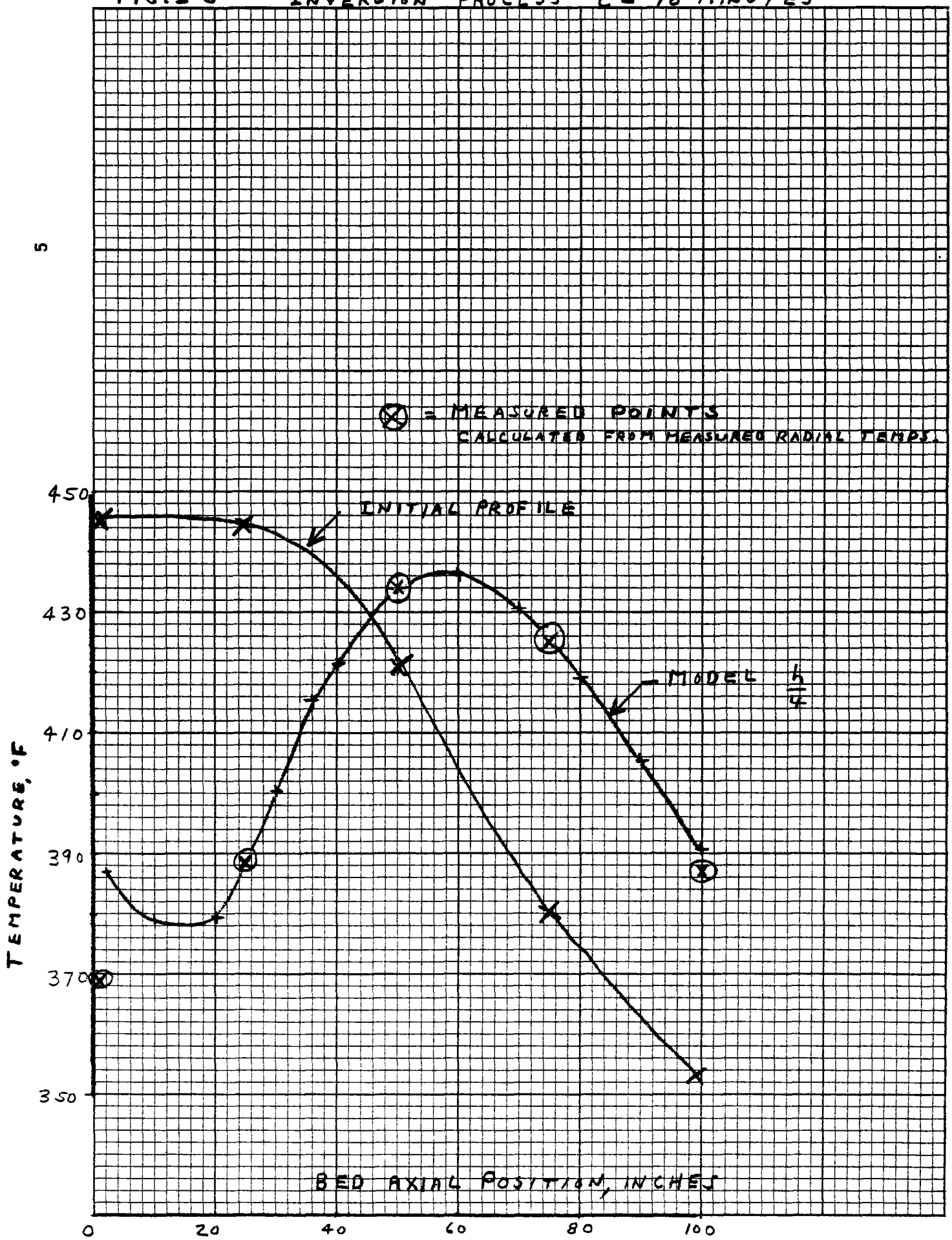

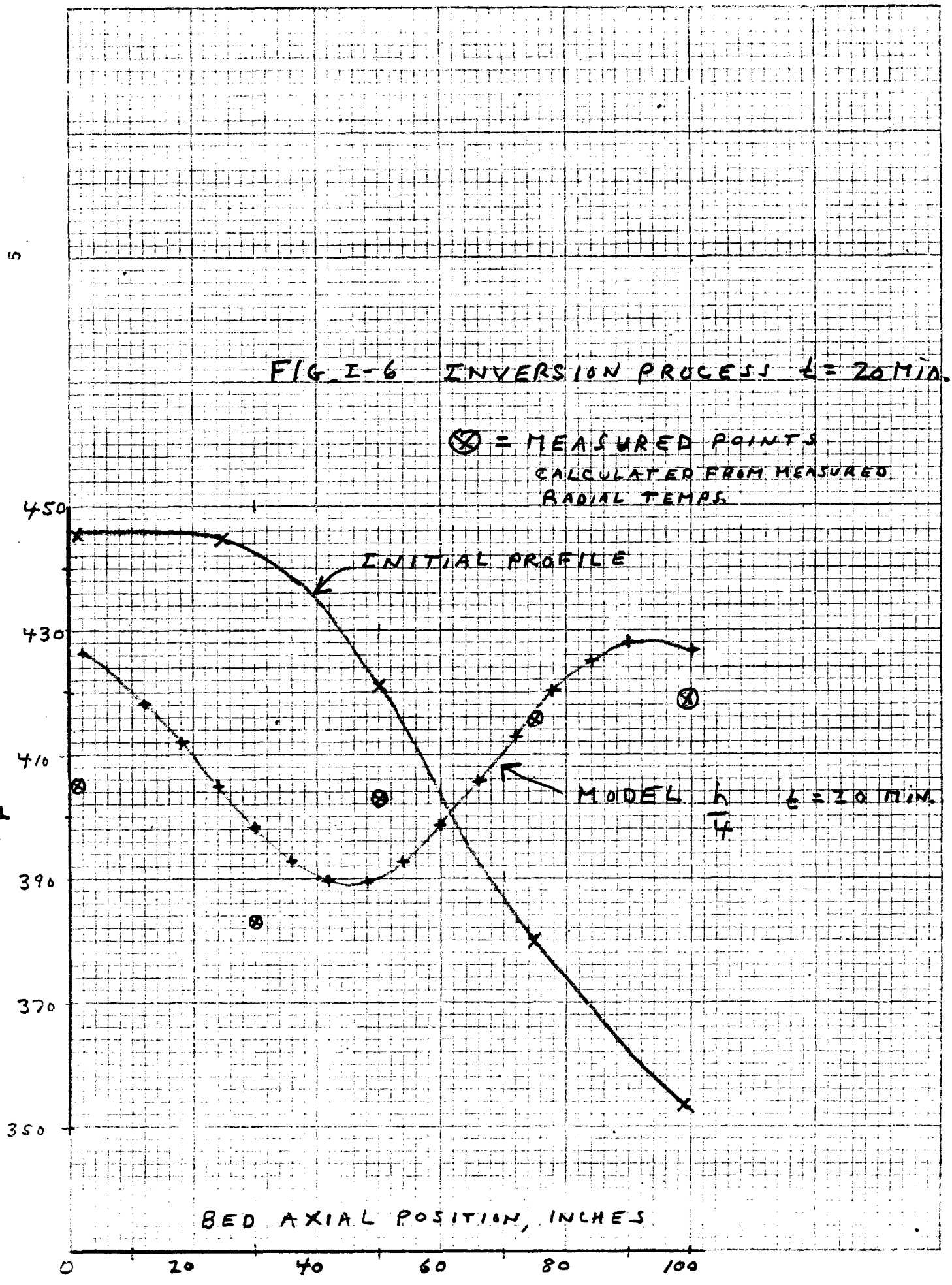
FIG. I-6 INVERSION PROCESS t = 20 MIN.
⊗ = MEASURED POINTS
CALCULATED FROM MEASURED RADIAL TEMPS.
INITIAL PROFILE
MODEL h/4 t = 20 MIN.
450
430
410
390
370
350
T °F
0
20
40
60
80
100
BED AXIAL POSITION, INCHES

5. Heat Transfer Coefficients

The model calculates a theoretical heat transfer coefficient based on variable fluid properties with temperature, the mass flow rate, and particle size. As seen in the charge and discharge test these theoretical values had to be reduced by a factor of 4 to provide a reasonable fit to the test data.

The magnitude of the heat transfer coefficient and its variation with mass flow rate is shown in figure C-1. The mass flow rate is defined in terms of the total bed cross sectional area. Values varied from 15 to 25 BTU/Ft^2hr^oF over the test range.

Figure C-2 shows the heat transfer coefficients in terms of Reynolds number, where the characteristic dimension in the Reynolds number is the particle diameter.

A more general correlation is shown in Figure C-3 where the Nusselt number is shown as a function of Reynolds number.

FIG. C-1

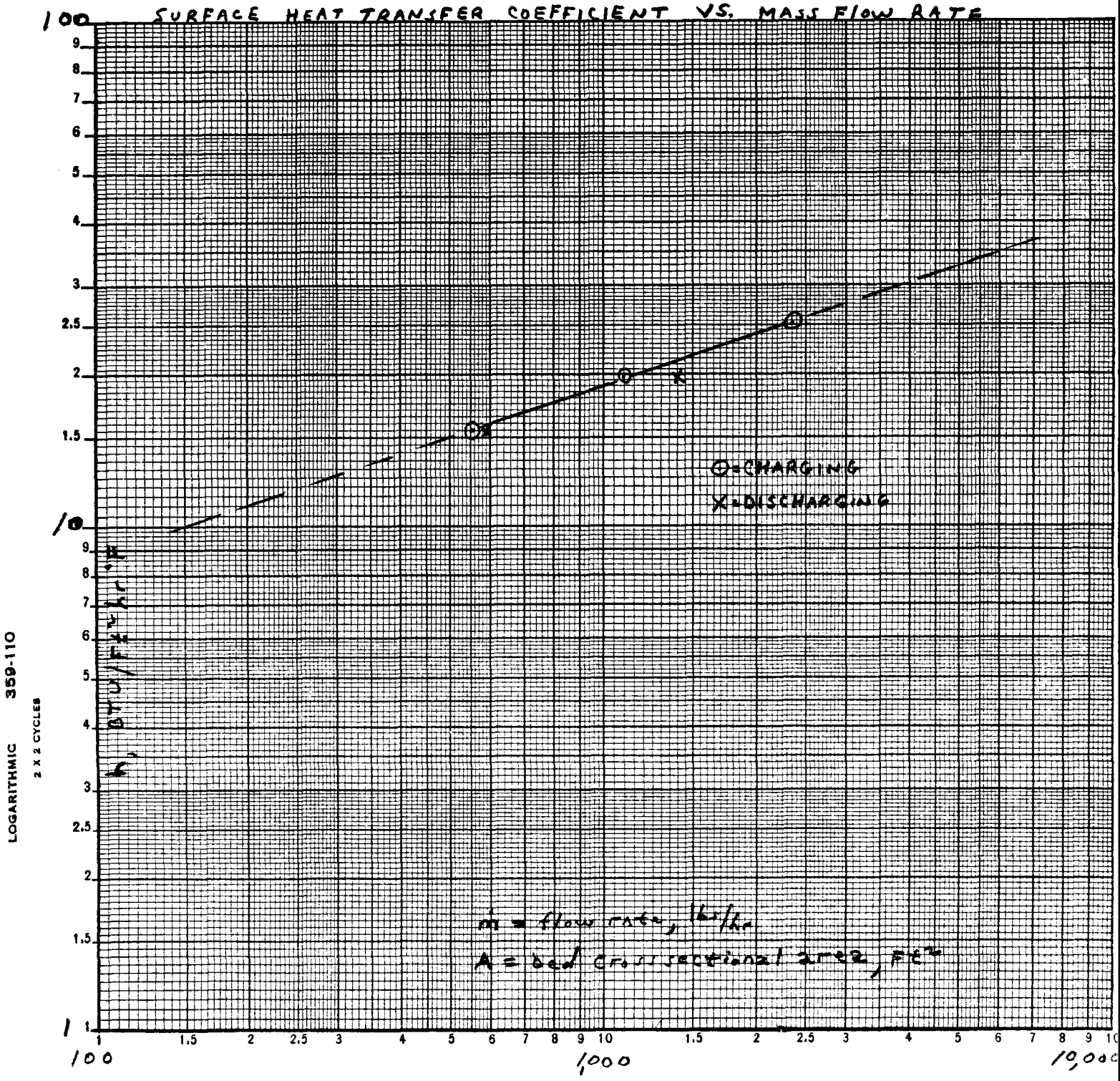

$G = \frac{\dot{m}}{A}$, SUPERFICIAL MASS FLOW RATE, lbs/ft²hr

FIG. C-2

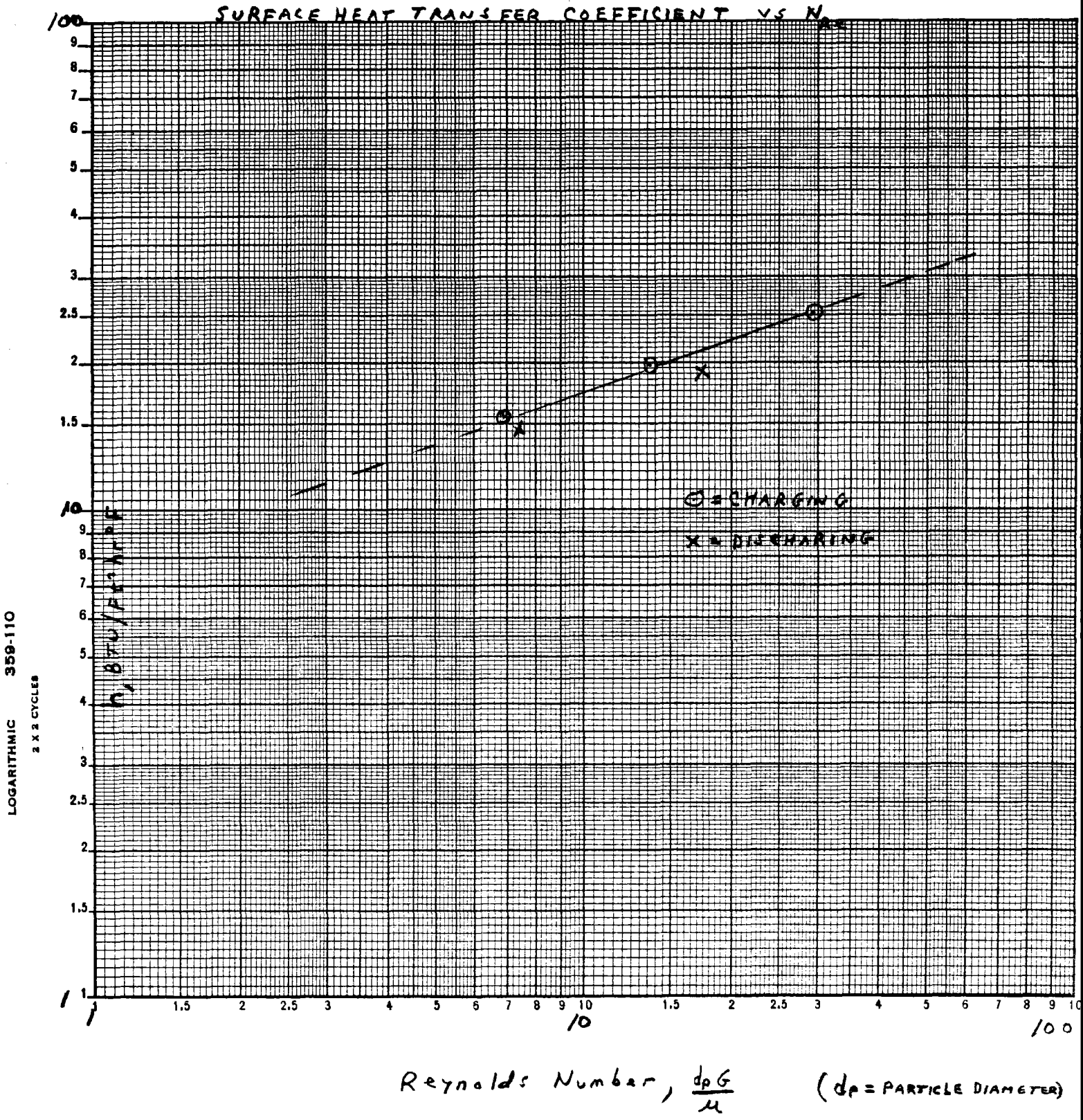
SURFACE HEAT TRANSFER COEFFICIENT VS N_{Re}
h, BTU/HR-FT²-°F
LOGARITHMIC 359-110
2 X 2 CYCLES
○ = CHARGING
X = DISCHARING
Reynolds Number, $\frac{d_p G}{\mu}$ (d_p = PARTICLE DIAMETER)

FIG. C-3

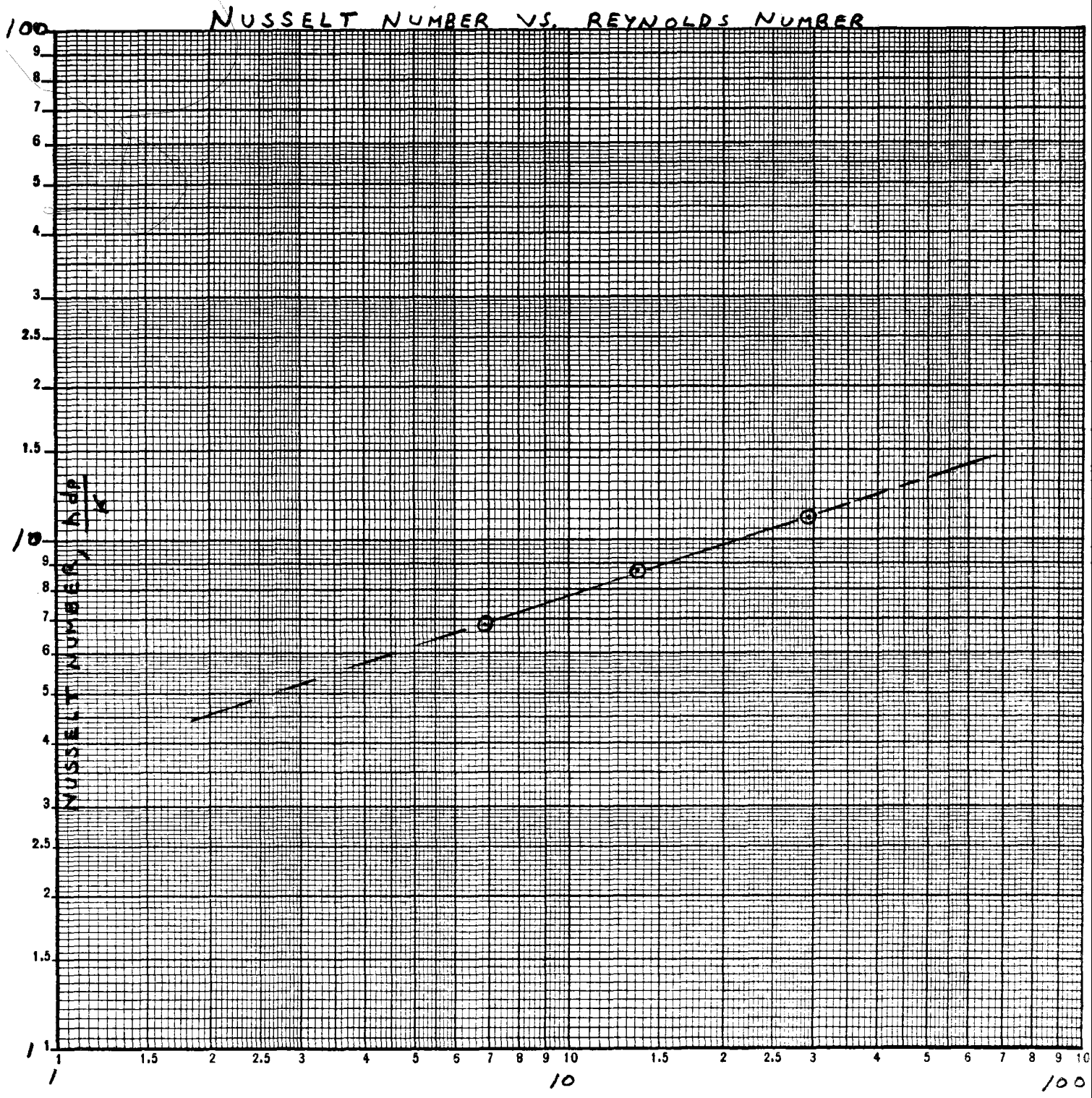
NUSSELT NUMBER VS. REYNOLDS NUMBER
NUSSELT NUMBER, $\frac{h\,d_p}{k}$
Reynolds Number, $\frac{d_p G}{\mu}$ (d_p = particle diameter)
LOGARITHMIC 359-110
2 X 2 CYCLES

5.6 Fluid Distributor Problem

The fluid distributor design was intended to provide uniform flow over the range of flow rates planned. This, however, did not turn out to be the case. At the lower flow rates, fluid preferentially flowed out the outer rings leaving the inner region fluid poor. The post test plot of the bed temperature profiles at the 1 GPM flow rate, showed that even after 5 hours of charging the bed centerline rose only a few degrees.

Prior to the start of testing, a test was run to check fluid distribution. This was accomplished by placing a series of cups of 2" diameter under the distributor. The test was run at 4 GPM. Fluid levels in the cups were compared and the deviation was approximately ±20% from the mean level. This was judged at the time to be acceptable with the intent of re-running tests if the thermoclines were poor. It is possible to vary the flow in each individual ring by means of a value in each ring inlet line, although it would be a time consuming operation.

The first charge/discharge runs were made at 8GPM, since thermocline spreading was expected to be most severe at the higher flow rates. When the 1 GPM temperature distributions were analyzed, detailed calculations were made of the pressure-flow relationships as shown in figure F-1. This showed that a head of only $\sim$ 9" was required to allow allfluid to flow out of the outer ring at 1 GPM. This was confirmed by a careful post test observation through the top view port at a flow of 1 GPM. This showed no flow from the inner rings. As the test data was being reduced, it became evident that a heat transfer coefficient of $\frac{h}{4}$ theoretical was a reasonable

fit to the thermocline slopes at the higher flow rates, compared to $\frac{h}{11}$ from the previous column test, and that acceptable full scale performance could be expected. These higher rates are representative of the great majority of rates for charging/discharging in the full scale system. Consequently, in the interest of cost economy, the decision was made not to fine tune the distributor and re-run the test at the lower flow rates.

FIG. F-1

COLUMN TEST DISTRIBUTOR FLOW

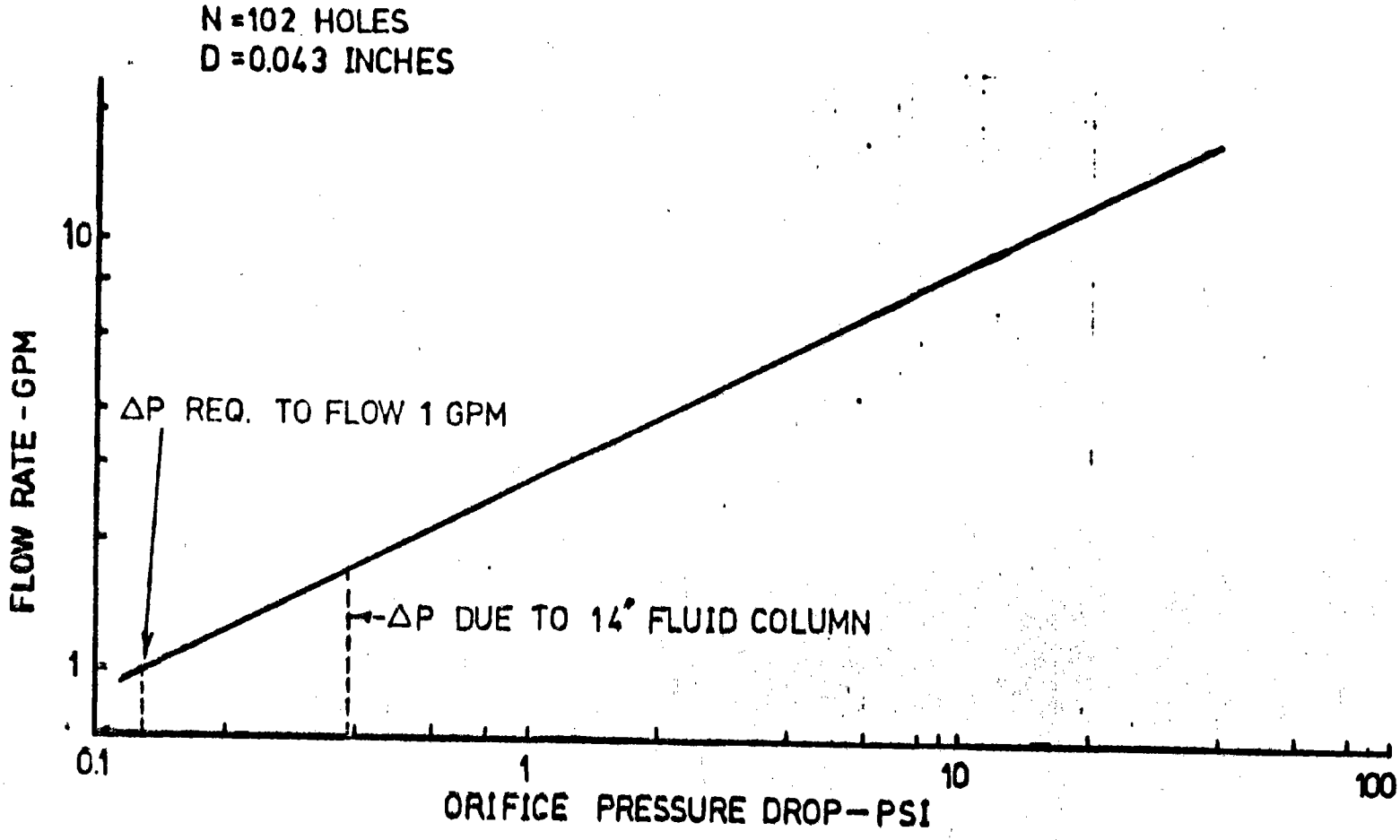

volume ratio of a small scale test compared to the full scale system. When this is considered, the holding tests indicate that significant distortion of the thermoclines will not result radially. Also, axial dispersion, (inherently lower in a trickle system), was seen to be small; convective losses at the top of the bed distort only the first 5 inches and holding tends to smooth out internal radial (not near the wall) gradients.

The inversion test results were distorted by the heat losses in the fluid exit line, but do indicate that the process is feasible.

In summary, the results of the Extended Column Test have established a rational engineering basis for the design of the trickle oil storage systems. The Extended Column Tests provide a higher degree of confidence than was provided by the previous short column test. It must be born in mind that the true criteria for judgement of trickle verus dual media mode lies not just in a direct comparison of thermocline shapes but in the overall system economics. With this in mind, it is a wise decision to carry the capability for both modes of operation into the Shenandoah system so that the economics and performance of both approaches can be comprehensibily evaluated.

volume ratio of a small scale test compared to the full scale system. When this is considered, the holding tests indicate that significant distortion of the thermoclines will not result radially. Also, axial dispersion, (inherently lower in a trickle system), was seen to be small; convective losses at the top of the bed distort only the first 5 inches and holding tends to smooth out internal radial (not near the wall) gradients.

The inversion test results were distorted by the heat losses in the fluid exit line, but do indicate that the process is feasible.

In summary, these test with due consideration to their limitations, do not provide an indictment against trickle mode operation nor do they provide the highest degree of confidence. They do provide a higher degree of confidence than provided by the previous short column test. It must be born in mind that the true criteria for judgement of trickle versus dual media mode lies not just in a direct comparison of thermocline shapes but in the overall system economics. With this, in mind it is a wise decision to carry the capability for both modes of operation into the Shenandoah Large Scale experiment.